

Applications of Nanotechnology in the Polymer and Textile Fields

**Von der Fakultät Chemie der Universität Stuttgart
zur Erlangung der Würde eines Doktors der
Naturwissenschaften (Dr.rer.nat.)
genehmigte Abhandlung**

Vorgelegt von
Master-Chem
Wael Sabry Mohamed
aus Kairo - Ägypten

Hauptberichter: Prof. Dr. Dr. h.c. Franz Effenberger

Mitberichter: Prof. Dr. rer. nat. Karl Brederick

Tag der mündlichen Prüfung: 28.September 2009

Universität Stuttgart

Institut für Polymerchemie

Lehrstuhl für Makromolekulare Stoffe und Faserchemie

2009

TO THE SPIRIT OF MY FATHER

Acknowledgements

First and foremost, I would like to present my sincere thanks to my advisor, **Prof. Dr. Dr. h.c. Franz Effenberger**, for all of his friendly support and guidance throughout my education at Stuttgart University. Words cannot express how much I have gained his wisdom, as well as from the many learning opportunities he afforded me during my tenure.

Additionally, I would like to thank **Dr. Michael Schweizer**, for without his insight, patience, and helpful suggestions that have shaped my development as a scientist, this thesis would not have been possible.

I would like also to express my sincere thanks and gratitude to **Dr. Gabriele Hardtmann** for her encouragement and support throughout my studying years at Stuttgart University.

Dr. Manuella Frick for her enormous helping.

Dr. Anette Hoffmann-Frey for her friendly interesting.

Dr. Gutmann for support in the melt spinning.

Dr. F. Harmanutz and **Mrs. Müller** for the manufacturing of X-rays.

Mr. Jan Pigorsch for assistance with laboratory work.

Mrs. Segel for measuring the mechanical properties.

Mrs. Henzler and **Mr. Hageroth** for the investigation by SEM.

Mr. Wölfl for melting intercalating process.

All of my colleagues in the institute for polymer chemistry and institute for textile and chemical fibres (Denkendorf) for the pleasant working climate and good cooperation.

I would like to express my sincere thanks and gratitude to Egyptian Government for the financial support and I would like also to extend my gratitude to the Egyptian Cultural Counsellor and all members of the Egyptian Culture Office in Berlin for their interest and enormous helping

Abstract

Intercalated modification of Montmorillonite clay (MMT) with three different amino acids - Alanine, Leucine, and Phenylalanine - in the presence of hydrochloric acid followed by surface modification by phenyl triethoxy silane coupling agent to produce double modified montmorillonite clay which is characterized by X-ray diffraction (XRD) and Thermogravimetric analysis (TGA). The data show an increase in d-spacing of modified clay as a result of cationic exchange. The ability of clay to make glucose and fructose absorption was kinetically studied and also the swelling degree of the clays was determined.

Double modified MMT clay was used in the preparation of Polyacrylate / clay nanocomposites by using an in situ redox emulsion polymerization of polyglycidylmethacrylate (PGMA) and polymethylmethacrylate (PMMA). The structure and properties of the prepared nanocomposites were achieved by XRD, TGA, and SEM. The results show that all weight loses temperatures for the nanocomposite samples are higher than that of pure polymer in both PGMA and PMMA. It is also obvious that the increasing in the clay content plays an effective role in the increasing of thermal stability of these materials. SEM shows that the clay is more homogenously dispersed in PMMA than in PGMA matrix.

Polyolefin nanocomposites were synthesized by using Na-MMT, Leucine-MMT and DM-MMT clay by solution polymerization method using anhydrous xylene solvent in case of polypropylene and using a co-solvent of xylene and benzonitrile (80:20wt %) in case of polyethylene. The structure and properties of the prepared nanocomposites were examined by XRD, TGA and SEM. The results show that a homogenous dispersion of MMT clay in the polymer matrix is observed only in the case of PP/DM-MMT up to 10%DM-MMT weight percentage.

The grafting emulsion polymerization of vinyl monomers onto cotton was carried out in the presence of double-modified montmorillonite clay. The obtained results show that grafting with glycidyl methacrylate/montmorillonite gave a higher rate of grafting than grafting with methyl methacrylate/montmorillonite in all clay percentages, and also, the grafting yield of glycidyl methacrylate monomer onto cotton in the presence of montmorillonite clay had a higher value than that in the absence of the clay for all factors studied. Cotton grafted with glycidyl methacrylate/ montmorillonite with a graft yield of about 50% was prepared according to the emulsion polymerization technique

and was treated with different concentrations of dibutylamine solutions ranging from 1 to 4%. The obtained samples were characterized according to nitrogen content, thermal stability, scanning electron microscopy, mechanical properties, water absorption, and colour strength according to acid, basic, and reactive dyes.

Polypropylene and nanocomposites polypropylene fibres were successfully prepared via melt spinning process. The prepared fibres were characterized according to thermal stability, scanning electron microscopy, mechanical properties, water absorption, and colour strength according to acid and disperse dyes.

Table of Contents

Chapter 1: Introduction and Objectives	1
1.1. Nanotechnology	1
1.1.1. Nanoscale systems and their properties	2
1.2. Nanocomposites	2
1.2.1. Types of Composite materials	2
1.2.2. The classification of nanocomposites	3
1.2.3. Nanoeffect	4
1.2.4. Polymer-Clay Nanocomposites	5
1.2.5. Applications of nanocomposites in Textile field	8
1.3. Objective of the study	8
Chapter 2: Clay Structure and Modification	10
2.1. Crystal Structure of Layered Silicate	11
2.1.1. Montmorillonite (MMT)	14
2.2. Modification of the Clay	16
2.2.1. Cation Exchange Process	16
2.2.2. Cation Exchange Capacity	17
2.2.3. Surface Charge Density	18
2.2.4. Types of Clay Modifications	18
A) Interlayer modification	18
I) Amino acids	18
II) Alkylammonium ions	19
B) Surface and edges modification	19
Chapter 3: Polymer Layered Silicate Nanocomposites (PLSN)	21
3.1. Polymer Matrices Used in Layered Silicate Nanocomposites	21
3.1.1. Vinyl Polymers	21
3.1.2. Polyolefin	22
3.2. Morphology of Polymer Layered Silicate Nanocomposites	22
3.2.1. Intercalated	22
3.2.2. Exfoliated	23
3.2.3. Flocculated	25
3.2.4. Intercalated-Exfoliated mix	26

3.3. Synthesis of Polymer Layered Silicate Nanocomposites	26
3.3.1. In-Situ Polymerization	26
3.3.2. Solution Mixing	29
3.3.3. Melt Intercalation	33
3.4. Characterization of Polymer Layered Silicate Nanocomposites	34
3.4.1. Wide Angle X-ray Diffraction (WAXD)	34
3.4.2. Transmission Electron Microscopy (TEM)	36
3.4.3. Rheology	36
3.5. Properties of Polymer Layered Silicate Nanocomposites	37
3.5.1. Young's modulus	37
3.5.2 Flexural modulus	38
3.5.3 Thermal degradation	38
3.5.4 Heat Distortion Temperature (HDT)	39
3.5.5 Barrier property improvements	40
Chapter 4: Grafting of Vinyl Monomers Nanocomposites onto Cotton Fabric	41
4.1. Cotton Fabric	41
4.1.1. Chemical Composition	41
4.1.2. Cotton Morphology	44
4.1.3. Cellulose Chemistry and Reactions	45
4.2. Grafting	47
4.2.1. Grafting Method	47
4.2.1.1. Grafting Initiated by Chemical Technique	47
4.2.1.1.1. Free-radical grafting	47
4.2.1.1.2. Grafting through living polymerization	48
4.2.1.1.3. Ionic grafting	50
4.2.1.2. Grafting Initiated by Radiation Technique	50
4.2.1.2.1. Free-radical grafting	50
4.2.1.2.2. Ionic grafting	51
4.2.1.3. Photochemical grafting	52
4.2.1.4. Plasma radiation induced grafting	52
4.2.1.5. Enzymatic grafting	53

Chapter 5: Fibre Reinforcement Polypropylene / Montmorillonite Nanocomposite	54
5.1. Polypropylene Based Nanocomposites	55
5.2. Processing Of PP/MMT Filament	56
5.2.1. Introduction to Spinnability Criteria	56
5.2.2. Melt Spinning Processing Techniques	59
5.2.2.1. Fibre Melt-spinning Principles	59
5.2.2.2. Film Extrusion-Calendering	59
Chapter 6: Experimental Part	61
6.1. Materials	61
6.2. Methods	62
6.2.1. Modification of MMT Clay	62
6.2.1.1. Intercalated Modification of MMT with Amino Acids	62
6.2.1.2. Surface Modification of MMT with Silane Coupling Agent	62
6.2.1.3. Double Modification of MMT with Amino acid and Silane Coupling Agent	62
6.2.2. The Swelling Degree	62
6.2.3. Glucose and Fructose Absorption Studies	63
6.2.3.1. Preparation of Calibration Curve	63
6.2.4. Preparation of Nanocomposites	63
6.2.4.1. Preparation of Polyacrylate / MMT Nanocomposites by In Situ Emulsion Polymerization	63
6.2.4.2. Preparation of Polypropylene / Montmorillonite Nanocomposite by Solution Polymerization	63
6.2.4.3. Preparation of Polyethylene / Montmorillonite Nanocomposite by Solution Polymerization	64
6.2.4.4. Preparation of Polypropylene / Montmorillonite Nanocomposite by Direct Melt Spinning Intercalation Method	64
6.2.5. Polypropylene / Montmorillonite Fibre Production Method	64
6.2.6. Grafting Polymerization Procedure	65
6.2.7. Dyeing Methods	65
6.2.8. Water Absorption	66
6.3. Characterization	67

Chapter 7: Modifications, Characterizations and Applications of Montmorillonite Nanoparticles	68
7.1. Introduction	68
7.2. Modification of Montmorillonite Clay	69
7.3. Characterization of Montmorillonite Clay	71
7.3.1. Thermal Gravimetric Analysis (TGA)	71
7.3.2. Morphology of MMT Clay by Scanning Electron Microscope(SEM)	72
7.4. Applications of Montmorillonite Clay	72
7.4.1. The Swelling Degree	72
7.4.2. Sugar Absorption Study	73
7.5. Conclusion	75
Chapter 8: Synthesis and Characterization of some Polyacrylate / Montmorillonite Nanocomposites by In Situ Emulsion Polymerization using Redox Initiation System	75
8.1. Introduction	75
8.2. Structures and Properties of nanocomposites	76
8.2.1. Thermal Gravimetric Analysis (TGA)	76
8.2.2. X-Ray Diffraction (XRD)	80
8.2.3. Scanning Electron Microscope (SEM)	80
8.3. Conclusion	82
Chapter 9: Solution Preparation of Polyolefin / Montmorillonite Nanocomposites	83
9.1. Introduction	83
9.2. Structure and Properties of Polyolefin Nanocomposites	84
9.2.1. Infra-Red (IR)	84
9.2.2. Thermal Gravimetric Analysis (TGA)	85
9.2.3. Melting Point (MP)	89
9.2.4. X-Ray Diffraction (XRD)	90
9.2.5. Scanning Electron Microscope (SEM)	92
9.3. Conclusion	94

Chapter 10: Elucidation of the Nanoparticles Effect in the Grafting of Vinyl Monomers onto Cotton Fabric	95
10.1. Introduction:	95
10.2. Factors Affecting Graft Polymerization of Vinyl Monomers onto Cotton Fabric	96
10.2.1. Effect of Double Modified Montmorillonite Clay Concentration:	96
10.2.2. Effect of Temperature	97
10.2.3. Effect of Time	98
10.2.4. Effect of Initiator Concentration	99
10.2.5. Effect of Monomer Concentration	99
10.3. Characterization of Cotton Fabric Grafted with GMA Monomer in the Presence of Double Modified MMT Clay and Treated with Dibutyl Amine	100
10.3.1. Nitrogen Content	101
10.3.2. Thermal Stability	102
10.3.3. Mechanical properties	103
10.3.4. Water absorption	104
10.3.5. Scanning Electron Microscope (SEM)	104
10.3.6. Colour Measurement	106
10.4. Conclusion	110
Chapter 11:Effect of Montmorillonite Clay Nanoparticles on the Properties of Polypropylene Fibres	112
11.1. Introduction	112
11.2. Structure and Properties of Polypropylene / Montmorillonite Fibres	113
11.2.1. Thermal Gravimetric Analysis (TGA)	113
11.2.2. Melting Point (MP)	114
11.2.3. Mechanical Properties	115
11.2.4. Water Absorption	115
11.2.5. Scanning Electron Microscope (SEM)	116
11.2.6. Colour Measurement	118
11.3. Conclusion	120
Summary	121
Zusammenfassung	125
References	129

List of Figures

- Figure 2.1:** Crystal structure of dioctahedral phyllosilicates. a) 1:1 layer. b) 2:1 layer
- Figure 2.2:** Structure of 2:1 phyllosilicates
- Figure 2.3:** Cation exchange reaction
- Figure 2.4:** The cation-exchange process between Alkylammonium ions and cation initially intercalated between the clay layers.
- Figure 3.1:** Intercalated silicate morphology. Straight lines represent silicate layers while curved lines represent polymer chains.
- Figure 3.2:** Exfoliated silicate morphology. Straight lines represent silicate layers while curved lines represent polymer chains.
- Figure 3.3:** Flocculated silicate morphology. Straight lines represent silicate layers while curved lines represent polymer chains.
- Figure 3.4:** Schematic of in-situ polymerization.
- Figure 3.5:** Schematic of solution mixing.
- Figure 3.6:** Schematic of melt intercalation.
- Figure 4.1:** Representation of the structure of a cotton fibre.
- Figure 4.2:** (a) Assembly of cellulose molecules in a sheet. (b) A schematic view of the crystal lattice of cellulose
- Figure 4.3:** Molecular structure of cellulose
- Figure 5.1:** Schematic description of (a) cohesive fracture and (b) capillary break-up failure mechanisms.
- Figure 5.2:** Maximum filament length predicted for the capillary break and cohesive fracture mechanisms
- Figure 5.3:** Schematic description of the melt spinning process.
- Figure 5.4:** Schematic description of the extrusion-calendering process.
- Figure 7.1:** XRD patterns of (A) pure MMT and treated with (B) Alanine, (C) phenyl Alanine and (D) Leucine amino acids.
- Figure 7.2:** XRD patterns of (A) pure MMT, (B) Silane surface MMT, (C) Double modified MMT and (D) Leucine MMT.
- Figure 7.3:** TGA thermograms of (A) Silane surface MMT, (B) Pure MMT, (C) double modified MMT and (D) Leucine-MMT.
- Figure 7.4:** SEM of (A) Pristine MMT and (B) double modified MMT.
- Figure 7.5:** Swelling degree of Leucine-MMT and DM-MMT

Figure 8.1: TGA thermograms of (A) Pure PGMA, (B)2%, (C)6%, (D)10% and (E)20% weight % MMT in PGMA-MMT nanocomposites.

Figure 8.2: TGA thermograms of (A) Pure PMMA, (B)2%, (C)6%, (D)10% and (E)20% weight % MMT in PMMA-MMT nanocomposites.

Figure 8.3: XRD patterns of (A) double modified MMT (B) PGMA-MMT nanocomposites (C) PMMA-MMT nanocomposites

Figure 8.4: SEM images of (A) pure PGMA, (B) PGMA-MMT

Figure 8.5: SEM images of (A) pure PMMA, (B) PMMA-MMT

Figure 9.1: FTIR spectrum of A) DM-MMT, B) Pure PE and C) PE + 5% DM-MMT nanocomposite.

Figure 9.2: FTIR spectrum of A) DM-MMT, B) Pure PP and C) PP + 5% DM-MMT nanocomposite.

Figure 9.3: TGA thermograms of pure PE and the prepared PE nanocomposites with different modified montmorillonite clay

Figure 9.4: TGA thermograms of pure PP and the prepared PP nanocomposites with different modified montmorillonite clay

Figure 9.5: TGA thermograms of the prepared PE nanocomposites with different double modified montmorillonite clay percentage

Figure 9.6: TGA thermograms of the prepared PP nanocomposites with different double modified montmorillonite clay percentage

Figure 9.7: Melting points of pure polyolefin and the prepared polyolefin / montmorillonite nanocomposites

Figure 9.8: XRD patterns of (A) PE/5%Na-MMT, (B) PE/5%Leucine/MMT and (C) PE/5%DM-MMT nanocomposites.

Figure 9.9: XRD patterns of (A) PP/5%Na-MMT, (B) PP/5%Leucine/MMT and (C) PP/5%DM-MMT nanocomposites.

Figure 9.10: XRD patterns of (A) PP/5%DM-MMT, (B) PP/10%DMMMT and (C) PP/15%DM-MMT nanocomposites.

Figure 9.11: SEM of pure PE and the prepared PE nanocomposites with different modified montmorillonite clay

Figure 9.12: SEM of pure PP and the prepared PP nanocomposites with different modified montmorillonite clay

Figure 10.1: Effect of MMT concentration on the grafting yields of A) GMA and B) MMA monomers onto cotton

Figure 10.2: Effect of Temperature on the grafting yields of A) GMA and B) GMA-MMT onto cotton

Figure 10.3: Effect of Time on the grafting yields of A) GMA and B) GMA-MMT onto cotton

Figure 10.4: Effect of initiator concentration on the grafting yields of A) GMA and B) GMA-MMT onto cotton

Figure 10.5: Effect of initiator concentration on the grafting yields of A) GMA and B) GMA-MMT onto cotton

Figure 10.6: Nitrogen percentages of unmodified cotton sample and treated samples

Figure 10.7: TGA thermograves of unmodified cotton sample and treated samples

Figure 10.8a: SEM of unmodified cotton sample

Figure 10.8b: SEM of cotton sample grafted with GMA

Figure 10.8c: SEM of cotton sample grafted with GMA-MMT

Figure 10.8d: SEM of cotton sample grafted with GMA-MMT and treated by DBA

Figure 10.9: Effect of acid dyes on colour strength unmodified cotton and treated samples

Figure 10.10: Effect of basic dyes on colour strength unmodified cotton and treated samples

Figure 10.11: Effect of reactive dyes on colour strength unmodified cotton and treated samples

Figure 11.1: TGA thermograms of polypropylene and nanocomposites polypropylene fibres

Figure 11.2: Melting point of polypropylene and nanocomposites polypropylene fibres

Figure 11.3(a): SEM of pure polypropylene fibre

Figure 11.3(b): SEM of polypropylene /Na-MMT fibre

Figure 11.3(c): SEM of polypropylene /DM-MMT fibre

Figure 11.4: Effect of acid dyes on the colour strength of polypropylene fibres

Figure 11.5: Effect of disperse dyes on the colour strength of polypropylene fibres

List of Tables

Table 2.1: Classification and nominal chemical composition of some layered silicates

Table 7.1: XRD data obtained for pure and modified MMT clay

Table 7.2: Effect of temperature on the absorption degree of glucose and fructose at sugar concentration 25% W/V.

Table 7.3: Effect of sugar concentration on the absorption degree of glucose and fructose at temperature 30 °C.

Table 8.1: TGA data obtained for pure PGMA and PGMA-MMT nanocomposites

Table 8.2: TGA data obtained for pure PMMA and PMMA-MMT nanocomposites

Table 8.3: Comparison in the weight loss % between PGMA-MMT and PMMA-MMT when 6 weight % MMT is added in different temperatures

Table 9.1: TGA data obtained for pure polyolefin and the prepared polyolefin nanocomposites

Table 9.2: TGA data obtained for pure the prepared polyolefin nanocomposites with different percentage of DM-MMT.

Table 9.3: Melting points of pure polyolefin and the prepared polyolefin / montmorillonite nanocomposites

Table 10.1: Degradation temperatures of unmodified cotton sample and treated samples.

Table 10.2: Variation of mechanical properties, colour strength and water absorption of unmodified cotton sample with treated samples

Table 11.1: Degradation temperatures of polypropylene and nanocomposites polypropylene fibres

Table 11.2: Variation of mechanical properties, colour strength and water absorption of polypropylene fibres

CHAPTER 1

Introduction and Objectives

1.1. Nanotechnology

Nanotechnology involves the investigation and design of materials or devices at the atomic and molecular levels. One nanometer, a measure equal to one billionth of a meter, spans approximately 10 atoms. Formulating a precise definition of nanotechnology, however, is a difficult task. Even scientists in the field maintain that it “depends on whom you ask. Biophysicist Steven M. Block [1] notes that some researchers “reserve the word to mean whatever it is they do as opposed to whatever it is anyone else does. For example, some researchers use the term to describe almost any research where some critical size is less than a micron (1,000 nanometer) while other scientists reserve the term for research involving sizes between 1 and 100 nanometer. There is also debate over whether naturally occurring nanoparticles, such as carbon soot, fall under the rubric of nanotechnology. Finally, some reserve the term “Nanotechnology” exclusively for manufacturing with atomic precision whereas others employ the term to describe the use of nanomaterials to construct materials, devices, and systems. According to the Foresight Institute, a nonprofit organization dedicated to preparing society for nanotechnology, molecular nanotechnology “will be achieved when we are able to build things from the atom up, and we will be able to rearrange matter with atomic precision [2]. The National Science Foundation, on the other hand, defines nanotechnology as “research and technology development at the atomic, molecular or macromolecular levels, in the length scale of approximately 1– 100 nanometer range, to provide a fundamental understanding of phenomena and materials at the nanoscale and to create and use structures, devices and systems that have novel properties and functions because of their small and/or intermediate size [3].

1.1.1. Nanoscale systems and their properties

Nanoscale and nanostructure materials, a new branch of materials research, are attracting a great deal of attention because of their potential applications in areas such as electronics[4,5], optics[6-8], catalysis[9], ceramics[10,11], magnetic data storage [12], and nanocomposites[13-15]. The unique properties and the improved performances of nanomaterials are determined by their sizes, surface structure and interparticle interactions. These systems have nanoscale dimensions with large surface area to volume ratio, important in the following aspects [16]:

1. Large surface area compared to small size provides a large interaction interface for these materials. The result is sensitivity of their properties to chemical and physical environment. Examples of this include sensitivity of nanoparticles properties like photoluminescence to surface ligands and chemical environment.
2. Small size and large surface area leads to strong influence of forces like van-der-Waals bonding, hydrogen bonding, columbic interaction and surface tension on these systems resulting in their unique physical characteristics, like self-assembly, morphology and sensitivity to environment.

1.2. Nanocomposite Materials

According to the International Organization for Standardization, nanocomposite materials are solid ones with multiple phases, which is a combination of two or more materials with different physical and chemical properties [17]. In composite materials, one phase is usually continuous and called the matrix, while the other phase is a reinforcing material called the dispersed phase. In self-assembled systems, the ordered structure is the dispersed phase, while the template film can be the continuous phase.

1.2.1. Types of Nanocomposite Materials

1- Organic–inorganic Nanocomposites.

In organic–inorganic composites, nanocomposites refer to composites in which the inorganic phase has nanoscale morphology such as particles, fibers and tubes. There is an additional type of organic–inorganic nanocomposite, where either the organic phase or the inorganic phase has Nanoscale morphology in an organic–

inorganic composite [18, 19]. For example, in emulsion systems of W/O or O/W, clay nanoparticles and silica are often used to stabilize the emulsions, which then form an organic–inorganic nanocomposite. In designing a system of thiol / FeOOH, heating the mixture would lead to the formation of thiol/Fe₂O₃ or thiol/Fe₃O₄ nanocomposites [18].

2- Polymer–Inorganic Nanocomposites.

Generally, it refers to a nanocomposite in which organic polymer forms a composite with inorganic nanoparticles, e.g., BiI₃–nylon nanocomposite [20], and montmorillonite–nylon (polyester) nanocomposites [21].

1.2.2. The Classification of Nanocomposites

1- Classification I. This classification is based on the nanomaterials dimensional (D) morphology.

- (a) 0-D nanopowder or nanoparticle;
- (b) 1-D nanowire, nanowisp, nanosilk, nanotube or nanocrystalline whisker;
- (c) 2-D nanomaterial with morphology of layer, lamellar or belt structure;
- (d) 3-D nanomaterial with morphology of cylinder, solid or block structure.

2- Classification II. This classification is based on polymer morphology, shape or state. In the nanocomposites, in which the inorganic particle is a 0-D nanoparticles [18, 22].

- (a) 1-D nanocomposite when the polymer in the composite is in solution;
- (b) 2-D nanocomposite when the polymer in the composite is in film or membrane shape;
- (c) 3-D nanocomposite when the polymer in the composite is in a powder state or morphology;
- (d) 0-D nanocomposite formed with two different nanopowders.

3- Classification III. This classification is based on a nanophase of tube- or non-tube like material in the nanocomposites.

- (a) Tube-like, e.g., single-wall carbon nanotubes, TiO₂ Tube, or Al₂O₃ tube.
- (b) Non-tube-like, e.g., layer of clay, lamellar, silk, belt or band-like shape.

Sometimes, the classifications are mixed to describe nanocomposites, e.g., carbon nanotubes or nanocrystalline whiskers with polymer powder construct a 1–3 type nanocomposite. Nanolayers of clay with polymer powder form 2–3 type of

nanocomposites, etc. The classifications for nanomaterials or nanocomposites are of definite significance with respect to the so-called “nanoeffect,” which is related to the material properties of the composite (mechanical, optical, thermal and magnetic) and the dependence of the properties on the size of the nanoparticles in the nanocomposite.

1.2.3. Nanoeffect

Besides the particle’s shape, surface or morphology, dispersion and aggregation in a matrix, attention needs to be paid to the properties and performance of a composite. How nanoparticles affect the properties of nanocomposite materials is of concern to engineers and scientists who are interested in the applications of nanocomposites.

The nanomaterials or nanocomposites and the theories related to them are based on a concept of “critical scale,” or nanoscale. For a critical scale of nanoparticles, the nanocomposite properties produce a superior property compared with the pure counterpart matrix if the nanoparticles are below a critical size.

When a material structure has one dimension less than the critical scale of 100 nm, can appear totally different the behaviour of its material properties. Based on such phenomena, scientists determined the abnormal phenomena to be produced on the scale level between single-atom molecules and clusters of many thousands of molecules. Properties of any nanocomposite must include two aspects: “nanoscale” and “nanoeffect.” At a critical scale, the properties of nanocomposite materials can sometimes produce an inverse transition of a property, e.g., the conduction behaviour of the metal Ag will change into that of an insulator at a particle scale less than 14 nm, while ferric magnetic performance is transformed into supermagnetic if the cluster size becomes less than several nanometers.

Nanoeffect in nanocomposites have several forms such as acceleration of polymer crystallization, induction of crystallization in a polymer, induction of liquid crystalline phenomenon, abnormal optical phenomenon, e.g., a blue shift, and abnormal multiple melting behaviour, e.g., double-melting behaviour in PET-layered clay nanocomposites. A nanoeffect can result from the transition of the performance due to aggregation, change of morphology or interactions, which leads to subsequent changes in the materials’ properties. As for nanocomposites, with many nanoeffects were not seen in each single composition, nanoeffects occurred during mixing, blending, compounding or in situ polymerization of the selected nanoparticles with

the matrix (matrix usually refers to macromolecules or polymers). Only after two kinds of matter come together to make a composite, where one phase is composed of nanoparticles, a nanoeffect can occur.

1.2.4. Polymer-Clay Nanocomposites

The polymer–clay nanocomposites area has received significant attention in recent years. However, work on layered clays has gone on for quite some time as it is of great importance to researchers studying soils. It was not until more recently that scientists have seen the applicability of such clays in materials science.

In 1990 a Toyota research group produced and characterized the first polymer/layered silicate nanocomposite (PLSN) material using Nylon-6 [23]. The unprecedented improvements that were achieved in a number of material properties showed tremendous promise for layered silicate material as a filler. In the years since, a flood of research has been carried out on nanocomposites using different polymer matrices, different layered silicates and multiple forms of compatibilizer. The layered silicates employed in this technology are most commonly phyllosilicates. Phyllosilicates make up a large family of naturally occurring clays whose basic layer structure is comprised of individual sheets of tetrahedral, oxygen rich layers and octagonal layers with silicon atoms at their core [24]. In case of the most commonly used layered silicate in this family (montmorillonite), Mg^{2+} and Al^{3+} cations occupy the spaces at the centre of the tetrahedral sheets [24]. Each silicate layer has a thickness of roughly a single nanometer and individual layers in their natural state are spaced approximately one nanometer apart [25]. Although there are a wide variety of silicate types, all layered silicates share the physical trait of high aspect ratio with length dimensions varying from 30 nm to several microns [25]. The high aspect ratio and nanometer scale dimensions give layered silicates a large surface area for interaction between silicate surface and polymer matrix. This large surface area is the primary difference between nanosilicate and traditional filler materials. Nanosilicate combined with polymer in only small quantities has been shown to dramatically increase the Young's modulus [23, 26], flexural modulus [23, 27] and impact strength [28] of a polymer matrix. Increases in thermal degradation temperature [29], decreases in thermal deformation [27] and improvements in barrier properties from neat polymer materials have all been recorded [30]. Each of these property improvements have been investigated in order to obtain a better

understanding of how layered silicate causes these enhancements. Results of past research have shown that there are a number of variables involved in determining the characteristics of a layered silicate nanocomposite including the compatibility of the polymer matrix and the silicate, the processing method used and the resulting morphology of the nanocomposite. The Toyota research group that first produced PLSNs chose to use Nylon-6 for their polymer matrix. The group found a 68% increase in tensile modulus, a 224% increase in flexural modulus and an 87°C increase in the heat distortion temperature [23]. Since that time many different polymer matrices have been used to form nanocomposites but all of them have failed to meet the impressive increases obtained in polyamide nanocomposite systems. There is a wealth of research that has attempted to mimic the strong compatibility between polymer and clay that is found in polyamide layered silicate nanocomposites. Multiple types of polyamides [31-40], polyolefin [41-48], polyesters [49, 50] and polycarbonates [51] have been combined with layered silicates modified to obtain maximum compatibility with the polymer matrix. It is well known that obtaining successful layered silicate nanocomposites requires excellent compatibility between the polymer matrix and the nanosilicate. A number of silicate surface modifications as well as a variety of compatibilizing compounds have been used for this purpose [52, 53].

Although considerable improvements in physical properties of nanocomposites have been realized with these techniques there is still ongoing research focused specifically on the enhancement of polymer/layered silicate compatibility. A large portion of the research carried out to date on PLSNs has been aimed at overcoming a number of challenges that are encountered when they are compounded. The two most critical challenges that need to be overcome in the production of a valuable PLSN are the inherent incompatibility of polymer and layered silicate as well as the tendency of layered silicates to assemble into ordered, layered domains. Natural layered silicate is highly hydrophilic due to the presence of interlayer cations that balance the negative charge generated by multiple surface oxygen atoms [25]. To make layered silicates compatible with many naturally hydrophobic polymer matrices, an ion exchange reaction can be carried out. In this way, highly hydrophilic layered silicates can be made miscible with polymer matrices. In addition to polymer/clay interactions that allow for miscibility, strong interactions between polymer and clay have been found to be a vital part of improving PLSN mechanical properties [48, 54].

Research has been heavily focused on a variety of techniques aimed to improve the interaction of polymer matrices and layered silicates. The development of oligomeric compatibilizers [48], novel reactive compatibilizers [50] and custom layered silicate surface modifications [52] has been an ongoing effort. In addition to promoting polymer/layered silicate compatibility, much attention has been focused on controlling the morphology of PLSNs. Layered silicates are naturally held together in sheets by strong Van der Waals forces [55]. Multiple layers of silicate stacked together are referred to as tactoids and can contain hundreds of individual layers. The tactoids themselves interact and can form large agglomerates within a polymer matrix. The advantage of high aspect ratio that layered silicates possess over traditional filler materials is lost when PLSN materials contain this type of large agglomerate. The presence of tactoids causes the effective aspect ratio of the silicates to decrease [56]. It has been shown that increasing the level of exfoliation in a PLSN results in improved mechanical, barrier and thermal properties [57, 58]. A number of processing techniques have been developed and implemented in an attempt to achieve PLSN systems with desired morphologies. Three compounding methods that have been used in the past are in-situ polymerization [52, 59], solution mixing [60] and melt compounding [61, 62]. In-situ polymerization and solution mixing have the disadvantage of requiring a suitable solvent. In addition, the logistics of each technique put a limit on what type of polymer matrix can be employed. Melt compounding has emerged as the most suitable industrial technique for the production of nanocomposites on a large, environmentally friendly scale. The difficulty associated with melt compounding is the inability of the technique to generate nanocomposites with a well exfoliated morphology. Many studies have shown that although high shear environments can increase exfoliation levels, complete exfoliation in certain polymer matrices cannot be achieved with melt compounding alone [38, 44, 53, 61, 62]. It has also been shown that extreme shear environments can decrease exfoliation levels as well as reduce nanosilicate aspect ratio by causing silicate fracture [53]. Efforts to expose PLSNs to an optimum amount of shear and back mixing have resulted in nanocomposite morphologies that still fall short of the desired exfoliated silicate state [42, 62].

1.2.5. Applications of Nanocomposites in Textile Field

Nanocomposites materials are widely used in various fields depending on the composite nature and structure [63], among these fields is the application in textiles where two principle ways can be considered for the use of nanocomposites in textile applications. Melt spinning of nanocomposite polymer [64] which can be subsequently woven or knitted has been demonstrated as a promising approach for textile fire retardant applications [65, 66]. Also coating of textile surfaces by nanocomposites formulation is another interesting way for the use of nanocomposites in textile application. In addition, the latter approach confers to textile surfaces other properties such as impermeability to water or gases for instance. Moreover, the incorporation of nanostructure in polymers for fire retardant applications makes it possible to limit the toxicity of the degradation products compared with the more traditional additives such as halogenated products [67-69]. In addition, the use of nanocomposites allows a reduction in the weight content of additives[66].

1.3. Objective of the Study

The overall focus of this study is synthesis, structure and properties of polymer / clay nanocomposites and its applications in the textile field. Specifically, the objectives are:

- 1- Developing the understanding of the surface and interlayer modification and to develop novel applications of the montmorillonite nanoclay.
- 2- Studying various factors that affect in the synthesis and characterization of some Polyacrylate / Montmorillonite nanocomposites by In-Situ emulsion polymerization using redox initiation system.
- 3- Studying the factors that affect in the solution preparation of Polyolefin / Montmorillonite nanocomposites

- 4- Elucidation of the effect of nanoparticles addition in the grafting of vinyl monomers onto cotton fabric.
- 5- Studying the effect of nanoclay on the properties of polypropylene nanocomposites fibers prepared by melt spinning technique.

A general introduction about the dissertation is given in chapter 1 together with its significance and the objectives of the study. Chapter 2 discusses in detail the structure and modifications of montmorillonite nanoclay. This is followed by a literature review of polymer layered silicate nanocomposites (PLSN) based on montmorillonite clay in chapter 3. Chapters 4 and 5 explain the applications of polymer nanocomposites in the textile field. Chapter 4 discusses in detail the structure of cotton fibre and the grafting of vinyl monomers nanocomposites onto cotton fabric. Fibre reinforcement polypropylene / montmorillonite nanocomposite is described in chapter 5. The experimental parts are explained in chapter 6. Surface and interlayer modification montmorillonite nanoclay, Determination of the swelling degree of the montmorillonite clay in different organic solvents and its applications in the sugar adsorption is studied in chapter 7. Chapter 8 presents the studying of various factors that affect in the synthesis and characterization of some polyacrylate / montmorillonite nanocomposites by in-situ emulsion polymerization using redox initiation system. Studying of the solution preparation of polyolefin / montmorillonite nanocomposites is presented in chapter 9. The applications of nanocomposites in textile field are studied in chapters 10 and 11 where chapter 10 presents the work of the elucidation of the effect of nanoparticles addition in the grafting of vinyl monomers onto cotton fabric and the studying of the effect of nanoclay on the properties of polypropylene nanocomposites fibers prepared by melt spinning technique is presented in chapter 11.

CHAPTER 2

Clay Structure and Modification

Clays are not the most abundant components in the mineral kingdom when compared to other components of the Earth's mantle or to feldspars of the continental crusts. However, they hold a special place in scientific research because their environment is criss-crossed constantly by human activity. Clays are at the centre of farming activities and civil engineering works; they are formed in diagenetic series prospected for petroleum resources; they crystallise in geothermal fields whose energy and mineral deposits prove valuable. Clays play an important part in everyday life, from the white-coated paper on which we write to the confinement of hazardous waste storage, from cosmetics to pneumatics, from paints to building materials.

Clays alone form an entire world in which geologists, mineralogists, physicists, mechanical engineers, chemists find extraordinary subjects for research. These small, flat minerals actually interface widely with their surrounding environment. They absorb, retain, release, and incorporate into their lattice a great variety of ions or molecules. Their huge external surface area (as compared with their volume) makes them first-class materials for catalysis, retention of toxic substances or future supports for composites. Clays are made up of particles that form stable suspensions in water. These suspensions have long served in drilling applications or tunnel piercing techniques. Suspended clays flow as liquids, thereby both helping to shape manufactured products such as ceramics, but also causing tragic mud flows, lahars or landslides.

Clay minerals belong to the phyllosilicates group (from the Greek "phyllon": leaf, and from the Latin "silic": flint). As a distinctive feature, they are very small (a few micrometers maximum) and their preferred formation occurs under surface (soils, sediments) or subsurface (hydrothermal alterations) conditions. Difficult to observe without using electron microscopy (scanning and transmission), they have been abundantly studied by X-ray diffraction, which is the basic tool for their identification. While the number of their species is relatively small, clay minerals exhibit a great

diversity in their composition because of their large compositional ranges of solid solutions and their ability to form polyphased crystals by interstratifications. The generic term "layered silicates" refers to not only natural clays but also to synthesised layered silicates such as magadiite [70], mica, laponite [71] and fluorohectorite [72]. Both natural clays and synthetic layered silicates have been successfully used in the synthesis of polymer nanocomposites. In the scope of this study, the focus will be on the use of montmorillonite natural clay from the smectite family because of its suitable layer charge density. Montmorillonite discovered in 1847 in France (Montmorillon) by Damour and Salvétat [73], is nowadays the most widely used clay as nanofiller. Montmorillonite is a common clay mineral with the numerous world-wide localities. In most cases, it has been formed by the weathering of eruptive rock material, usually tuffs and volcanic ash [74] (bentonite). In the pristine form, montmorillonite contains in addition varying amounts of cristobalite, zeolite, biotite, quartz, feldspar, zircon and other minerals found in volcanic rocks [75].

2.1. Crystal Structure of Layered Silicate

The crystal structure of all phyllosilicates is based on two types of layers [76, 77]:

- a) 1:1 layers in which one tetrahedral sheet is bonded to one octahedral sheet (Figure a)
- b) 2:1 layer in which one octahedral sheet is sandwiched between two tetrahedral sheets (Figure b).

The theoretical structures of both types of layers depend on the hexagonal symmetry of the tetrahedral and octahedral sheets which are linked to each other. The apical oxygen of the tetrahedral becomes the vertices of the octahedral. Thus, the six vertices of the octahedral in a 1:1 layer are formed by 4 OH⁻ radicals and 2 apical oxygen of the tetrahedral. In 2:1 layers, they are formed by 2 OH⁻ radicals only because the other four vertices are the apical oxygen of the two tetrahedral sheets.

The layers may be electrostatically neutral or possess negative electrostatic charge, due to the isomorphous substitution of the cations (in either the tetrahedral or octahedral sheets) by cations with low valence [78, 79]. Table (2.1) summarizes some of the phyllosilicates related to layered silicates [80, 18].

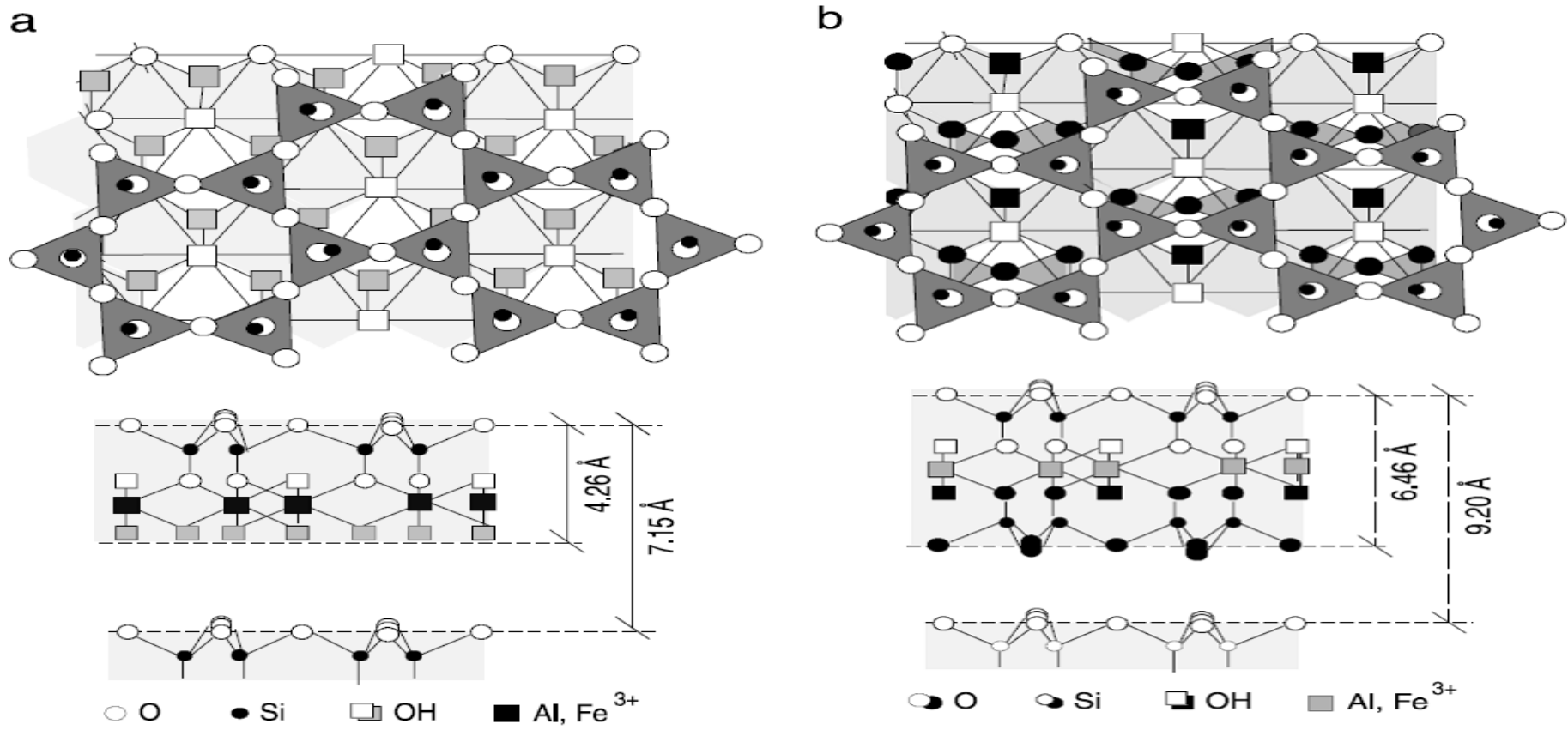


Figure 2.1: Crystal structure of dioctahedral phyllosilicates. a) 1:1 layer. b) 2:1 layer

Table 2.1: Classification and nominal chemical composition of some layered silicates

a: Commonly used in polymer nanocomposites fabrication

b: Synthetic layered silicates.

c: M represents a monovalent, charge compensating cation in the gallery.

Mineral Group (Layer Charge)		Subgroup	
1:1 (x~0)	Kaoline	Kaolinite	
		$[Al_4](Si_4)O_{10}(OH)_3$	
		Dioctahedral	Trioctahedral
2:1 (x~0)	Pyrophyllite-Talc	Pyrophyllite	Talc
		$[Al_2](Si_4)O_{10}(OH)_2$	$[Mg_3](Si_4)O_{10}(OH)_2$
Smectite (0.25<x<0.7)	Montmorillonite ^{a, c}	Hectorite ^{a, c}	
		$M_x[Al_{2-x}Mg_x](Si_4)O_{10}(OH)_2$	$M_x[Mg_{3-x}Li_x](Si_4)O_{10}(OH)_2$
		Saponite ^{a, b, c}	
		$M_{y-x}[Mg_{3-x}Fe_x^{3+}](Si_{4-y}Al_y)O_{10}(OH)_2$	
		Fluorohectorite ^{a, b, c}	
		$M_x[Mg_{3-x}Li_x](Si_4)O_{10}F_2$	
		Laponite ^{a, b, c}	
		$M_{x-y}[Mg_{3-x}Li_y](Si_4)O_{10}(OH)_2$	
		Beidellite ^c	
		$M_x[Al_2](Si_{4-x}Al_x)O_{10}(OH)_2$	
Vermiculite (0.6<x<0.9)	Dioctahedral Vermiculite	Trioctahedral Vermiculite	
		$M_x[Al_2](Si_{4-x}Al_x)O_{10}(OH)_2^c$	$M_x[Mg_3](Si_{4-x}Al_x)O_{10}(OH)_2^c$
Mica (x~1)	Muscovite	Phlogopite	
		$K[Al_2](Si_3Al)O_{10}(OH)_2$	$K[Mg_3](Si_3Al)O_{10}(OH)_2$

One of the most important aspects of some clay minerals is that they can have a great increase in their volume by adsorbing water molecules or other molecules into their gallery space, called swelling. According to their swelling behaviour, clay minerals can be divided into swelling and non-swelling; the swelling clays are called smectites which belongs to 2:1 [82, 83] layered silicates. Smectites can be further divided into two groups: dioctahedral and trioctahedral. In the former, all the octahedral sites (nominally) are occupied by divalent cations; while in the latter trivalent cations occupy two thirds of the octahedral central sites. In all the layered

silicates with negative surface charge, this negative charge is balanced by the counter hydrated alkali metal and alkali earth cations, which reside between the layers (gallery). The Vander Waals force between layers leads to the stacking of layers (crystallites) with an interlayer spacing about 1nm. At the edge, the charge is not fully balanced due to the crystal defect, and therefore a positive charge shows at the layer edge [14]. Depending on the nature of particular silicate (natural or synthetic), the lateral dimension can vary from 20 nm (laponite) to microns (montmorillonite, fluorohectorite) [24]. The most widely used smectites is montmorillonite (MMT), which has been used in this work.

2.1.1. Montmorillonite (MMT)

Montmorillonite is a raw material which is used in the preparation of polymer/ clay nanocomposites where Montmorillonite is a very soft phyllosilicate mineral that typically forms in microscopic crystals (Figure 2.2) [25]. Montmorillonite, a member of the smectite family, is 2:1 clay, meaning that it has two tetrahedral sheets sandwiching a central octahedral sheet. The particles are plate-shaped with an average diameter of approximately 1 micrometer. Montmorillonite water content is variable and it increases considerably in volume when it absorbs water [84].

Chemically, it is hydrated sodium calcium aluminum magnesium silicate hydroxide $(\text{Na, Ca})_{0.33}(\text{Al, Mg})_2(\text{Si}_4\text{O}_{10})(\text{OH})_2 \cdot n\text{H}_2\text{O}$. Potassium, iron, and other cations are common substitutes; the exact ratio of cations varies with source. The montmorillonite minerals occur in very small micron size less than 2 μm . They are fine-grained and thin-layered. The building blocks model structure of MMT, proposed by Hoffmann, Endell and Wilm consists of two fused silicon-oxygen tetrahedral sheets sandwiching an edge-shared octahedral sheet of either aluminium or magnesium hydroxide. Excess of negative charges within the montmorillonite layers is due to isomorphous substitution of Si^{4+} for Al^{3+} in the tetrahedral and of Al^{3+} for Mg^{2+} in the octahedral sheet [85]. These negative charges are counterbalanced by cations such as Ca^{2+} and Na^+ situated between the layers. These cations between the layers are part of the cation exchange capacity (CEC) of clay. Montmorillonite has a particularly large surface area when it is dispersed in water; one gram of MMT has a surface area of up to 800 square meters. The clay layers are held together by weak bonding between the oxygen in the tetrahedral and the charge-balancing cations and they can be easily separated. The gallery space between clay layers

depends on the type of cations (monovalent cations like Na^+ lead to more expansion than divalent cations like Ca^{2+}) and the concentration of ions. The sum of the single layer thickness and the interlayer represents the repeat unit of the multilayer material, so called d-spacing or basal spacing, and is calculated from the (001) harmonics obtained from X-ray diffraction patterns.

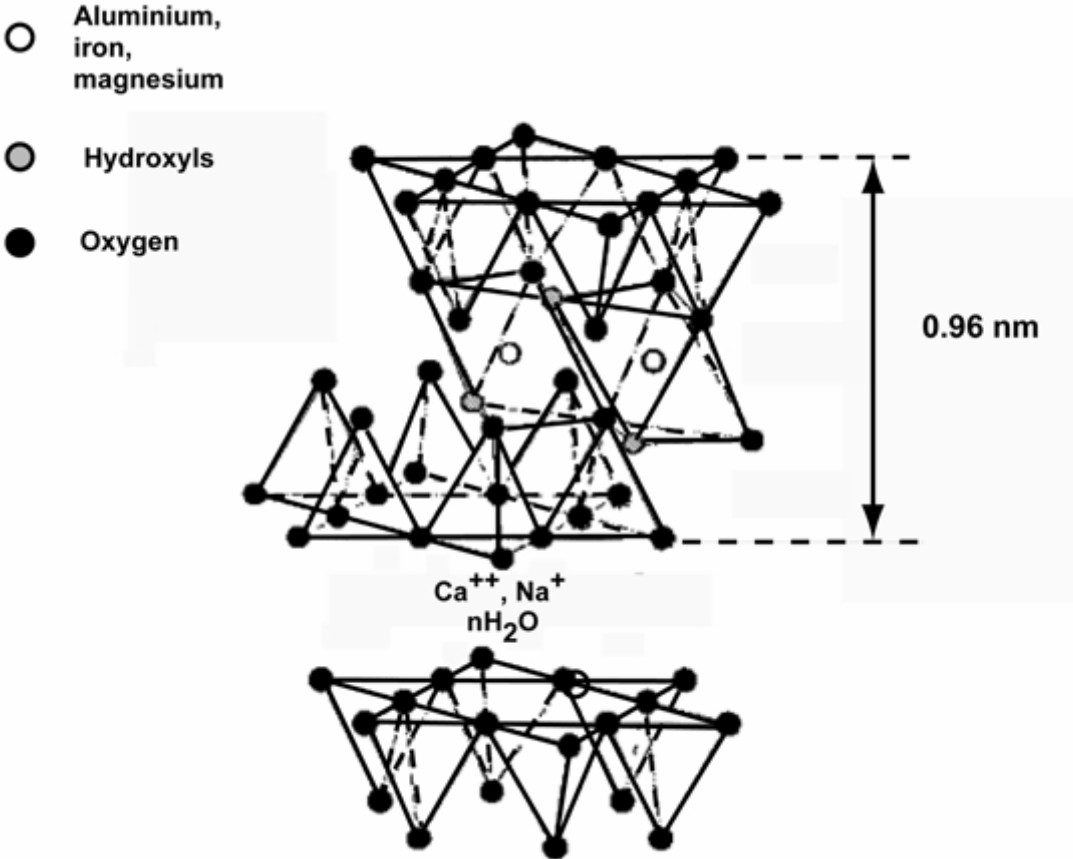


Figure 2.2: Structure of 2:1 phyllosilicates

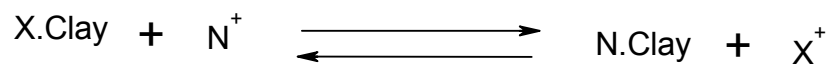
The physical dimensions of MMT give it unique properties as a filler material. The basic 2:1 sheet structure results in high aspect ratio sheets with a thickness of 1 nm and lengths of up to 300 nm. A consequence of this high aspect ratio is that small amounts of silicate have very large surface areas. The presence of a large surface area for interaction is a valuable characteristic in fillers. The tremendous surface area available for polymer-clay interaction allows polymer chains to effectively transfer stress into filler particles [54]. In addition, high aspect ratio particles can be used to improve the barrier properties of polymer membranes by increasing the tortuosity of the material [30].

2.2. Modification of the Clay

Clays are hydrophilic in nature, resulting from the hydration of the interlayer alkali metal or alkali earth metal cations. This leads to the incompatibility of the clay with most of the polymers as well as most hydrocarbons. However, the interlayer cations are readily exchangeable with organic cations, e.g., alkyl ammonium or phosphonium cations, which lowers the surface energy of the silicate surface and improve the wetting with polymer matrix [86, 87]. This is characterized by the cations exchange capacity and is directly related to the surface charge density of the silicate layers. The modified layered silicates have been widely used in petroleum and paint industry as a thickening agent to adjust the rheological properties [88, 89]. In addition to improving the wetting characteristic of clay with polymer, the organic cations also expand the gallery and weaken the Van der Waals force. Other than organic cations, silane coupling agent can also be used to modify the clay surface, relying on the reaction between the silanol group and the hydroxyl group on the clay surface [90, 91].

2.2.1. Cation Exchange Process

A characteristic feature of smectites such as montmorillonite is their ability to make absorption for certain cations and to retain them in an exchangeable state. It means that these intercalated cations can be exchanged by treatment of other cations in water solution. The most common exchangeable cations are Na^+ , Ca^{2+} , Mg^{2+} , K^+ , H^+ and NH_4^+ [25]. If the clay is placed in a solution of a given electrolyte, an exchange occurs between the ions of the clay (X^+) and these of the electrolyte (N^+): [92, 93]



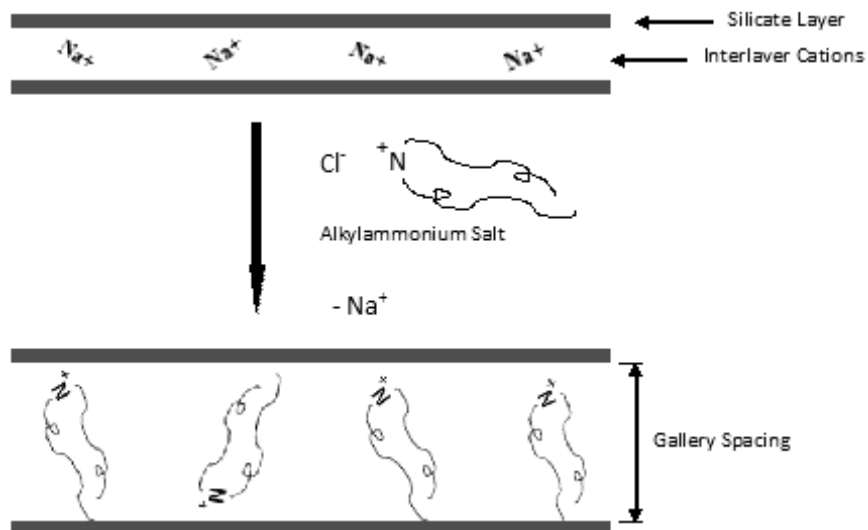


Figure 2.3: Cation exchange reaction

As indicated, this reaction is balanced and the extent to which the reaction proceeds from the left to right depends on the nature of the cations X^+ and N^+ , on their relative concentrations and often on secondary reactions.

Although the Law of Mass is not obeyed quantitatively in the equation above, the equilibrium of the reaction can be moved to the right by increasing the concentration of the added cations N^+ .

The cation-exchange process is controlled by the diffusion of the ion replacing the existing resident on the cation-exchange site. It is considered to occur in two stages:

- A) Diffusion from the bulk of the solution through the individual layers (film diffusion) surrounding the clay particles (Nernst diffusion).
- B) Diffusion within the particle itself (particle diffusion).

Using crystals of vermiculite as models, it has been demonstrated that the reaction starts at the edges of the particles, progressing towards the centre in a highly regular fashion. Rate measurements have shown that the penetration rate is linearly related to the square root of time of immersion, which confirms a diffusion-controlled process [94].

2.2.2. Cation Exchange Capacity

For the clay, the maximum amount of cations that can be taken up is constant and is known as the cation-exchange capacity (CEC). It is measured in milliequivalents per gram (meq/g). Although the convention is to use the unit, it represents a charge per unit mass and, in SI units, is expressed in coulombs per unit mass (C/g). A CEC of 1

meq/g is 96.5 C/g in SI units. Cation-exchange capacity measurements are performed at a neutral pH 7. The CEC of montmorillonite varies from 80 to 150 meq/100g. Determination of the cation-exchange capacity is a more or less arbitrary matter and no high degree of accuracy can be claimed. The measurement is generally made by saturating the clay with NH_4^+ and determining the amount held at pH 7 by conductometric titration [95, 96]. Another method consists in saturating the clay with Alkylammonium ions and evaluating the quantity of ions intercalating by ignition of the sample [97].

2.2.3. Surface Charge Density

Surface charge density (σ) can be estimated in different ways. If the CEC and the specific surface of the clay (S) are known:

$$\sigma = \text{CEC} / S$$

This formula gives an average value of the surface charge density in the clay [98].

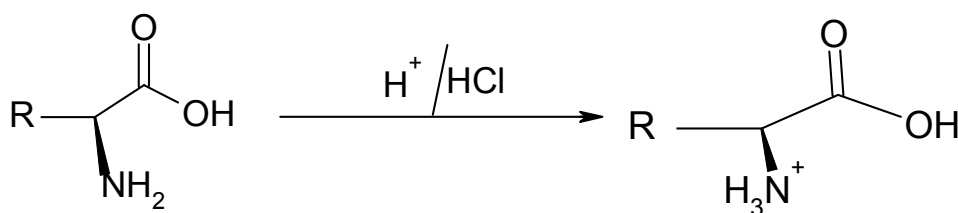
2.2.4. Types of Clay Modifications

A) Interlayer Modification

Interlayer galleries modification in which the MMT clay is treated with a compatibilizing agent as amino acid or alkyl ammonium ions because they can exchange easily with ions between the silicate layers, hence resulting in increasing in the distance between the clay layers [94].

I) Amino Acids

Amino acids are molecules which consists of a basic amino group ($-\text{NH}_2$) and an acidic carboxyl group ($-\text{COOH}$). In an acidic medium, a proton is transferred from the COOH group to the intermolecular $-\text{NH}_2$ group. A cation-exchange is then possible between the $-\text{NH}_3^+$ function formed and a cation such as Na^+ and Ca^{2+} intercalated between the clay layers so that the clay becomes organophilic [97, 99].



II) Alkylammonium Ions

Montmorillonite exchanged with long chain Alkylammonium ions can be dispersed in polar organic liquids, forming gel structures with high liquid content. This property was first discovered by Jordan [100] and summarised later by Weiss [101]. Alkylammonium ions can be intercalated easily between the clay layers and offer a good alternative to amino acids for the synthesis of nanocomposites based on other polymer systems than polyamide 6. The most widely used ammonium ions are based on primary alkyl amines put in an acidic medium to protonate the amine function. Their basic formula is $\text{CH}_3-(\text{CH}_2)_n-\text{NH}_3^+$ where n is between 1 and 18. Alkylammonium ions based on secondary amines have also been successfully used [102]. The cation-exchange process of linear Alkylammonium ions is described in Figure 2-4.

Depending on the layer charge density of the clay, the Alkylammonium ions adopt different structures between the clay layers (Monolayer, bilayer, pseudotrimolecular layers and paraffin type monolayer) [103]. Alkylammonium ions permit to lower the surface energy of the clay so that organic species with different polarities can get intercalated between the clay layers [104].

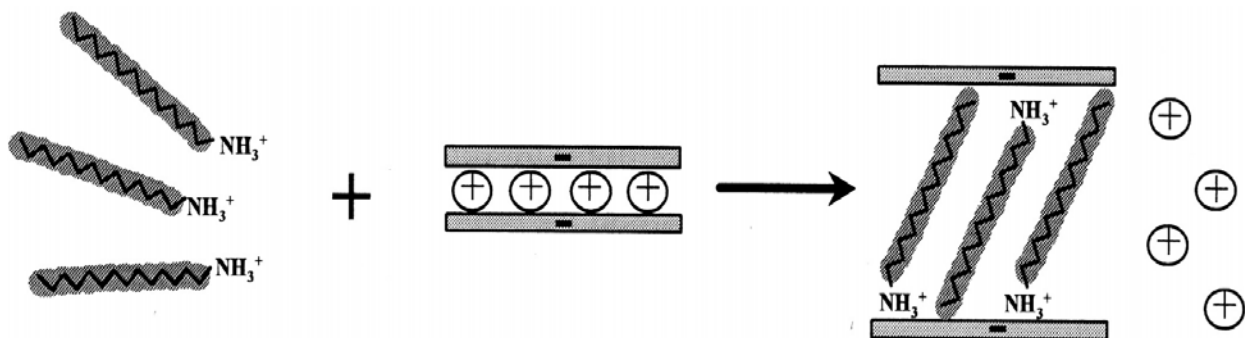


Figure 2.4: The cation-exchange process between Alkylammonium ions and cation initially intercalated between the clay layers.

B) Surface and Edges Modification

Silane coupling agents are used in surface and edges modification to generate an organophilic surface and edges. An interlayer galleries modifier is not enough for MMT surface and edges modification. Although quaternary ammonium ions can adsorb on the MMT surface, this adsorption is unstable [105]. The modification by a

CHAPTER 3

Polymer Layered Silicate Nanocomposites (PLSN)

Polymer layered silicate nanocomposites (PLSN) are commonly defined as the combination of a polymer matrix and nano-reinforcement additives that have at least one dimension in the nanometer range. The nano additives can be one dimensional (examples include nanotubes and fibres), two dimensional (which include layered mineral like clay), or three dimensional (including spherical particles) [108]. Over the past decades, polymer nanocomposites have attracted considerable interests in both academia and industry, owing to their outstanding mechanical properties [37,109,110] like elastic stiffness [111] and strength with only a small amount of additives. This is caused by the effect of large surface area to volume ratio of nano additives when compared to micro- and macro-additives [112]. Other superior properties of polymer nanocomposites include barrier resistance [113], gas permeability [114,115], thermal stability [116], flame retardancy [117], scratch/wear resistance [118] as well as optical [119], magnetic [120] and electrical properties [121].

3.1. Polymer Matrices Used in Layered Silicate Nanocomposites

The large variety of polymer systems used in polymer layered silicate nanocomposites preparation with layered silicate can be conventionally classified as:

3.1.1. Vinyl Polymers

These include the vinyl addition polymers derived from common monomers like methyl methacrylate [122–136], methyl methacrylate copolymers [137–143], acrylic acid [144, 145], acrylonitrile [146–149], styrene (S) [150–177], 4-vinylpyridine [178], acrylamide [179,180], poly(N-isopropylacrylamide) [181] and tetrafluoro ethylene [182]. In addition, selective polymers like PVA [183–187], poly(N-vinyl pyrrolidone) [188–192], poly(vinyl pyrrolidinone) [193,194], poly(vinyl pyridine) [195], poly(ethylene glycol) [196], poly(ethylene vinyl alcohol) [197], poly(vinylidene fluoride) [198], poly(p-phenylenevinylene) [199], polybenzoxazole [200],

poly(styrene-co-acrylonitrile) [201], ethyl vinyl alcohol copolymer [202], polystyrene–polyisoprene diblock copolymer [203, 204] and others [205] have been used

3.1.2. Polyolefin

Polyolefin such as polypropylene (PP) [206–241], polyethylene (PE) [242–250], polyethylene oligomers [251], copolymers such as poly (ethylene-covinyl acetate) (EVA) [24], ethylene propylene diene methylene linkage rubber (EPDM) [252] and poly (1-butene) [253] have been used.

3.2. Morphology of Polymer Layered Silicate Nanocomposites

Silicate morphology refers to the way in which silicate layers are ordered in a PLSN system. A number of distinct silicate morphologies and the effect these structures on the final PLSNs have been identified in literature. The two most common clay morphologies are intercalated and exfoliated [60,254,255]. Additional clay structures include a flocculated morphology and a mixture of both exfoliation and intercalation in the same nanocomposite [203]. As a result of the fact that each silicate morphology type has a significant impact on PLSN properties, tremendous efforts have been made to understand how these structures form and how they can be controlled.

3.2.1. Intercalated

Intercalated clay morphology occurs when polymer chains diffuse into the gallery spacing of layered silicate [25]. The ordered, layered structure of individual tactoids remains, but the presence of polymer chains within gallery spacing forces the silicate layers farther apart. The gallery spacing in intercalated structures are on the order of a few nanometer. An example of intercalated silicate morphology is shown in Figure 3.1. Confining polymer chains in the narrow gallery spacing between layers of silicate results in an entropic loss. In order to make intercalation thermodynamically favourable either an increase in entropy in the surfactants used as surface modifiers must occur, or enthalpic gains must be made. Vaia et al. [151] proposed that the entropic loss due to the confinement of polymer chains must be offset by large numbers of polymer-clay interactions thus making intercalation an enthalpically driven process. The enthalpic change involved with the interaction of polymer chain segments with the surfactant molecules and clay surface is small. To make intercalation favourable a large number of these interactions are necessary. The

kinetics governing the diffusion of polymer chains between silicate layers are an important topic that have the most relevance when polymer and clay are combined using melt processing techniques. Vaia et al. [256] used in-situ x-ray diffraction to monitor the direct intercalation of polystyrene into organoclay galleries. The authors found that the activation energy for polymer diffusion between silicate layers was similar to that measured for polystyrene self diffusion. The implication is that the amount of chain mobility between clay layers is similar to that of chain mobility in the bulk polymer. Prior to this it was thought that the extreme confinement of polymer chains in gallery spacing would limit chain mobility and their rate of diffusion. The knowledge that diffusion leading to intercalation is on the same order of magnitude as polymer self diffusion means that a fully intercalated morphology can be achieved using traditional melt compounding methods.

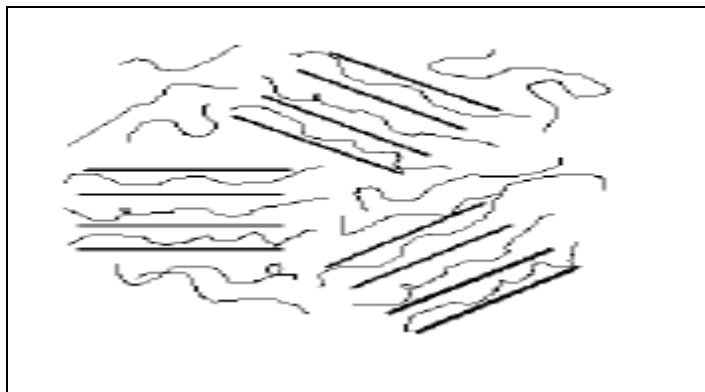


Figure 3.1: Intercalated silicate morphology. Straight lines represent silicate layers while curved lines represent polymer chains.

3.2.2. Exfoliated

An exfoliated structure occurs when silicate layers are separated by regions of polymer matrix at distances on the order of the radius of gyration of the polymer chains [24]. Compared to intercalation the silicate layers are separated by much greater distances. An example of exfoliated silicate morphology is shown in Figure 3.2. An exfoliated structure can maintain a partially oriented state called an ordered exfoliate where layers have localized order despite their separation, or the silicate layers can be in an entirely disordered state called a disordered exfoliate. The benefit of an exfoliated structure is the ability to take advantage of the high aspect ratio of individual silicate layers. An intercalated system can be represented by

effective clay particles made up of multiple clay layers resulting in an effective aspect ratio lower than that of a single clay layer [56]. Exfoliated morphologies maximize polymer/clay contact by obtaining the highest aspect ratio and surface area possible. Boo et al. [57] used alpha zirconium phosphate (α -ZrP) nanoparticles to examine the effect that exfoliation has on the mechanical properties of nanocomposites. α -ZrP particles are well suited to form model systems for layered silicate nanocomposites since their geometry is highly controllable. The length and width of these particles can be controlled to produce particles with a very small distribution of sizes. With thickness dimensions on the order of a single nanometer, α -ZrP is an ideal analog to layered silicate nanoparticles. As a result of the narrow particle size distributions and the relative ease in attaining an exfoliated state, α -ZrP nanocomposites are useful to examine the effect of morphology on layered nanocomposite materials while eliminating a host of other variables. The authors formed nanocomposites with varying levels of exfoliation of α -ZrP and found that the nanocomposite with excellent exfoliation had a 40% improvement in Young's modulus over nanocomposite with poor exfoliation. The model system of α -ZrP particles showed that exfoliation has a large impact on nanocomposites formed using high aspect ratio particles.

Hbaieb et al. [257] also found that mechanical properties of PLSNs are dependent on the morphology of the final composite. The authors compare a 2D and 3D finite element model of PLSNs to the Mori-Tanaka and Halpin-Tsai models developed from composite theory. The results show that as clay volume and weight fraction increase, clay layers collapse to form ordered exfoliates and regions of intercalation. The Mori-Tanaka and Halpin-Tsai models assume complete layer exfoliation. The finite element models incorporate the potential for clay layer collapse. As a result, the 3D finite element estimates for composite modulus fall below those of the composite theory models at increasing clay content. Sheng et al. [56] found with the use of a multi-scale micromechanical model that the advantages of exfoliation may not be as great as expected. The model results show that there is no abrupt stiffness increase due to the formation of exfoliated silicate layers from stacked, intercalated layers. Instead the model predicts a steady, gradual increase in stiffness up to a fully exfoliated state. [258]

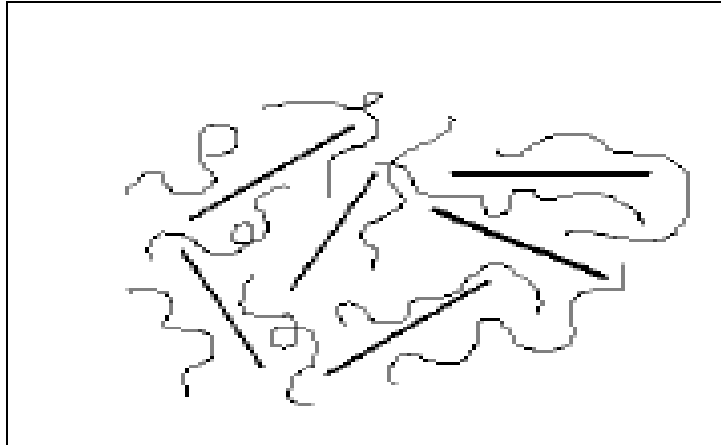


Figure 3.2: Exfoliated silicate morphology. Straight lines represent silicate layers while curved lines represent polymer chains.

3.2.3. Flocculated

A less commonly found clay morphology is flocculation. Flocculation occurs when the edges of silicate layers are attracted to one another end to end. An example of flocculated silicate layers is shown in Figure 3.3. Wu et al. [49] proposed that this structure forms because the edges of layered silicates have unshielded hydroxyl groups that tend to interact with one another. The authors report that the formation of flocculation increases the chance of particle-particle interaction under flow conditions. This behaviour is consistent with what one would expect from an increase in effective particle aspect ratio resulting from the combination of layers in an end to end fashion. It has been reported that flocculation results in a large increase in the aspect ratio of the layered silicate due to the combination of clay layers through end to end hydrogen bonding [25].

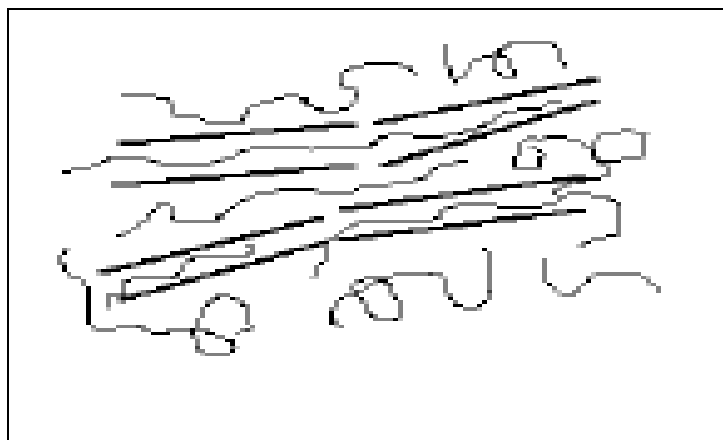


Figure 3.3: Flocculated silicate morphology. Straight lines represent silicate layers while curved lines represent polymer chains.

3.2.4. Intercalated-Exfoliated Mix.

The most common silicate morphology is a mixture of both intercalated clay layers and exfoliation. Clay loading, strength of polymer-clay interaction and the compounding technique used all have an effect on the resulting clay morphology. More often than not, clay morphology is characterized as a point in-between the extremes of intercalation and exfoliation. The various processing methods employed to compound PLSNs including in-situ polymerization, solution mixing and melt compounding have been found to generate composites with varying degrees of exfoliation and intercalation.

3.3. Synthesis of Polymer Layered Silicate Nanocomposites

The methods used in synthesis of nanocomposites have a significant effect on silicate morphology and the resulting composite properties. In addition to property concerns, the processing method employed puts limits on both the type of polymer that can be used and the volume of nanocomposite material that can be produced. Three methods that have been used successfully in producing nanocomposites are in-situ polymerization, solution mixing and melt intercalation. Each method has advantages as well as disadvantages and much research has been devoted to understanding each of them.

3.3.1. In-Situ Polymerization

In In-Situ polymerization, monomer is first mixed with layered silicates and then polymerization takes place. A schematic of this technique is shown in Figure 3.4. Because of the low viscosity of a monomer in comparing to a polymer, it is much easier to break up particle agglomerates using a high shear device, and achieve more uniform mixing of particles in the monomer. In addition, the low viscosity and high diffusivity results a higher rate of monomer diffusion into the interlayer region of layered silicate. Furthermore, it is possible to control nanocomposite morphology through the combination of reaction conditions and clay surface modification. The greatest disadvantage to this technique is the extended processing time as well as the necessity for solvent while polymerization certain types of polymer.

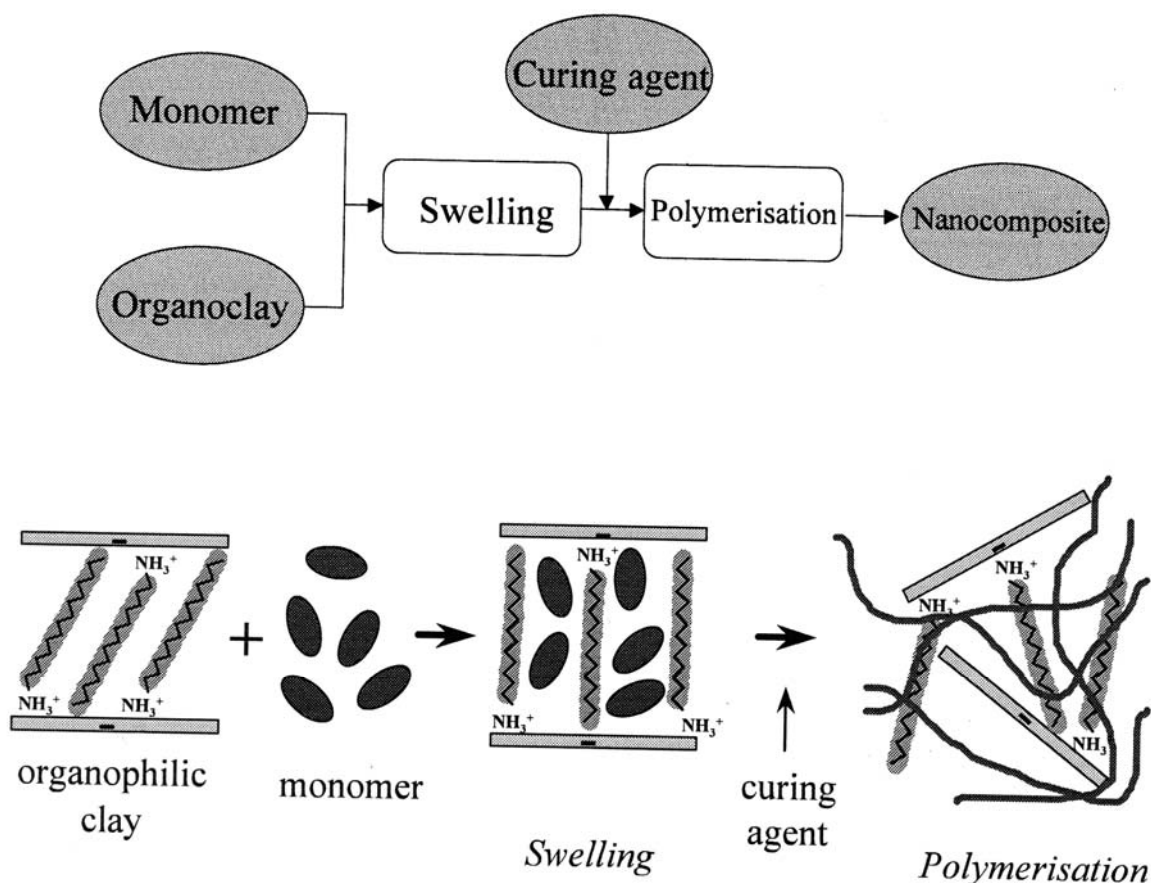


Figure 3.4: Schematic of in-situ polymerization.

In-Situ polymerization has been studied since the 1960s. In most of the early studies, natural clay without surface modification was used. Blumstein et al [259] used both Gamma radiation and initiator (AIBN and BPO) to polymerize MMA / MMT nanocomposite. It was found that PMMA chain can lie flat within the gallery region to form a monolayer. Solomon et al [260-262] did a series study of styrene and MMA polymerization in the presence of different clays as MMT and talc. They conclude that the lewis acidity of the silicate edge has a profound effect on the polymerization. The first systematic study on the polymer layered silicate nanocomposites was done by the research team at Toyota [93, 99]. They prepared nylon 6 nanocomposites via in-situ polymerization using ϵ -caprolactam as a monomer. They used a series of protonated amino acids to modify the layered silicate surface. It was found that with the increase of chain length, the organic ammonium cations could change the orientation from monolayer, bilayer, to paraffin like structure with the tail inclined away from the silicate surface. Nylon 12 clay nanocomposites were also prepared via in-situ polymerization under elevated temperature and pressure, using 12-aminolauryl acid as both the surface modifier and monomer. Intercalated and

partially exfoliated nanocomposites were obtained [263]. Messersmith et al [30] used an approach similar to Toyota to synthesize poly (ϵ -Caprolactam) layered silicate nanocomposites. They also used protonated 12-aminolauryl acid to modify the layered silicate surface. In their study, they did not see gallery expansion upon (ϵ -Caprolactam) intercalation in the gallery region under room temperature. But once heated to an elevated temperature (170°C), they observed significant increase in matrix viscosity, possibly indicating further monomer intercalation and interlayer expansion. After polymerization, the silicate layers were exfoliated in the polymer matrix.

Free radical polymerization is one of the major methods in preparing many industrial important thermoplastic polymers, e.g., polystyrene (PS), acrylic polymers and poly (vinyl chloride) (PVC). In-situ polymerization is also used to prepare nanocomposites based on these polymer matrices. Intercalated PMMA and PS nanocomposites have been synthesized through either emulsion [162, 264] or bulk polymerization [265-266]. It was found that the structural affinity between the styrene monomer and the organic cation played an important role in the PS / clay hybrid structure [159]. By improved dispersion of clay in the PMMA / clay nanocomposites was obtained when MMA was co-intercalated and copolymerized with lauryl metacrylate (LMA). The authors attribute this improvement to a better compatibility of LMA with the organic cation functionalized clay surface [267]. Okamoto et al [140] also reported the polar comonomer played an important role in delaminating clay layers in PMMA. However, there seems to be an optimal polarity as well as the amount of comonomer for exfoliation. Very high polarity or amount of comonomer leads to strong aggregation and flocculation of clay. Akelah et al [268] reported the preparation of polystyrene nanocomposites and it was found the interlayer spacing was affected by solvent used during polymerization. Efforts have also been made to anchor a living free radical polymerization (LFRP) initiator in the interlayer region to improve the interlayer polymerization rate, in order to achieve an exfoliated PS nanocomposite [163]. Chen et al [269] took an interesting approach to prepare PS nanocomposite. The MMT clay is modified by cetyltrimethyl ammonium bromide. Instead of using a styrene soluble initiator, they used a hydrophilic initiator dissolved in water along with sodium dedecyl sulphate as the emulsifying agent. The whole mixture was then polymerized and partially exfoliated nanocomposite was obtained. Recently a suspension polymerization route was adopted by Huang et al [131], using

organoclay as the suspension stabilizer. Three different organics were used to modify the clay surface, a long chain Alkylammonium salt, a cationic free radical initiator and a polymerized ammonium salt. Exfoliation occurred when the second and third organics were used and the author speculated that the growth of polymer from the clay surface being the main driving force. Exfoliation of clay in PMMA was also reported in the emulsion polymerization [130]. It is noteworthy that in Huang work, the polymer is prepared via emulsion polymerization in the presence of polymerized surfactant as the emulsifying agent and thus the polymer particle has a positive charge. Clay is then delaminated in water and mixed with polymer emulsions. It is not necessary to use organic cations to modify clay surface, and the process can occur at room temperature.

To summarize, a wide variety of polymer nanocomposites were synthesized via in-situ polymerization. The silicate layers can be either delaminated first, after which polymerization occurs, or during polymerization by promoting polymer chain growth within the gallery region.

3.3.2. Solution Mixing

In solution mixing, a common solvent or solvent mixture is used to disperse the layered silicate and at the same time, dissolve the polymeric matrix. A schematic of this technique is shown in Figure 3.5. Depending on the interaction of the solvent and the layered silicate, the crystallite may be delaminated in an adequate solvent due to the weak van der Waals force to stack the layer together. Polymer chains then can be adsorbed on the delaminated individual layer. However, upon solvent removal, the layers can reassemble to reform the stack with polymer chains sandwiched in between, forming a well ordered intercalated nanocomposites. Few exfoliated nanocomposites were prepared via this method. Another disadvantage of this method is the large amount of solvent needed, resulting in a higher cost. Also the types of polymers that can be used to prepare nanocomposite ultimately depend on the selection of proper solvent, limiting the applicability of this method.

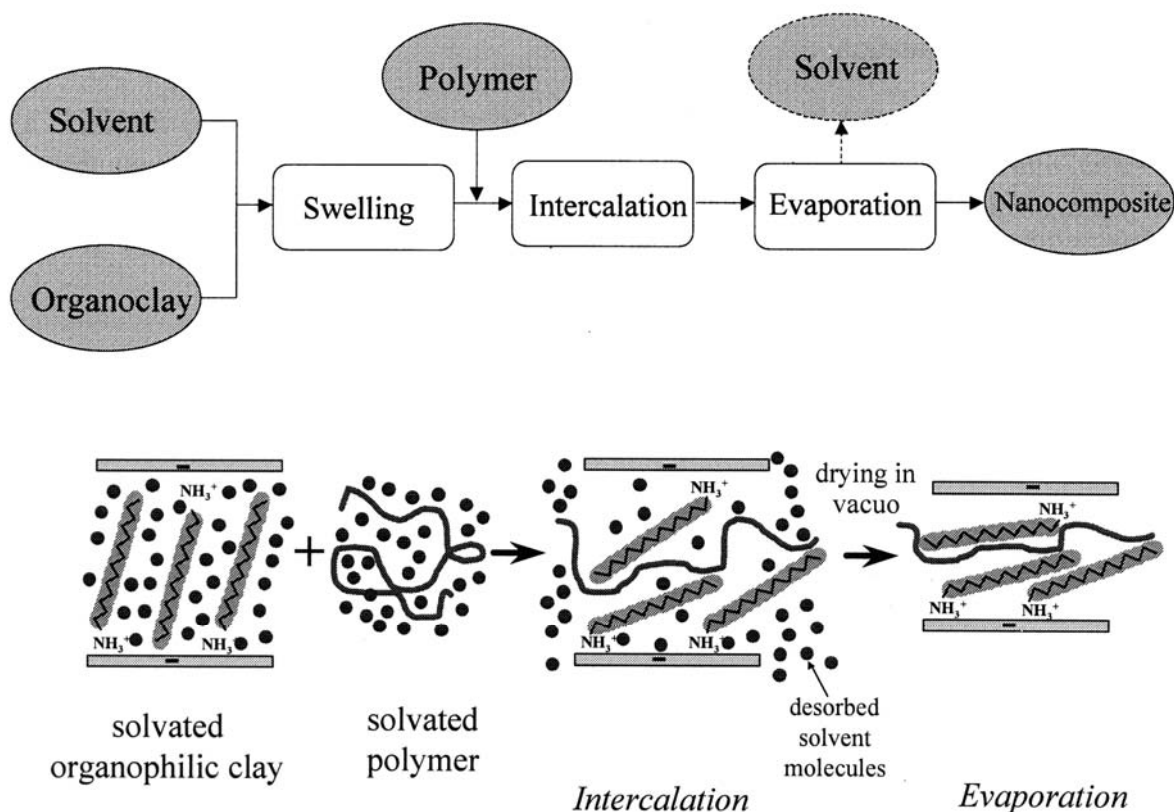


Figure 3.5: Schematic of solution mixing.

Krishnamoorti et al. [60] used solution mixing with a polystyrene-polyisoprene block copolymer in toluene as the solvent. The toluene used as a solvent had to be removed with extensive drying in a vacuum oven at 100°C. The resulting PLSN was comprised of a mixture of intercalated and exfoliated silicate layers as shown by x-ray diffraction. Ding et al [270] prepared PP / MMT nanocomposite by directly dissolving of PP in modified MMT in xylene system at 130 °C. Jeon et al [271] used solution mixing to prepare HDPE / MMT nanocomposite using a co-solvent of xylene-benzonitrile (80-20 wt %) at 110°C. polyethylene oxide (PEO) [197,272-275], polyvinyl alcohol (PVA) [140,163] and polyacrylic acid (PAA) [245] nanocomposites were also prepared via this method.

3.3.3. Melt Intercalation

Melt intercalation involves the combination of layered silicate and polymer at or above the melt temperature of the polymer. When little or no shear history is applied to the PLSN the technique is referred to as direct intercalation [151]. More often the technique is carried out in a mixer or an extruder where shear forces are imparted

into the composite material. The combination of mobile polymer chains and shear force facilitates intercalation when suitable levels of polymer-clay compatibility exist. The relative ease in utilizing this technique has made it the most popular compounding method of the three detailed here. Figure 3.6 shows a simple schematic of melt intercalation. Of the three syntheses of nanocomposites melt intercalation has the advantage of being simple, fast and compatible with current industrial techniques. The primary challenge to melt intercalation that must be overcome is the inability to disperse and fully exfoliate organoclay in certain polymer matrices such as polypropylene.

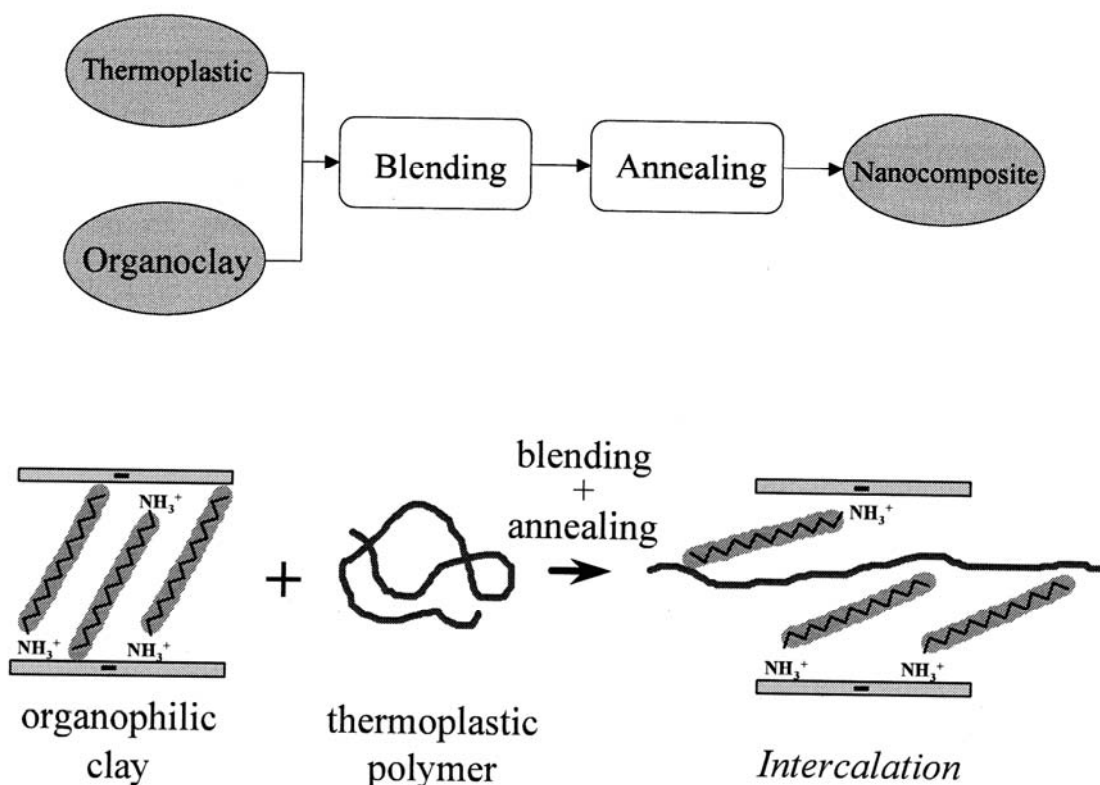


Figure 3.6: Schematic of melt intercalation.

The finding of Vaia et al. [151] that directs intercalation of polymer chains into clay gallery spacing is viable compounding techniques opened up the possibility of melt intercalation. In a follow up paper, Vaia et al. [256] used in-situ x-ray diffraction to determine that the rate of diffusion of polymer chains between silicate layers was on the same order of magnitude as polymer self diffusion. This work showed that melt

intercalation was not only possible but it could be carried out under the same conditions as one would melt process a pure polymer material.

Cho et al. [38] carried out one of the first extensive studies on the effects of melt intercalation conditions on silicate morphology and PLSN properties. Both a single screw and a twin screw extruder were employed to produce polyamide based PLSNs. Results from samples produced using the single screw extruder at 40rpms showed poor exfoliation. A second pass through the single screw extruder was also attempted but poor exfoliation still existed. PLSNs produced using the twin screw extruder showed considerable property improvements as compared PLSNs processed with the single screw extruder. Exfoliation in the twin screw processed PLSN material was found to be extensive after only a single pass. The young's modulus improved over the single screw PLSNs and a 15% increase in yield strength was achieved. The authors used a number of different screw speeds and barrel temperatures in the twin screw extruder to consider the effect these conditions might have on the final PLSN properties. Results showed that material properties remained the same over the full range of processing conditions employed. It is important to note that all of the PLSNs produced using the twin screw extruder showed complete exfoliation. The excellent compatibility of polyamide and the organoclay used may have made it difficult to consider the effect that barrel temperature and screw speed have on the silicate morphology and PLSN properties. A more in depth analysis of the effect of extruder conditions on PLSN properties was carried out by Dennis et al. [53]. A single screw extruder as well as a co and counter rotating twin screw extruder were used in their study. Variable screw speeds and multiple screw configurations were used in order to control the amount of shear and back mixing that occurred during the formation of polyamide-6 based PLSNs. The authors use two commercially available organoclays containing different surfactant modifications in order to obtain the proper degree of polymer/clay compatibility necessary to study the effect of melt processing conditions. Very strong polymer/clay compatibility would dampen the effect of melt processing conditions by resulting in an exfoliated morphology under low shear conditions. In agreement with the findings of Cho et al. [38], PLSN material produced using the single screw extruder showed minimal exfoliation and poor material properties. The twin screw results showed a high degree of variability in exfoliation levels depending on the degree of back mixing and residence time. The results indicate that an optimal level of back mixing

exists and that excessive levels of shear lead to reduced exfoliation and dispersion. The relationship between extruder conditions and silicate morphology is linked by the amount of shear imparted to the PLSN in the melt as well as the transfer of shear throughout the PLSN in the melt. Fornes et al. [37] showed that the molecular weight of the PLSN affects silicate morphology due to the ability of high molecular weight polymers to transfer shear stresses more effectively than low molecular weight polymers. A twin screw extruder was used in the preparation of PLSNs using low, medium and high molecular weight polyamide resins. The low molecular weight PLSNs showed incomplete exfoliation and inferior mechanical properties while the medium and high molecular weight PLSNs showed excellent exfoliation. The differences in exfoliation levels are attributed the trend of increasing melt viscosity and stress transfer ability of the polymer melt with increasing molecular weight. Extruder screw rotational speed is another important melt processing condition. Peltola et al. [42] examined the effect of rotational screw speed on polypropylene based PLSNs. A twin screw extruder was used to produce PLSNs at screw speeds of 200, 500 and 1000rpms. Results show an increase in intercalation and a modest increase in exfoliation with increasing screw speed but no improvement in PLSN mechanical properties are seen. The modest improvements in exfoliation that are seen in TEM images may not have been enough to noticeably alter the mechanical properties of the PLSNs. Modesti et al. [62] carried out an extensive study of the effect of both temperature and screw speed on the morphology and mechanical properties of polypropylene based PLSNs. Screw speeds of 200 and 350 rpms were used in an intermeshing, co-rotating twin screw extruder. The two different melt temperatures employed were approximately 170°C and 200°C. The results of both the silicate morphology tests and the mechanical property test were conclusive in showing that the most effective melt compounding condition was that of low temperature and high screw speed. The authors conclude that conditions which maximize the shear stress exerted on the polymer are the most effective at forming highly dispersed and exfoliated PLSNs. In addition to the effect of temperature and screw speed on silicate morphology, the authors show that the effect of residence time is far less influential in achieving silicate exfoliation than shear stress during processing. This conclusion might be expected since the rate of polymer diffusion into silicate galleries is on the same order as the rate of polymer self diffusion.

In summary, melt intercalation offers a simple way of preparing nanocomposites. However, very careful attention has to be paid to finely tune the layered silicate surface chemistry to increase the compatibility with polymer matrix. Processing conditions have profound effects on the structure evolution of polymer nanocomposites by melt intercalation.

3.4. Characterization of Polymer Layered Silicate Nanocomposites

Identification of the silicate morphology within a PLSN can be accomplished using a number of analytical techniques. The simplest, most common analysis technique used for this purpose is wide angle x-ray diffraction (WAXD). Gallery spacing values can be determined from diffraction peaks and evidence of silicate exfoliation can be seen from peak intensities. In addition to WAXD, an optical image of the silicate morphology can be generated using transmission electron microscopy (TEM). Finally, multiple studies on the rheological properties of PLSNs have attempted to find qualitative relationships between silicate morphology and rheology with limited success.

3.4.1. Wide Angle X-ray Diffraction (WAXD)

X-ray diffraction is a powerful tool for identifying crystalline structures on the nanoscale. WAXD involves the use of x-ray diffraction at low angles between 1 and 10 degrees where reflections are the result of crystalline structures having length dimension on the order of tens of nanometer. WAXD is particularly useful for the identification of intercalated structures due to their nanometer dimensions and their repetitive crystalline order [76]. Exfoliated structures are not visible as peaks in WAXD curves as the lack of system order prevents the constructive interference necessary for peaks in diffraction curves to form.

Intercalated silicate structures are seen in WAXD curves as distinct peaks rising out of a flat baseline curve. The location of the peak with respect to the angle 2θ can be related to the basal spacing of the intercalated silicates using the Bragg equation [27]:

$$2d\sin\theta = n\lambda$$

Where d is the average basal spacing of the silicate tactoids, θ is one half of the 2θ location of the diffraction peak, n is the wave number taken to be 1 and λ is the x-ray

wavelength. The Bragg equation is an effective way to measure the changes that occurs in basal spacing values due to the formation of an intercalated structure. At angles of 2θ between 1 and 15 degrees, basal spacing values calculated from peaks with widths less than 2 degrees of 2θ are expected to have less than 2% error [76].

In addition to reflection peak location relative to 2θ , peak width with respect to 2θ can be a useful characteristic in determining relative silicate tactoid sizes. The full width of a reflection peak measured at half of its maximum intensity (FWHM) can be related to the average tactoid size present in the sample by the Scherrer equation:

$$d' = K\lambda / L \cos\theta$$

Where d' is the value of the FWHM, θ is one half of the peak location at its 2θ value, L is the average tactoid size, k is a proportionality constant equal to approximately 0.93 [276, 277] and λ is the x-ray wavelength. Calculation of the average tactoid size combined with basal spacing information attained from the Bragg equation allows for calculation of the average number of silicate layers per tactoid [278]. The accuracy of the Scherrer equation in determining the correct average silicate tactoid size in layered silicates has been shown to be poor in past literature [279]. The nature of this inaccuracy is primarily due to experimental conditions which skew the size results in one direction. By maintaining the same experimental conditions, the precision of tactoid size values calculated from the Scherrer equation allows for semi-quantitative tactoid size comparisons between multiple samples.

In addition to the effect of particle size on the FWHM, crystalline disorder can have a measureable effect on the FWHM [280]. Disorder in silicate layer structure can be in the form of bent silicate layers or irregularities in the chemical structure. The flexible nature of the silicate layers makes it possible to have bends or folds in the layers. The irregular geometry of these bent layers has been shown to increase the FWHM of diffraction peaks. The individual contributions of particle size and crystal structure disorder to FWHM broadening can be isolated if higher orders of the same diffraction peak are present in the WAXD curve [276]. Diffraction peaks that occur from wave numbers (n) greater than 1 are higher order peaks that are less intense than primary peaks. These higher order peaks are more sensitive to crystal structure disorder and often cannot be resolved due to high levels of FWHM broadening.

3.4.2 Transmission Electron Microscopy (TEM)

Images generated using TEM can be used to confirm results obtained from WAXD. The primary advantage of TEM over WAXD is the ability to confirm the presence of exfoliation in a PLSN sample. WAXD can be strongly affected by particle size, sample preparation, silicate concentration and sample orientation. WAXD curves indicating exfoliation can be the result of low silicate concentration or poor sample preparation. In the case of a WAXD curve indicating exfoliation, TEM can be used to confirm the presence of exfoliation. A severe limitation to the use of TEM is the highly localized nature of the images that are obtained. The extremely high magnification of TEM means the operator must choose a representative image for the entire sample from only a very small portion of the actual sample. For this reason, levels of intercalation and exfoliation can be highly variable if obtained from TEM images.

3.4.3 Rheology

The rheology of PLSNs has been studied for a wide variety polymer and filler types. The primary characteristic of interest in rheological studies is the formation of yield stress behaviour during dynamic oscillatory rheological testing. Krishnamoorti et al. [281] found increasing yield stress behaviour in polyamide-6 PLSNs with increasing silicate loading. This behaviour was attributed primarily to the tethering of polyamide chains to the surface of the layered silicate. Lim et al. [282] used dynamic oscillatory shear in the linear viscoelastic regime of three different polymer systems in an attempt to identify the behaviour of exfoliated and intercalated PLSNs. In agreement with previous studies the authors found an increase in yield behaviour with clay loading. It was also found that for exfoliated silicate morphologies yield stress behaviour was caused by the formation of a percolated network structure. Intercalated PLSNs showed yield like behaviour at low frequencies only when strong interactions between the polymer and silicate existed. Li et al. [43] found similar results in their study of polypropylene based PLSNs. A percolated network structure appeared to form at 3 wt% silicate loading in polypropylene due to particle-particle interactions among the silicate tactoids. Non-linear rheology using steady shear showed that the percolated network structure can be destroyed when the silicate layers become preferentially aligned in the flow direction. Letwimolnun et al. [283] attempted to use yield stress values to quantify the level of exfoliation present in a

PLSN system. The results showed that there is a relationship between yield stress and exfoliation but the models that were implemented in an attempt to quantify this relationship failed to describe the experimental results.

The use of rheology in characterizing PLSN systems has led to an improved understanding of how silicate layers interact with themselves as well as the polymer matrix. Polymer chains that are highly compatible with the silicate surfaces tether to the silicate layers and create a percolated network structure that is responsible for the yield like behaviour seen at low frequencies during dynamic oscillatory rheological testing. At higher clay loadings beyond a percolation threshold, particle-particle interactions between silicate tactoids may also contribute to the formation of a yield stress. Under strong shear forces in the non-linear viscoelastic regime, the preferential orientation of silicate layers has been observed. The alignment of silicate layers destroys any network structure that exists and eliminates yield like behaviour upon further testing. Efforts to quantify the level of exfoliation in a PLSN using rheology have not been successful. Qualitative conclusions based on previous studies and our current understanding of the formation of percolated networks in PLSNs can be made.

3.5. Properties of Polymer Layered Silicate Nanocomposites

Layered silicates have provided tremendous property enhancement of the polymer matrices. A number of material properties where enhancements have been reported in the literature include tensile modulus [23, 278], flexural modulus [23, 27, 62], thermal degradation [24, 26, 29, 58, 68, 284,], heat distortion temperature [26, 27] and barrier ability [30, 58].

3.5.1. Young's Modulus

Kojima et al. [23] was the first to record significant improvements in the tensile modulus of PLSNs over their neat polymer matrices. A 69% increase in tensile modulus was realized in a polyamide based PLSN containing 4.7 wt% layered silicate. The authors also found that the length or aspect ratio of the layered silicate used has a significant effect on the tensile modulus of the final PLSN. The tensile property improvements are attributed to increases in the amount of constrained region in the PLSN due to the presence of the layered silicate. The constrained region includes all portions of the PLSN that are not amorphous and is shown to

increase with both silicate loading and length. Estimations of the constrained region correlate well with improvements in physical properties that are realized.

Galgali et al. [278] studied the effect of silicate orientation as well as polymer/clay compatibility on the tensile modulus of polypropylene based PLSNs. Using 2D x-ray diffraction to quantify the amount of silicate orientation the authors found a strong correlation between the tensile moduli and the average silicate orientation present in the samples. The polymer/clay compatibility was altered in some samples by the addition of an isotactic polypropylene-g-maleic anhydride compatibilizer. It was found that samples containing compatibilizer had average silicate orientations that were dependent on the amount of shear they were exposed to during melt compounding. The tensile modulus of the compatibilized samples correlated very well with the average silicate orientation resulting in large modulus improvements. The uncompatibilized samples had average silicate orientations that were independent of the amount of shear they were exposed to during melt compounding. As a result, no improvement in the tensile modulus of the uncompatibilized samples with increasing shear exposure was found.

3.5.2 Flexural Modulus

Modesti et al. [62] found that improvements in the flexural modulus were highly dependent on melt compounding conditions. Using a compatibilized polypropylene a 35% increase in the flexural modulus was realized over the neat polymer matrix.

Uncompatibilized polypropylene PLSNs showed a maximum increase of 26% over the neat polymer matrix. This difference in improvements between the uncompatibilized and compatibilized samples was attributed primarily to improvements in polymer/clay compatibility. The authors propose that improvements in polymer/clay interaction should decrease polymer chain mobility and increase the stiffness of the material.

3.5.3. Thermal Degradation

Materials with high moduli and high thermal degradation temperatures are valuable as potential parts in high performance automotive applications. Vaia et al. [284] studied the ablation performance of polyamide-6 based PLSNs. It was found that the degradation kinetics was unaltered by the presence of layered silicate but the ablation performance increased. The addition of layered silicate in amounts as small

at 2 wt% resulted in over an order of magnitude decrease in the rate of mass loss as compared to neat polyamide. This behaviour was attributed to the formation of char on the surface of the PLSN during exposure to high temperature air. The inorganic char is said to be responsible for decreasing degradation by insulating the material beneath it. In addition to having insulating properties, the uniform char formation makes the diffusion of volatile degradation products out of the sample more difficult by increasing the tortuosity of the sample.

Pramoda et al. [29] also used polyamide-6 to examine the thermal degradation behavior of PLSNs. The results showed that the presence of silicate did not affect the type of gas evolved during thermal degradation. The onset temperature for thermal degradation however, was 12°C higher for the PLSN containing 2.5 wt% silicates than the neat polyamide-6. The authors also found that the state of exfoliation has a significant effect on the thermal degradation tendency of the PLSNs. Composites only showed an increase in thermal degradation temperature when they contained an exfoliated silicate morphology. Agglomerated clay particles did not alter the thermal stability of the PLSNs. The behavior seen in this study can be attributed to silicate layers acting as barriers to the diffusion of volatile degradation products out of the PLSN samples.

3.5.4 Heat Distortion Temperature (HDT)

Limiting the amount of deformation a material undergoes when exposed to heat is important for many applications that involve high temperatures. Ke et al. [26] found that the addition of 5 wt% layered silicate to a poly (ethylene terephthalate) (PET) matrix caused a 40°C increase in the heat distortion temperature (HDT). This dramatic increase in the HDT is attributed to the confinement of polymer chains between silicate layers. The extreme confinement of the polymer chains decreases their ability to move freely. The authors claim that the observed increase in the HDT is a direct result this reduction in chain mobility.

Wang et al. [27] also found improvements in the HDT of PET PLSNs. At a 1 wt% silicate loading a 35°C increase in the HDT was found. The HDT increased with the addition of layered silicate until a 49°C improvement in HDT was realized for a 5 wt% silicate loading PLSN over the neat polymer matrix. The authors do not point to a single reason for this behavior but instead suggest that it could be the result of both

increased crystallinity and a loss of polymer chain mobility due to extreme confinement between silicate layers.

3.5.5 Barrier Property Improvements

Adding high aspect ratio particles to a polymer matrix dramatically increases the tortuosity of a membrane formed from that polymer material. Engineering polymers with improved barrier properties have the potential for use in industrial, military and packaging applications. Ray et al. [58] examined the Oxygen permeability coefficient of poly (butylene succinate) (PBS) based PLSNs as a function of clay loading. The results show a monotonic decrease in the permeability of Oxygen with an increase in silicate loading. The decrease in permeability is the result of an increase in tortuosity of the PBS membrane due to the presence of layered silicate. At a silicate loading of 3.6 wt% there is a steep drop in the Oxygen permeability that the authors attribute to the formation of a flocculated structure. In order to achieve the maximum increase in tortuosity possible, an exfoliated structure must be achieved. Intercalated tactoids are far less effective at limiting the diffusion of small molecules through a PLSN membrane.

CHAPTER 4

Grafting of Vinyl Monomers Nanocomposites onto Cotton Fabric

4.1. Cotton Fabric:

The first use of natural fibres in composite systems was from 3000 years ago in the ancient Egypt, where straw and clay were used together to build walls. In the past decade an enormous interest in the development of new composite materials with natural fibres has been shown by important industries such as the automotive, construction or packaging industry.

Compared to inorganic fibres, natural fibres present some advantages such as lower density and lower price, they are less abrasive to the processing equipment, harmless, biodegradable, renewable, and their mechanical properties can be comparable to those of inorganic fibers [286-291]. All these properties have made natural fibres very attractive for industries like the automotive industry, that search a product with mechanical properties comparable with glass fibre reinforced thermoplastics, but lighter and harmless to workers.

Cotton fibers are the purest form of cellulose, nature's most abundant polymer. Nearly 90% of the cotton fibers are cellulose. All plants consist of cellulose, but to varying extents. Bast fibers, such as flax, jute, ramie and kenaf, from the stalks of the plants are about three-quarters cellulose. Wood, both coniferous and deciduous, contains 40–50% cellulose, whereas other plant species or parts contain much less cellulose. The cellulose in cotton fibers is also of the highest molecular weight among all plant fibers and highest structural order, i.e., highly crystalline, oriented and fibrillar. Cotton, with this high quantity and structural order of the most abundant natural polymer. [292].

4.1.1. Chemical Composition

Cotton fibers are composed of mostly α -cellulose (88.0–96.5%) [293]. The noncellulosics are located either on the outer layers (cuticle and primary cell wall) or inside the lumens of the fibers whereas the secondary cell wall is purely cellulose. The specific chemical compositions of cotton fibers vary by their varieties, growing environments (soil, water, temperature, pest, etc.) and maturity. The noncellulosics

include proteins (1.0–1.9%), waxes (0.4–1.2%), pectins (0.4–1.2%), inorganics (0.7–1.6%), and other (0.5–8.0%) substances. In less developed or immature fibers, the non-cellulosic contents are much higher. The primary cell walls of cotton fibers contain less than 30% cellulose, noncellulosic polymers, neutral sugars, uronic acid, and various proteins [293, 295]. The cellulose in the primary cell walls has lower molecular weight, with the degree of polymerization (DP) between 2,000 and 6,000 and their distributions are broader [296]. The secondary wall of the cotton fibre is nearly 100% cellulose. The DP of the cellulose in the secondary wall is about 14,000, and the molecular weight distribution is more uniform [297]. The high molecular weight cellulose characteristic of mature cotton has been detected in fibers as young as eight days old. In the later stage of elongation or 10–18 days following initiation, the higher molecular weight cellulose decreases while the lower-molecular weight cell wall components increase, possibly from hydrolysis [298]. Between the ages of 30 and 45 days, the DPs estimated from intrinsic viscosities of fibers have been shown to remain constant [299]. Of the non-cellulosic components in the cotton fibers; the waxes and pectin are most responsible for the hydrophobicity or low water wettability of raw cotton fibers. The term ‘cotton waxes’ has been used to encompass all lipid compounds found on cotton fibre surfaces including waxes, fats, and resins [300]. True waxes are esters, including gossypyl carnaubate, gossypyl gossypate, and montanyl montanate. Alcohols and higher fatty acids, hydrocarbons, aldehydes, glycerides, sterols, acyl components, resins, cutin, and suberin are also found in the wax portion of the cuticle in varying quantities. Pectins are composed primarily of poly (b-1,4- polygalacturonic acid) and rhamose to make up the rhamnogalacturonan backbone [301]. The side chains are composed of arabinose, galactose, 2-O-methylfucose, 2-O-methylxylose and apiose. Eighty-five percent of the polygalacturonic acid groups are methylated leading to a highly hydrophobic substance. Proteins are located primarily in the lumen, but small amounts of hydroxyproline rich proteins are present on the fibre surface [302]. The far lower extents of the non-cellulosics than cellulose make their detection in mature cotton fibers challenging. Extraction and reaction techniques are often employed to separate the non-cellulosic cell wall components for characterization. These procedures, however, tend to disrupt their organization and possibly alter their chemical compositions. The amounts of the noncellulosic components change during fibre elongation and the transition from primary to secondary wall. Some of

the protein constituents (enzymatic, structural or regulatory) are unique to cotton fibre cells and have been found to be developmentally regulated [303]. The non-cellulosic constituents in developing cotton fibers through the onset of secondary cell wall synthesis can be clearly identified by analytical techniques, including FTIR/ATR, DSC, TGA, and pyrolysis-GC/MS methods [304]. The waxy compounds in developing fibers up to 17 days old are detected by their melting endotherms in the DSC. Pectin can be detected by FTIR in the 14-day-old as well as the mature fibers. FTIR/ATR measurements indicated the presence of proteins in developing fibers up to 16 dpa. The presence of proteins can be measured by FTIR/STR methods in up to 16-day-old fibers and by pyrolysis-GC/MS in up to 14-day-old fibers. Only pyrolysis-GC/MS could detect the presence of the non-cellulosic compounds in 27-days-old fibers. The detection of the non-cellulosics diminished as the proportion of cellulose rapidly increased at the onset of secondary cell wall synthesis. The presence of hydrophobic compounds on the surfaces of cotton fibers of all ages and their removal by alkaline scouring are easily determined by their water contact angles. Among the inorganic substances, the presence of phosphorus in the form of organic and inorganic compounds is of importance to the scouring process used to prepare fibers for dyeing. These phosphorus compounds are soluble in hot water, but become insoluble in the presence of alkali earth metals. The use of hard water, therefore, can precipitate alkali earth metal phosphates on the fibers instead of eliminating them [305].

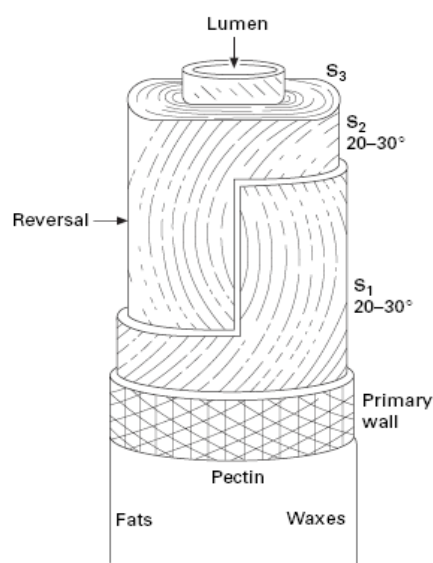


Figure 4.1 Representation of the structure of a cotton fibre.

4.1.2. Cotton Morphology

From a physical viewpoint the cellulose molecule is a ribbon-like structure of linked six-membered rings with hydroxyl groups projecting out in the plane of the ribbon. The covalently bonded chain molecule is further stiffened by internal hydrogen bonds, which, as shown in Figure 4-2 (a), parallel the oxygen bridges between the rings. In tension, the molecule has high modulus and high strength, and it has high rigidity for bending in the plane; but it can easily twist or bend out of the plane. As discussed by Rouselle [306], exact determination of molecular weight (MW) is difficult, because of the problems of dissolving cellulose. The use of a new solvent after a pre-(mercerisation) swelling treatment of cotton print cloth shows a distribution of molecular weights with a peak at 2×10^5 and most values between 10^4 and 5×10^6 ; the peak value corresponds to a chain length of about 0.5 mm with a molecular aspect ratio of about 1000:1. Timpa and Ramey [307] report higher values of molecular weight.

Cellulose crystallises with lattices in which hydrogen bonds between hydroxyl groups link the molecules into sheets, Figure 4-2 (a); between the sheets, there are weaker van der Waals forces. Natural cellulose fibres, including cotton, have a crystal lattice known as cellulose I, which differs from cellulose II in cellulose regenerated from solution or treated with a strong swelling agent. The classical X-ray diffraction studies of Meyer and Misch [308] proposed a unit cell for cellulose I, with 1.03 nm for two repeats along the chain axis, 0.835 nm for spacing between neighbouring chains in the sheets, and 0.79 nm between two equivalent sheets, which are separated by a staggered sheet of anti-parallel chains. Only small variations in the size of the unit cells have been proposed by other workers. However, the question of whether the chains were parallel or anti-parallel was controversial. Sarko and Muggli [309] made a more detailed study of Valonia cellulose. They found that the chains were all aligned in the same direction in the cellulose I lattice. Since there were no differences from the pattern for cotton and ramie, except those attributable to the larger crystallite size in Valonia, they inferred that the cotton crystal lattice had the same cellulose I lattice, containing staggered sheets of parallel chains. There are minor differences in unit cells proposed around the same time by other studies [310]. Figure 4-2 (b), which is a modification of the Meyer and Misch lattice, shows the features essential to an understanding of the role of crystalline cellulose in cotton. Unlike the monomeric glucose molecules, the crystals do not dissolve in water, but

can be disrupted by caustic soda and some solvents. In growing cells, cellulose is synthesised by the condensation of glucose molecules at enzyme complexes, each of which generates 30 cellulose molecules. These naturally lie in the same direction and crystallise into long microfibrils, which are about 7 nm in width. In this sense, natural cellulose can be regarded as virtually 100% crystalline. The evidence, from moisture absorption, density, X-ray diffraction and other techniques that cotton is about 2/3 crystalline can be explained by the imperfect packing of the microfibrils, which are normally separated by absorbed water. X-ray diffraction of ground cotton fibres gives crystallinity values of 92.6 to 94.7% [307].

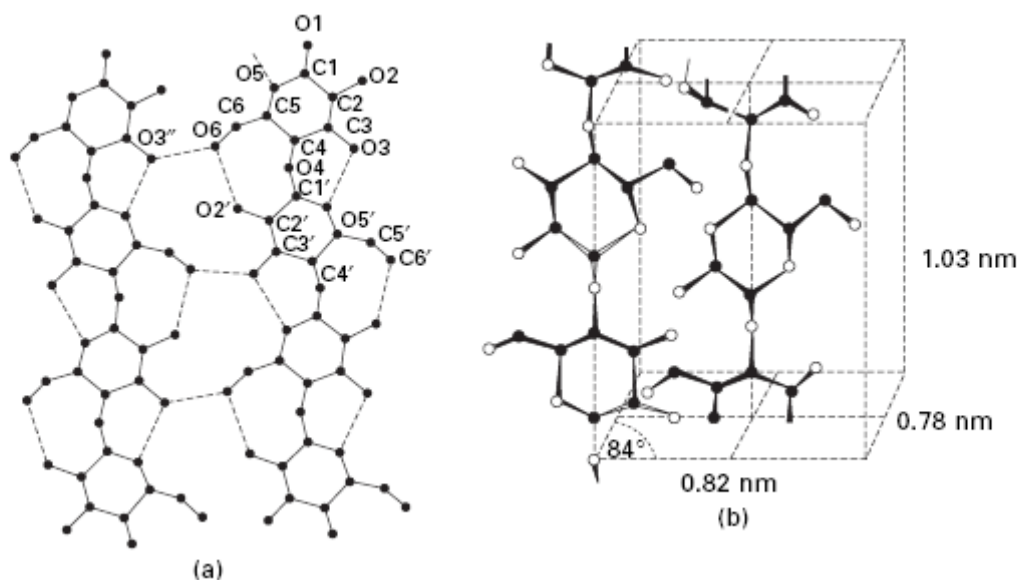


Figure 4.2 (a) Assembly of cellulose molecules in a sheet. C1, O1, etc., are positions of carbon and oxygen atoms; hydrogen atoms complete the valences; hydrogen bonds are shown by dotted lines. [310]. (b) A schematic view of the crystal lattice of cellulose I, adapted from the drawing by Meyer and Misch [308], which had anti-parallel chains. Hydrogen bonded sheets are in the plane of the paper. The sheets in the middle of the cell are staggered with respect to those on the front and back faces.

4.1.3. Cellulose Chemistry and Reactions

Cotton cellulose is highly crystalline and oriented. Cellulose is distinct in its long and rigid molecular structure. The β -1, 4-D (+)-glucopyranose building blocks in long cellulose chain are linked by 1, 4-glycosidic bonds. The steric effects prevent free rotation of the anhydrogluco-pyranose C-O-C link. Each anhydroglucose contains three hydroxyl groups, one primary on C-6 and two secondary on C-2 and C-3. The abundant hydroxyl groups and the chain conformation allow extensive inter-

molecular and intra-molecular hydrogen bonding to further enhance the rigidity of the cellulose structure.

Chemical reactions and heating effects on cotton cellulose depends on the supermolecular structure as well as the activity of the C-2, C-3 and C-6 hydroxyl groups. Heat or reactions begin in the more accessible amorphous regions and the surfaces of crystalline domains. Chemical reactivity of the cellulose hydroxyl groups follow those of aliphatic hydroxyl groups, i.e., higher for the C-6 primary than the secondary on the C-2 and C-3. Etherification and Esterification are the two main categories of reactions. Esterification reactions, such as nitration, acetylation and phosphorylation are usually carried out under acidic conditions. Etherification, on the other hand, is favoured in an alkaline medium. Cellulose is readily attacked by oxidizing agents, such as hypochlorites, chlorous, chloric, and perchloric acids, peroxides, dichromate, permanganates, periodic acid, periodate salts, and nitrogen tetroxide [311]. Most oxidizing agents are not selective in the way they react with the primary and secondary hydroxyl groups. Oxidation of cellulose can lead to two products, reducing and acidic oxycellulose. In reducing oxycellulose, the hydroxyl groups are converted to carbonyl groups or aldehydes, whereas in acidic oxycellulose, the hydroxyl groups are oxidized to carboxyl groups or acids. The oxycellulose can be further oxidized to acidic oxycellulose.

Reducing oxycellulose is more sensitive to alkaline media and the chain lengths are often reduced. Periodic acid and periodate salts break the anhydroglucose ring between C-2 and C-3, converting the two secondary hydroxyl to aldehydes which can be further oxidized to carboxyl groups. Nitrogen tetraoxide reacts specifically with the primary hydroxyl groups on C-6, oxidizing it to carboxyl group directly forming polyglucuronic acid.

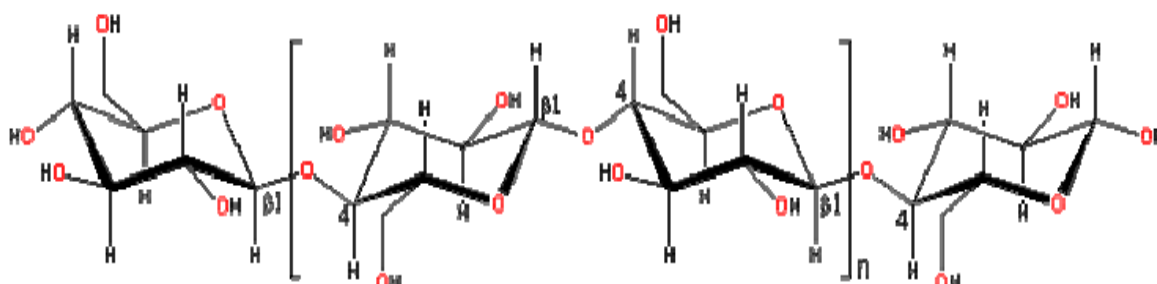


Figure 4.3 Molecular structure of cellulose

4.2. Grafting

Graft co-polymerization is an attractive method to impart a variety of functional groups to a polymer.

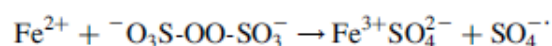
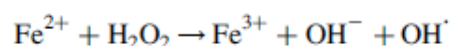
4.2.1. Grafting Method

4.2.1.1. Grafting Initiated by Chemical Technique

4.2.1.1.1. Free-radical Grafting

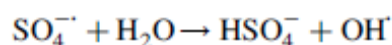
In the chemical process, free radicals are produced from the initiators and transferred to the substrate to react with monomer to form the graft co-polymers. In general, one can consider the generation of free radicals by indirect or direct methods.

An example of free radicals produced by an indirect method is the production through redox reaction, M^{n+}/H_2O_2 , Persulphates [312-316]:

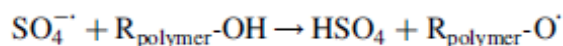


It may be observed that the active species in the decomposition of H_2O_2 and potassium-persulphate induced by Fe^{2+} are OH^- and $SO_4^{\cdot-}$ respectively.

There are different views regarding the activity of $SO_4^{\cdot-}$. Some authors reported that initially formed $SO_4^{\cdot-}$ reacts with water to form OH^\cdot , subsequently producing free radicals on the polymeric backbone:

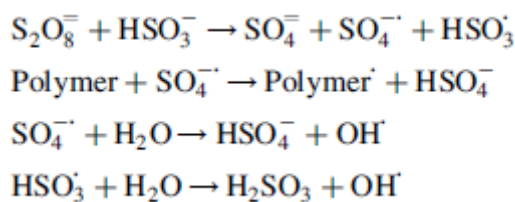


An alternate view is that $SO_4^{\cdot-}$ reacts directly with the polymeric backbone (e.g. cellulose) to produce the requisite radicals

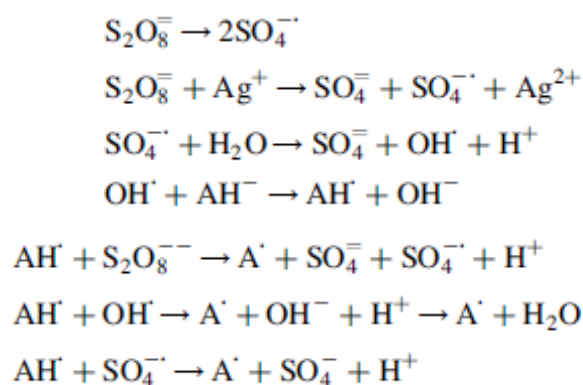


However, Misra et al. [29] established that during grafting of vinyl monomers onto wool/cellulose, OH^\cdot reacts faster than $SO_4^{\cdot-}$.

Similar electron transfer reaction may also occur when organic hydroperoxides, persulphates, Fe^{3+} , Cu^{2+} , etc. are used in place of H_2O_2 together with a reducing reagent such as sodium bisulphite, thiosulphate or Ag^+ :



Bajpai et al. [317] reported peroxydisulphate–ascorbic acid initiated graft co-polymerization. In this case, the reaction between peroxydisulphate and ascorbic acid involves chain reaction catalyzed by Ag^+ , because of the production of sulphate ion radicals, which are well-known chain carriers



Where AH refers to ascorbic acid.

It is apparent from the above that $\text{SO}_4^{\bar{\cdot}}$ or AH^{\cdot} may initiate graft co-polymerization by hydrogen abstraction from a polymer chain.

4.2.1.1.2. Grafting Through Living Polymerization

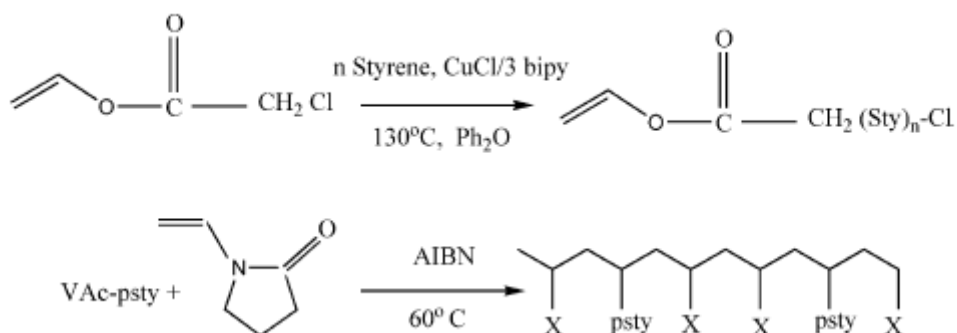
In recent years, methods of ‘Living Polymerization’ have developed to provide a potential for grafting reactions. The most plausible definition of a ‘living polymer’ is ‘that retains their ability to propagate for a long time and grow to a desired maximum size while their degree of termination or chain transfer is still negligible’ [318]. Controlled free-radical polymerizations combine features of conventional free-radical and ionic polymerizations. Conventional free-radical polymerization requires continuous initiation, with termination of the growing chain radicals in coupling or disproportionation reactions, and as a result leads to unreactive (‘dead’) polymers and essentially time invariant degrees of polymerization and broad molecular weight distribution. In case of a living polymerization, it provides living polymers with regulated molecular weights and low polydispersities [319–326].

Controlled free-radical polymerization may be effective through ATRP. ATRP of styrene and various methacrylates has been reported, using various catalytic

systems [327, 328]. In that method, dormant chains are capped by halogen atoms, which are reversibly transferred to metal complexes in the lower oxidation state. This generates the transient growing radicals and complexes in the higher oxidation state. The key reaction of ATRP is the activation–deactivation dynamic equilibrium process.

As controlled radical polymerization involves (essentially) simultaneous initiation of individual growing polymer chains with negligible transfer or termination and simultaneous growth (or fast exchange of the active growing species) between all polymer chains, it is the most suitable technique for the synthesis of gradient copolymers. The technique has also proved its potential for the preparation of molecular brushes, i.e. high grafting density polymer, using a ‘grafting from’ approach. It has been used successfully to prepare molecular brushes with methacrylate or polystyrene backbones and various polyacrylates, polymethacrylates and polyethylene side chains [329–332].

The ATRP/controlled living radical polymerization technique would provide an excellent means of expanding the versatility of macromonomer method, as it increases the number of monomers available for making macromonomers and the ease with which they can be made. Grafting through using macromonomers from PVE, PMMA, PDMS, PLA, PE and PS has been reported [333–338]. A reaction scheme using polystyrene is presented as follow:



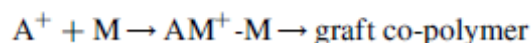
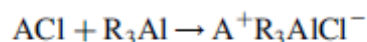
Vinyl acetate–polystyrene macromonomer is prepared via ATRP and then copolymerized with NVP by a conventional free-radical polymerization. Both steps can be performed by the combination of two living polymerization steps for poly (n-butyl acrylate)-graft-ranched polyethylene [339].

Surface grafting by controlled radical polymerization has been reported from polymeric substrates, colloidal particles and inorganic materials [340–349].

For example, Carlmark and Malmstroem [348] immobilized 2-bromoisobutyryl bromide by reaction with the hydroxyl groups on the filter paper. Then, grafting is accomplished by immersing the modified paper into a reaction mixture containing methyl acrylate, Cu(I)Br, tris 2-(dimethyl amino)ethyl amine, sacrificial initiator and ethyl acetate.

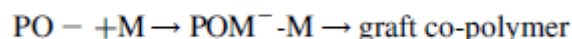
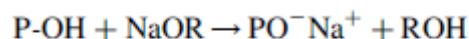
4.2.1.1.3. Ionic Grafting

Grafting can also proceed through an ionic mode. Alkali metal suspensions in a Lewis base liquid, organometallic compounds and sodium naphthalenide are useful initiators in this purpose. Alkyl aluminum (R_3Al) and the backbone polymer in the halide form (ACl) interact to form carbonium ions along the polymer chain, which leads to copolymerization. The reaction proceeds through cationic mechanism.



Cationic catalyst BF_3 can also be used.

Grafting can also proceed through an anionic mechanism. Sodium–ammonia or the methoxide of alkali metals form the alkoxide of polymer ($PO^- Na^+$), which reacts with monomer to form the graft co-polymer.



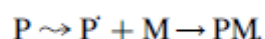
4.2.1.2. Grafting Initiated by Radiation Technique

4.2.1.2.1. Free-radical Grafting

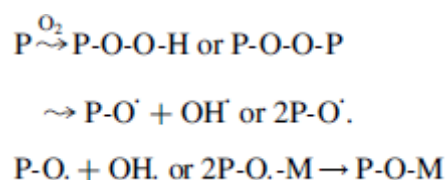
The irradiation of macromolecules can cause homolytic fission and thus forms free radicals on the polymer. In the radiation technique, the presence of an initiator is not essential. The medium is important in this case, e.g. if irradiation is carried out in air, peroxides may be formed on the polymer. The lifetime of the free radical depends upon the nature of the backbone polymer. Grafting proceeds in three different ways: (a) pre-irradiation (b) peroxidation and (c) mutual irradiation technique. In the pre-irradiation technique [350–354], the polymer backbone is first irradiated in vacuum or in the presence of an inert gas to form free radicals. The irradiated polymer substrate is then treated with the monomer, in liquid or vapour state or as a solution in a suitable solvent. In the peroxidation grafting method, the trunk polymer is subjected

to high-energy radiation in the presence of air or oxygen to form hydroperoxides or diperoxides, depending on the nature of the polymeric backbone and the irradiation conditions. The stable peroxy products are then treated with the monomer at higher temperature, whence the peroxides undergo decomposition to radicals, which then initiate grafting. The advantage of this technique is that the intermediate peroxy products can be stored for long periods before performing the grafting step. On the other hand, with the mutual irradiation technique, the polymer and the monomers are irradiated simultaneously, to form free radicals and subsequent addition [355–361]. Since the monomers are not exposed to radiation in the preirradiation technique, the obvious advantage is that the method is relatively free from homopolymer formation, which occurs with the simultaneous technique. However, the decided disadvantage of the preirradiation technique is scission of the base polymer due to its direct irradiation, which can result in the formation of block co-polymers. These processes are represented through simple mechanisms described below.

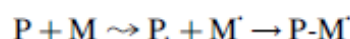
(a) Grafting (pre-irradiation)



(b) Grafting (peroxidation)



(c) Grafting (mutual irradiation)



4.2.1.2.2. Ionic Grafting

Radiation grafting can also proceed through an ionic mode, with the ions formed through high-energy irradiation. Ionic grafting may be of two different types: cationic or anionic. The polymer is irradiated to form the polymeric ion, and then reacted with the monomer to form the grafted co-polymer. The potential advantage of the ionic grafting is high reaction rate. Thus, small radiation doses are sufficient to bring about the requisite grafting.

Radiation induced grafting differs from chemical initiation in many aspects. In a mechanistic way, as in a radiation technique the initiator is not required, free radical formation is on the backbone polymer/monomer whereas in a chemical method, a free radical forms first on to the initiator and then it is transferred to the

monomer/polymer backbone. Unlike the chemical initiation method, the radiation-induced process is free from contamination, so that the purity of the processed products may be maintained. Chemical initiation is limited by the concentration of the initiator, and it may be difficult to determine an accurate concentration of the initiator in pure form. Chemical initiation often brings about problems arising from local heating of the initiator, an effect that is absent in the formation of free-radical sites by radiation, which is only dependent upon the absorption of high-energy radiation. Due to large penetrating power of higher energy radiation, methods using radiation initiation provide the opportunity to carry out grafting at different depths of the base polymer matrix. Moreover, the molecular weight of the products can be better regulated in radiation techniques, and these are also capable of initiation in solid substrates. Regarding its limitation, nuclear radiation energy is usually expensive in comparison with chemical reactions. The length of irradiation time and setting up the optimum conditions present limitations of the radiation technique. Moreover, it should be well known whether the polymer is stable in the radiation range of interest [362-363].

4.2.1.3. Photochemical Grafting

When a chromophore on a macromolecule absorbs light, it goes to an excited state, which may dissociate into reactive free-radicals, whence the grafting process is initiated. If the absorption of light does not lead to the formation of free-radical sites through bond rupture, this process can be promoted by the addition of photosensitizers, e.g. benzoin ethyl ether, dyes such as Na-2,7 anthraquinone sulphonate or acrylated azo dye or aromatic ketones (such as benzophenone, xanthone). That means the grafting process by a photochemical technique can proceed in two ways: with or without a sensitizer [364, 365]. The mechanism without sensitizer involves the generation of free radicals on the backbone, which react with the monomer free radical to form the grafted co-polymer.

On the other hand, in the mechanism 'with sensitizer', the sensitizer forms free radicals, which can undergo diffusion so that they abstract hydrogen atoms from the base polymer, producing the radical sites required for grafting.

4.2.1.4. Plasma Radiation Induced Grafting

In recent years, the plasma polymerization technique has received increasing interest. Plasma conditions attained through slow discharge offer about the same

possibilities as with ionizing radiation [366, 367]. The main processes in plasmas are electron-induced excitation, ionization and dissociation. Thus, the accelerated electrons from the plasma have sufficient energy to induce cleavage of the chemical bonds in the polymeric structure, to form macromolecule radicals, which subsequently initiate graft co-polymerization

4.2.1.5. Enzymatic Grafting

The enzymatic grafting method is quite new. The principle involved is that an enzyme initiates the chemical/electrochemical grafting reaction [368]. For example, tyrosinase is capable of converting phenol into reactive o-quinone, which undergoes subsequent non-enzymatic reaction with chitosan. Enzymatic grafting on a poly (dicarbazole- hydroxysuccinimide) film was reported by Cosnier et al. [369], thionine and toluidine blue have been irreversibly bound to the poly (dicarbazole) backbone and the grafting of polyphenol oxidase (PPO) on polydicarbazole has been reported.

CHAPTER 5

Fibre Reinforcement Polypropylene / Montmorillonite Nanocomposite

Classical structural polymer composite materials contain a strong load-bearing phase, typically in the form of a reinforcing fibre, embedded in a polymer matrix. The fibers provide the mechanical strength and stiffness, and the polymer matrix ensures the transfer of loads between the fibers, and protects them from environmental degradation. Such materials have traditionally been used in applications where high stiffness/weight and strength/weight ratios are required. However, the next generation of polymer composites may need not only to fulfil structural requirements but also to incorporate one or more non-structural functions such as sensing, actuation, and electrical energy absorption or power generation, gas barrier or heat resistance. Multifunctional polymer composites are already of interest for a wide variety of applications. The transport industry represents a large part of this demand [370, 371], but they may also be integrated into sporting goods, for example, such as skis or tennis rackets in order to reduce vibration [372], or into artificial prostheses to restore, repair or replace the structural and functional performance of natural tissues [373]. The performance of polymer composites may be improved and/or expanded by modifying the properties of either the reinforcing fibers or the polymer matrix. The fibre properties may be modified during synthesis or by specific surface treatments, but extensive work has already been carried out in this area, and the perspectives are relatively restricted. Tuning the physical properties of the matrix, on the other hand, offers far greater potential, and the focus in the present work is therefore on improving the polymer matrix properties, whilst maintaining the load bearing function of the fibers. In order to achieve this objective, it is necessary to develop polymer matrices with controlled composition and morphology as well as methods for their incorporation into the final composite. However, to ensure the competitiveness of this approach, it is of interest to exploit conventional manufacturing techniques as far as possible [374-376].

5.1. Polypropylene Based Nanocomposites

Polypropylene is a nonpolar semicrystalline thermoplastic with a low surface tension. It is produced by coordination addition polymerization of propylene monomer. The chain configuration of polypropylene is a symmetrical helix molecule with three monomeric units per single revolution (0.65 nm). The methylene side groups are aligned in three columns parallel to the helix axis [377]. Most frequently, stereospecific Ziegler-Natta catalysts are used in industrial processes to produce either highly crystalline isotactic polypropylene (iPP) or syndiotactic polypropylene (sPP). Under usual solidification conditions, iPP crystallizes in its stable monoclinic α -form [378]. At high undercoolings or at high pressures, the less stable hexagonal β - and triclinic γ -crystal modifications may dominate [379]. Typically, iPP contains 40 – 60 wt% of crystalline phase, with a melting point ranging from 167 °C to 180 °C, depending on the crystal form and lamellar thickness. Neat iPP crystallized from the melt exhibits a spherulitic morphology. Spherulites are typically composed of twisted lamellae, typically 10 nm thick and 1 – 10 μ m wide. iPP spherulites exist in five main forms. The three types of α -spherulites are distinguished by their cross-hatched lamellar structure, while β -spherulites exhibit leaflike lamellae [380]. iPP is an extremely attractive candidate for many engineering applications. Relatively low price, excellent chemical resistance, good processability and the possibility of modifying its mechanical properties over a wide range by adding fillers and dispersions of secondary polymeric inclusions have contributed to the massive expansion of iPP in automotive, land transport, home appliances and other industries [381-383]. Therefore iPP is one of the fastest-growing classes of commodity thermoplastics, with a market share growth of 6 % - 10 % per year [384]. However, brittleness and inadequate stiffness are among its most important deficiencies, so that expensive engineering thermoplastics are generally required in more demanding applications [385]. To reduce cost or enhance physical and mechanical properties, fillers and reinforcements are commonly added in iPP [386-387]. These include talc [388], CaCO₃ [389], mica [390], wollastonite [391], glass fibre [392], carbon fibre [393] and jute [394].

5.2. Processing Of PP/MMT Filament

5.2.1. Introduction to Spinnability Criteria

In this section, different criteria that affect the spinnability of polymer melts are defined and discussed in the context of iPP/MMT nanocomposites. They are divided into two categories:

A) Mechanisms of filament breakage; these depend on processing parameters and melt viscosity and include:

- Cohesive brittle fracture
- Capillary waves

B) Flow instabilities; these cause non-uniformity in the filament diameter:

- Die swell
- Melt fracture
- Draw resonance

A fluid is spinnable under a given set of deformation conditions if steady-state, continuous elongation of the fluid jet proceeds without rupture of any kind [395]. Thus, a lack of spinnability is usually manifested by filament breakage, and the maximum elongation of the fluid thread is a measure of spinnability. Two principal physical mechanisms control the breakage of the fluid threads. These are (i) cohesive, brittle fracture, and (ii) capillary waves. A schematic description of these two failure mechanisms is given Figure 5-1.

Cohesive brittle fracture occurs when the tensile stress in the jet exceeds a critical value (the tensile strength). In this case, the elasticity of the fluid plays a determinant role. Whereas an ideally viscous fluid would deform to an infinite extent, the deformation energy being dissipated instantaneously, a viscoelastic polymer melt stores part of this energy. When the stored energy reaches a critical value, depending on the deformation rate and the relaxational characteristics of the polymer melt, cohesive, brittle fracture occurs. The probability of failure is reduced when the relaxation of the stored energy is rapid [396]. A similar failure mode has been identified by Ide and White [397], called ductile failure. The latter mode of failure is due to the growth of a neck generated in the filament by high local stresses. Capillary waves are associated with the viscosity and the surface tension of the fluid. They correspond to the growth of distortions of the jet surface that lead to the formation of droplets.

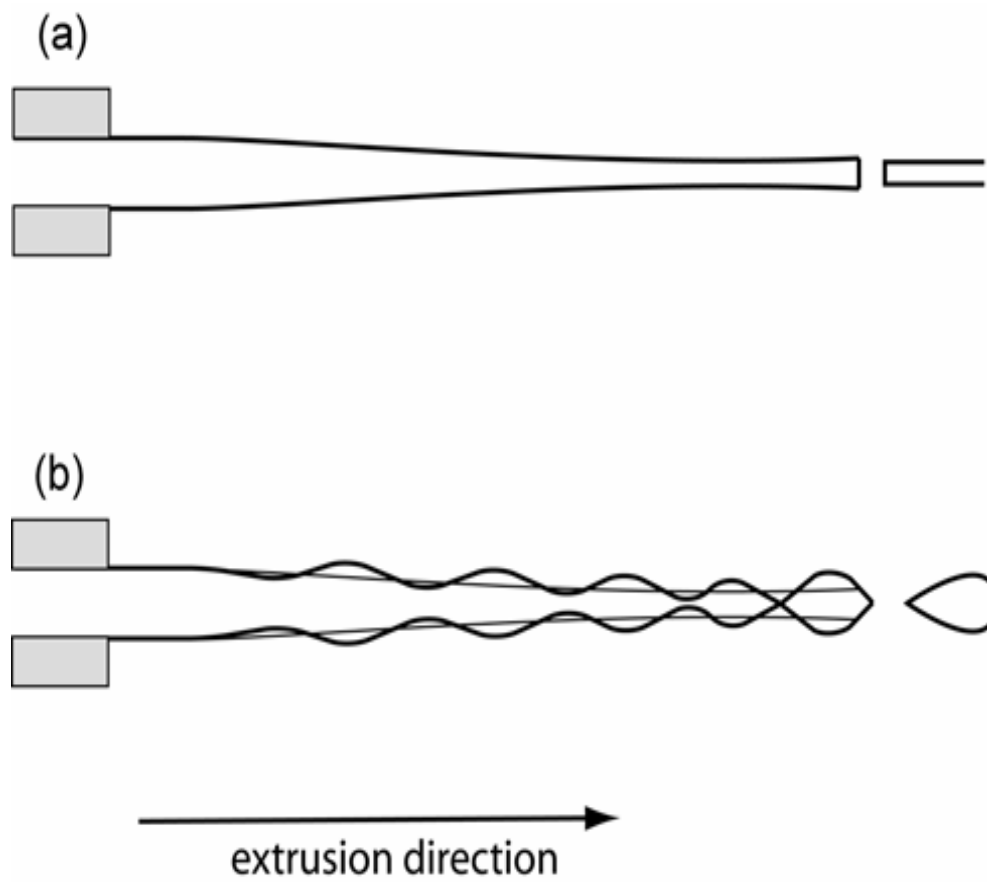


Figure 5.1: Schematic description of (a) cohesive fracture and (b) capillary break-up failure mechanisms.

To obtain a qualitative idea of how the spinnability i.e. the maximum filament length is affected by these two modes of fracture, it is useful to consider the ideal case of a linear viscoelastic polymer subjected to a steady-state, isothermal stress distribution during melt spinning. Ziabicki [395] has shown that if only the cohesive fracture mode is considered, the maximum filament length increases linearly with the product $V_0\eta$, where V_0 is the extrusion velocity and η is the melt viscosity. For the same conditions, he has also shown that for the capillary wave failure mode, the dependence is more complex and that the maximum filament length increases monotonically with η , and decreases with the surface tension of the liquid.

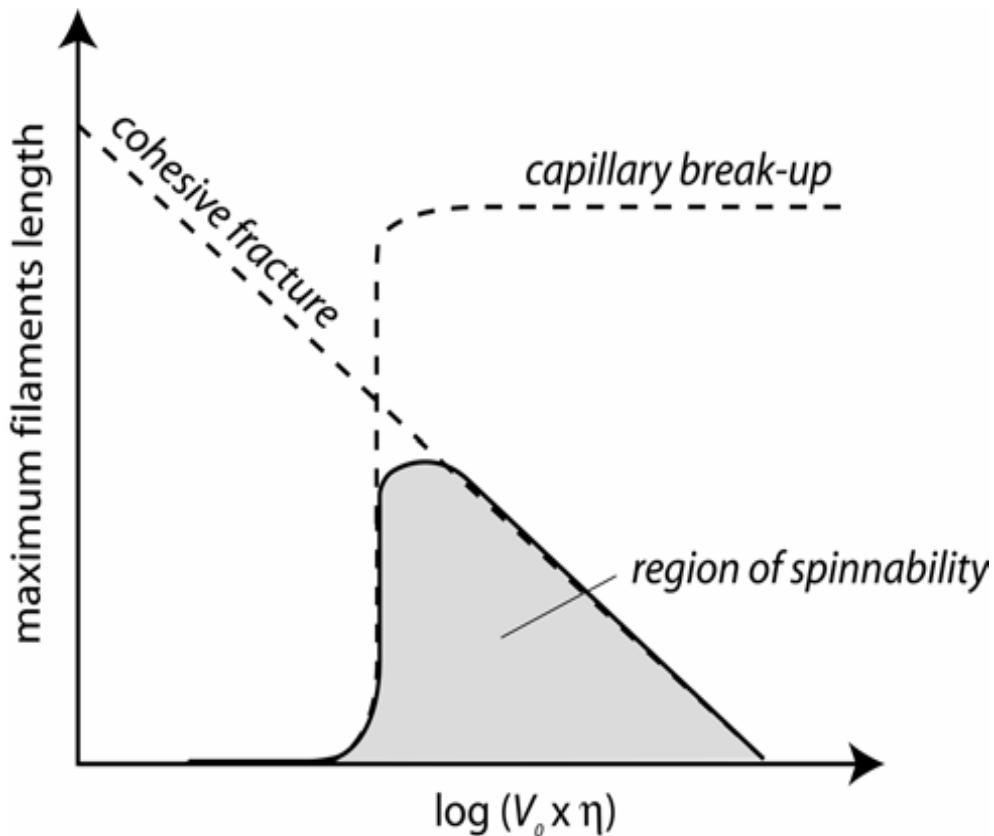


Figure 5.2: Maximum filament length predicted for the capillary break and cohesive fracture mechanisms

In practice, neither isothermal nor steady state conditions are encountered in the melt spinning process. Moreover, the variation of the maximum filament length in the cohesive and capillary wave failure mode would be much more complex in the case of a viscoelastic polymer melt. However, the above analysis, summarized in Figure 5.2, highlights factors that may be used to assess the spinnability of polymer melts. These include not only experimental variables (the extrusion temperature and velocity, the dimensions and number of the spinneret orifices, the fluid flow rate, etc.), but also the intrinsic properties of the fluid. In order to compare the ease of processing of the different iPP1/MMT formulations, it is assumed here that the processing variables, except for V_L , are constant. Thus, the parameters pertinent to the spinnability may be divided in two groups: (i) those that affect the intrinsic rheological properties of the polymer melt and (ii) the spinning conditions. This chapter focuses on the rheological properties of the melt, and, in particular on their dependence on MMT concentration. Spinning conditions are discussed in terms of drive-roll velocity and the physical characteristics of the filaments.

5.2.2.Melt Spinning Processing Techniques

5.2.2.1. Fibre Melt-spinning Principles

The melt spinning process is commonly used for polymer resins and inorganic glasses. The process involves the melting and the extrusion of the material to be processed through multi orifice capillary die, followed by cooling and solidification of the filaments, which can be wound on a bobbin or otherwise processed [398]. A basic form of the melt spinning process is illustrated in Figure 5.3. The polymer, in the form of dried granules is fed into the extruder where it is melted and conveyed to a metering pump. The metering pump ensures a steady flow of polymer to the spin pack where the polymer is filtered and forced through the capillaries of the spinneret. The filaments are then cooled and solidified by blowing air into the quench chamber, while being drawn down by the action of heated godet rolls and then wound onto a bobbin. The winding speed corresponds to the spinning speed and is called the drive-roll velocity.

5.2.2.2. Film Extrusion-Calendering

The calendering of thermoplastics is an operation used for the production of continuous sheets or films of uniform thickness by squeezing the molten material between a pair of heated driven rolls⁴. A schematic of the extrusion-calendering process is given Figure 5.4. Films of about 75 mm wide and 0.7 μm thick were produced by this method using a standard Prism twinscrew extruder (TSE) and a Prism TSE system calender.

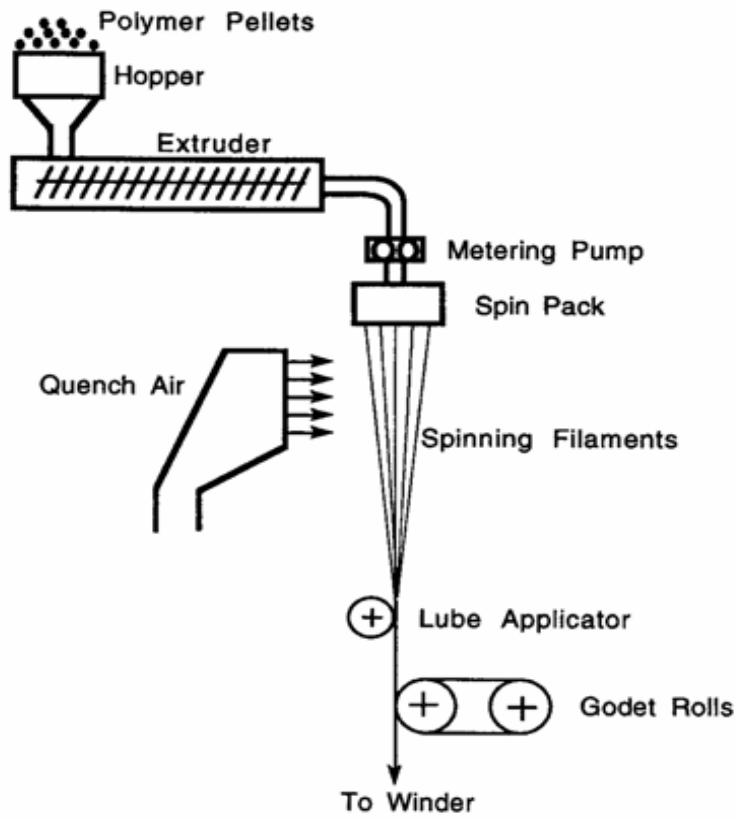


Figure 5.3: Schematic description of the melt spinning process.

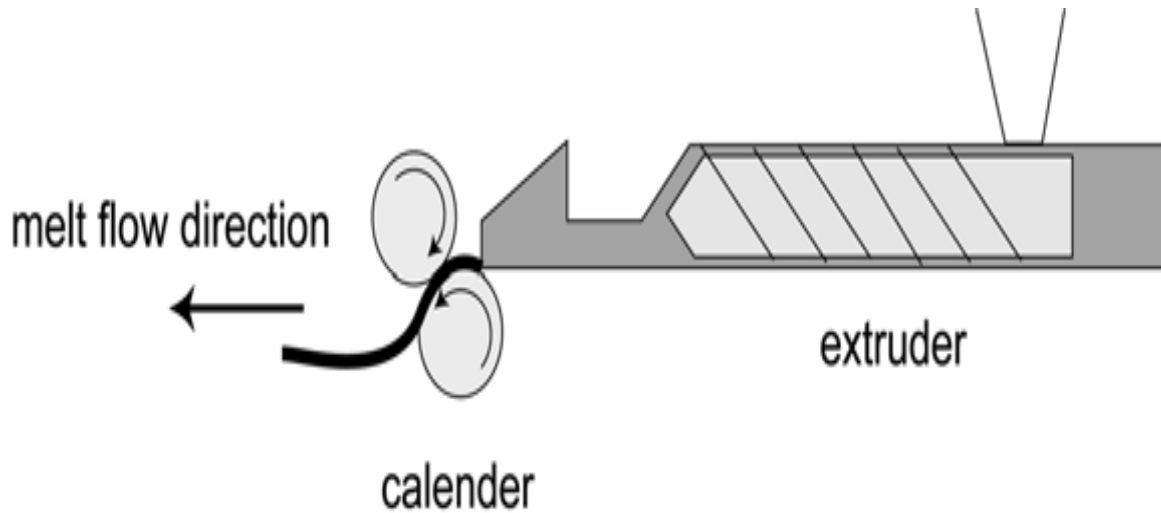


Figure 5.4: Schematic description of the extrusion-calendering process.

CHAPTER 6

Experimental Part

6.1. Materials

The cotton fabric we used consisted of normal bleached fibers (obtained from the Institute for Textile Chemistry and Chemical Fibers, Denkendorf, Germany).

The materials used for the preparation of polyolefin / montmorillonite nanocomposites are commercial homopolymer polypropylene (HP561T) with melt flow rate (MFR) of 1.6g / 10 min, commercial homopolymer polyethylene (TIPELIN 7700M) with melt flow rate (MFR) of 0.28g / 10 min. Polypropylene and polyethylene were supplied from ITCF-Denkendorf (Germany).

Montmorillonite clay (MMT) with cation exchange capacity (CEC) 100 meq per 100g was supplied by Süd-Chemie – Moosburg –Germany.

The monomers Glycidyl methacrylates (GMA) and Methyl methacrylate (MMA) were provided by Acros (KMF Laborchemie Handels GmbH, Sankt Augustin, Germany). The monomers were redistilled and stored at -20 °C. The monomers were redistilled and stored at -20°C.

We used acid dye, namely, Acid Red 8 (Aldrich); reactive dye namely, remazol-brill. Blue FB (Hoechst), basic dye, namely, malachite green and disperse dye, namely, Resolin Red GR and which were supplied by Bayer AG (Leverkusen, Germany).

Most of the chemicals used in this study, including alanine, leucine, phenylalanine, glucose, fructose, methanol, benzene, methyl ethyl ketone, butanol, sodium per sulphate (SPS), sodium bisulphite (SBS) and phenyl triethoxy silane were acquired from Aldrich Chemical - Germany.

Sodium dodecyl sulphate (SDS), Hydrochloric Acid, dibutyl amine and sodium hydroxide were obtained from Merck – Darmstadt – Germany. Ferrous ammonium

sulphate, sodium citrate, sodium carbonate, copper sulphate and sodium sulfate decahydrate (Glauber salt) were supplied from BDH (Köln, Germany).

The solvents xylene and benzonitrile were supplied from Acros (Belgium).

6.2. Methods

6.2.1. Modification of MMT Clay [399-400]

6.2.1.1. Intercalated Modification of MMT with Amino Acids

MMT (2.5g) was dispersed into 250 ml deionized water; the mixture was stirred for 1h and then heated to 70 °C to obtain aqueous suspension of clay. The desired amount of amino acid (1x and 2x concentrations of the clay based on CEC) and 2 ml of hydrochloric acid in 50 ml deionized water was added into the mixture, The PH value of the solution was adjusted to 6-8 and stirring was continued for 4h. A white liberated precipitate was filtered and washed with deionized water. The obtained wet precipitate was dried under vacuum at 80 °C for 24h.

6.2.1.2. Surface Modification of MMT with Silane Coupling Agent

A mixture of MMT and phenyl triethoxy silane (10% weight of MMT) was added to a solution of deionized water and ethanol (10/90 volume), The PH value was adjusted to 5.5 and stirred for 2h. The treated MMT was filtered and dried at 80 °C for 24h.

6.2.1.3. Double Modification of MMT with Amino acid and Silane coupling agent

A silane coupling agent solution with MMT was prepared as described above in the surface modification. A separated solution of amino acid and 2 ml of hydrochloric acid in 50 ml deionized water was added to the solution. The mixture was then stirred for 3h at 70 °C. The white precipitate was obtained by filtration and dried under vacuum at 80 °C for 24h.

6.2.2. The Swelling Degree [401]

The swelling degree was determined by taking a definite weight of a dry sample and introduced into a small sintered glass and allowed to imbibe for 24 h in different solvents. The excess solvent was removed by gentle centrifugation. The swelled sample was weighted and re-suspended in the solvent. This procedure was repeated until obtaining a constant weight for the swelled sample. The swelling degree of each sample is expressed as the amount of sorbed solvent per 100g of dry sample.

6.2.3. Glucose and Fructose Absorption Studies [402, 403]

The ability of MMT clay to make sugar absorption is studied by using Benedict solution which is used as a test for the presence of all monosaccharide and prepared by dissolving 173g sodium citrate, 100g sodium carbonate (hydrated) 17,3g copper sulphate and diluting to 1 litre with distilled water.

6.2.3.1. Preparation of Calibration Curve

- 1- 0.02M glucose solution is used to make up samples ranging in concentration from 2 to 20 mM.
- 2- 5cm³ of Benedict's solution is added to 5cm³ of each dilution.
- 3- Each sample is placed in a boiling water bath for 6 minutes.
- 4- The tubes are replaced in a rack. Make sure each tube is labelled. Allow precipitated copper to settle to the bottom of the tubes overnight.
- 5- Next day, the intensity of the unprecipitated blue Cu (II) ions is measured by using a colorimeter against a blank (water only) in all wavelengths available range.
- 6- A graph of light absorbance against concentration of sugar is plotted. This is the calibration curve.
- 7- Unknown solutions can be taken through the same procedure and their absorbance converted to concentration with the help of the calibration curve.

6.2.4. Preparation of Nanocomposites

6.2.4.1. Preparation of Polyacrylate / MMT Nanocomposites by In Situ Emulsion Polymerization [404]

In 250 ml round flask, monomer, 50 ml water, 0.2g KOH, 0.5g emulsifier sodium dodecyl sulphate (SDS) and double modified clay were added and stirred for 30 min at room temperature, and then the mixture was heated to 80 °C. Then the initiator (SPS/SBS) is added to the mixture and stirring was continued for 5h. After cooling, the product was precipitated in methanol. The precipitated nanocomposites hybrid was filtered, washed with methanol, and finally dried under vacuum for 24h at 60 °C. The different composite mixtures were prepared following the same procedure with different acrylate monomer and with different clay / monomer weight percent.

6.2.4.2. Preparation of Polypropylene / Montmorillonite Nanocomposite by Solution Polymerization [270]

Polypropylene / montmorillonite nanocomposite was prepared as follow, In a 500 ml three-necked round flask equipped with a condenser and a magnetic stirrer were

added 100 ml of anhydrous xylene, the desired amount of MMT clay and polypropylene pellets. Under the protection of N₂, the flask was brought up to 160 °C to have the polypropylene dissolved. The clear solution was kept being stirred for 5 h, after which it was poured into excess methanol with vigorously stirring. The precipitate was filtered off, washed with methanol several times, and dried at 60 °C under vacuum for 8 h.

6.2.4.3. Preparation of Polyethylene / Montmorillonite Nanocomposite by Solution Polymerization [271]

Polyethylene / montmorillonite nanocomposite was prepared by solution blending. A desired ratio of MMT clay and HDPE was dissolved in a co-solvent of xylene and benzonitrile (80:20wt %) at 160 °C to have the polyethylene dissolved. The clear solution was kept being stirred for 5 h, after which it was poured into a large amount of vigorously stirred THF. The precipitated powder was filtered and washed several times with THF to remove the residues of xylene and benzonitrile. The product was dried at 70 °C under vacuum for 8 h.

6.2.4.4. Preparation of Polypropylene / Montmorillonite Nanocomposite by Direct Melt Spinning Intercalation Method

Polymer melt-direct intercalation is an approach to make polypropylene / Montmorillonite nanocomposites using a conventional polymer extrusion process. Polypropylene was melt mixed with the clay (5% wt) using a 5 litre reactor. The rotational speed 400rpm for 6 hours in order to have high shear stress and the temperatures of the reactor reached to 250°C.

6.2.5. Polypropylene / Montmorillonite Fibre Production Method

Before the fibre production, the polypropylene / montmorillonite nanocomposite was dried at 0,1 bar and 160 °C. Continuous fibres were produced via spinning process using extruder Haake 9000 (Germany). The solid polymeric pellets were introduced in the spinning machine which has three independent temperature areas and is equipped with a pressure sensor. In order to process the PP/MMT clay nanocomposite filament, the heating temperature is regulated between 180 and 230 °C. As a spinning pump a toothed wheel pump (or gear pump) is available, whose delivery volume is 0.6 Cm³/U. The control of the temperature at the pump and the spinneret is affected by a thermal element where a spinning nozzle a 10-hole-spinneret (diameter of pore 200 µm) is used after turning the spinning-fiber around

two gallettes it is spooled on a coil by a coiler (winder) from Barmag, Type SW 66 SSD.

6.2.6. Grafting Polymerization Procedure [405]

Pieces of cotton samples about 3 gm in weight was placed in 250 ml stopped glass vessel containing the grafting solution at a specific temperature (50, 60, 70 and 80°C) using thermostatic shaker water bath. The grafting solution consists of water, double modified MMT clay, monomer, butanol and emulsifier. The content of the reaction vessel was shaken vigorously for 30 min. Ferrous ammonium sulphate and initiator are added to the flask and the graft polymerization is hold under shaking for the desired time (15 to 120 min) at the desired temperature. After the desired polymerization time, the grafted cotton sample was quickly removed from the grafting solution and the homopolymer is extracted from the grafted cotton by soxhlet extraction using methyl ethyl ketone in case of GMA monomer and Benzene solvent in case of MMA monomer . Extraction of homopolymer was repeated till constant weight of cotton sample. The grafting percentage was calculated according to the following equation:

$$\text{Grafting \%} = (W_2 - W_1 / W_1) \times 100$$

Where, W_2 = Weight of grafted cotton and W_1 = weight of ungrafted cotton.

6.2.7. Dyeing Methods [406,407]

Each of ungrafted cotton sample, Cotton sample grafted with GMA, Cotton sample grafted with GMA in the presence of MMT clay and Cotton sample grafted with GMA in the presence of MMT clay and treated with dibutyl amine were independently dyed with three types of dyestuff namely Acid, basic and Reactive dyes. Where polypropylene yarns and polypropylene/montmorillonite yarns were dyed with two types of dyestuff namely acid and disperse dye. In case of acid dye, the dye bath was prepared by dissolving the dye in hot water; sample was introduced into the bath at 60 °C and held for 10 min. The temperature of the bath was raised to 90 °C over a period of 60 min. The sample was rinsed with cold water. Then, soaped with a solution containing 5 g/l Na_2CO_3 and 1 g/l detergent, washed with cold water and then dried. For Basic dye and disperse dye the dyeing process was carried out by

pasting the dye with 1% acetic acid (based on sample weight) and then dissolved in boiling water. The dissolved dye was added to the bath at 60 °C and the temperature was then raised slowly to 90 °C. The dyeing was continued for 60 min during which Glauber salt (20% based on sample weight) was added, the samples were rinsed with cold water then soaped and washed as mentioned in the acid dye. In the use of reactive dye, the dye was first dissolved using boiling water. Sample was entered the bath containing glauber salt (80 g/l) and Na₂CO₃ (5 g/l) at 25 °C for 10 min. The dissolved dye was then added to the bath. After 15 min the temperature was raised to 60 °C over a period of 30 min then, the alkali sodium hydroxide (1 ml/l for 32.5%) was added. Again the dyeing was continued for 30 min. Sample was rinsed with cold water and acidified with 1 ml/l acetic acid (60%) at 40 °C. The sample was then soaped for 10-15 min. Finally, the sample was washed with cold water and air dried. All dyeing processes were carried out using conventional exhaustion method at dye concentration of 0.2 % and Liquor ratio of 1:50. After dyeing, the colour strength (K/S) was followed by measuring the reflectance (R) using a spectrophotometer. This was followed by substituting the measured value of (R) in the following Kubelka-Munk equation [406].

$$K/S = [(1-R)^2 / 2R] - [(1-R_t)^2 / 2R_t] = A . C$$

Where R is the decimal fraction of the reflectance of the colored sample

R_t is the decimal fraction of the reflectance of the uncolored sample

K is the adsorption coefficient

S is the scattering coefficient

C is the dye concentration

A is the proportionality factor.

6.2.8. Water Absorption [408]

The Water absorption test was based on immersion of cotton fibers onto water for different interval time (30min, 60min and 120min) at room temperature. Water absorption percentage (S %) values were determined from the following equation [408]

$$S\% = (M - M_0 / M_0) \times 100$$

Where M is the mass of the swollen cotton fibers in distilled water at room temperature and M_0 is the mass of the same cotton fibers dried at $50\text{ }^\circ\text{C}$.

6.3. Characterization

X-ray diffraction (XRD) measurements were performed using a Philips powder – Diffractogram PW 1050 with ADM software and with Ni-filtered Cu-K radiation. The accelerating voltage was 40 KV, and the current was 30 mA.

Thermogravimetric analysis (TGA) was determined on TGA 7 thermogravimetric analyzer (Perkin Elmer instrument) under a nitrogen flow at heating rate $10\text{ }^\circ\text{C min}^{-1}$.

The morphology and fracture surface of the clay and composites were examined by Scanning electron microscope (SEM) analysis using Zeiss, DSM 962 microscope.

Melting point was determined by using electrothermal-digital melting point apparatus. Light absorbance of the sugar solutions was determined by Perkin Elmer UV/VIS spectrometer (Lambda2).

The nitrogen content was determined according to Kjeldal method [409] using Büchi 322 as distillation unit and Büchi 343 as control unit.

The mechanical properties [410] of the cotton samples and polypropylene fibre were measured by using Zugprüfgerät machine by force 10 KN.

Colour strength was measured using Textfash datacolor GmbH, Zubehoer 3381.

The Fourier transfer infrared (FTIR) spectra were scanned using Bruker IFS 28 spectrometer

CHAPTER 7

Modifications, Characterizations and Applications of Montmorillonite Nanoparticles

7.1. Introduction

Montmorillonite (MMT) clay is a common natural layered silicates and the suggested crystallographic structure of Montmorillonite is based on pyrophyllite consisting of two fused tetrahedral silica sheets sandwiching an edge-shared octahedral sheet of either aluminium or magnesium hydroxide. Isomorphous substitution of Si^{4+} with Al^{3+} in the tetrahedral lattice and of Al^{3+} with Mg^{2+} in the octahedral sheet cause an excess of negative charges within the Montmorillonite layers. These negative charges are counterbalanced by cations such as Ca^{2+} and Na^{+} situated between the layers [411].

Montmorillonite clay is hydrophilic. It is very important to improve the organophilicity, so that it can be compatible with organic polymers. The organophilicity of Montmorillonite clay is increased by two types of modifications:

1) Interlayer galleries modification in which the MMT clay is treated with compatibilizing agents as amino acids [93, 99] or alkyl ammonium ions [103], because they can exchange easily with ions between the silicates layers, hence increasing in the distance between the clay layers results.

2) Surface and edges modification using silane or titanate coupling agents to generate organophilic surfaces and edges. Although quaternary ammonium salts can be adsorbed on the MMT surface, interlayer galleries modifiers are not enough for MMT surface and edges modification because this adsorption is unstable and the modification by a coupling agent on the surface and edges can form a stable covering [105]. The coupling agent is expected to react with the hydroxyl groups at the clay edges and surfaces [106, 107].

7.2. Modification of Montmorillonite Clay

Three different amino acids result in different intercalation effects and structures. Figure 7.1 displays XRD patterns of the pure MMT clay and intercalating agent-treated MMT clays depends on amino acid concentration 2x based on MMT clay CEC, Alanine-MMT, Leucine-MMT and Phenylalanine-MMT. The basal spacing (d_{001}) values of these samples are calculated from the peak position using Bragg's equation:

$$n\lambda = 2d \sin \Theta$$

Each sample has one peak at $2\Theta = 10.5^\circ$, 7.0° , 6.5° and 6.9° respectively. The data for d-spacing are listed in table 7.1 which shows that the diffraction peaks of all modified MMT clay samples are shifted to smaller angles compared with the pure MMT. This indicates that MMT clay was successfully intercalated with amino acids. The results also show that - in all modifiers – the addition of 2x concentration of amino acid based on clay CEC give increment in interlayer spacing more than in the addition of 1x concentration. The listed data in table 7.1 concluded that the more interlayer spacing is given by using 2x concentration of Leucine amino acid based on MMT CEC. Figure 7.2 shows XRD curves of pure MMT, silane surface modified MMT, Leucine-MMT and double modified MMT clays, these peaks are assigned to the d-spacing of MMT [399, 412]. The data for d-spacing of each sample is given in table 7.1. From the table, it can be seen, that silane surface treatment did not cause any positive significant difference in the basal spacing of pure MMT clay, and the d-spacing of double modified MMT clay was found to be 11.94 nm which is lower than the d-spacing of Leucine- MMT (12.9nm). This is due to the effect of the silane coupling agent which coat the surface of the MMT clay and then the clay layer becomes closed for amino acid penetration between the silicate layers [399].

Table 7-1: XRD data obtained for pure and modified MMT clay

Sample	Modifier conc.	2 Θ	d ₀₀₁ (nm)
Pure MMT	-	10,5	7,74
Silane surface MMT	10 % weight of MMT	10,9	7,50
Alanine-MMT	1x	7,4	11,01
	2x	7,0	11,55
Leucine-MMT	1x	6,6	12,36
	2x	6,5	12,59
Phenylalanine-MMT	1x	7,1	11,38
	2x	6,9	11,75
Double modified MMT	10 % weight of MMT and 2x Leucine conc.	6,8	11,94

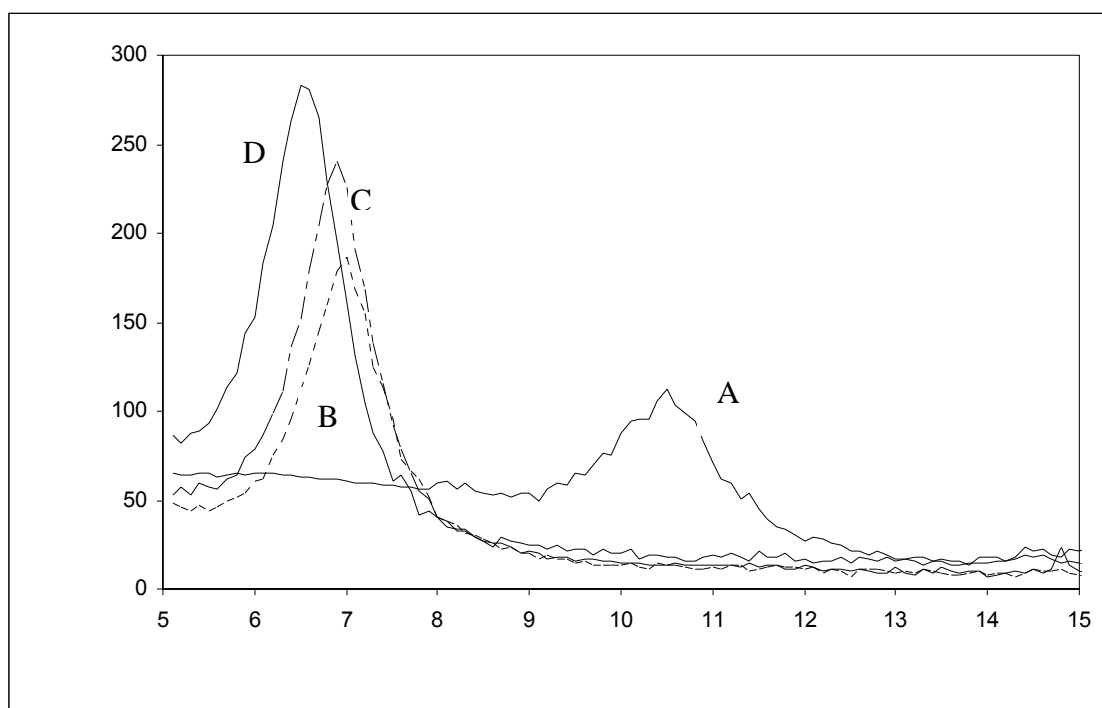


Figure 7.1: XRD patterns of (A) pure MMT and treated with (B) Alanine, (C) Phenyl Alanine and (D) Leucine amino acids.

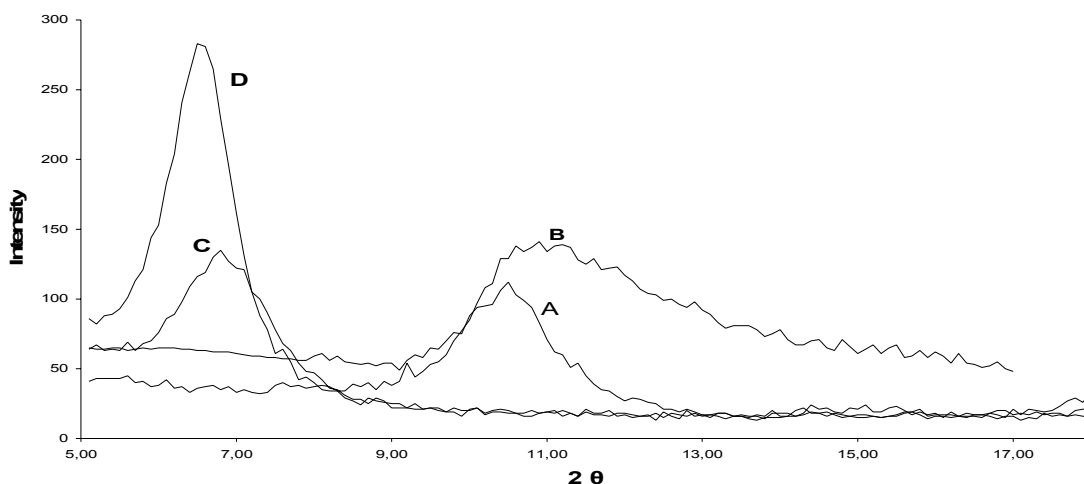


Figure 7.2: XRD patterns of (A) pure MMT, (B) Silane surface MMT, (C) Double modified MMT and (D) Leucine MMT.

7.3. Characterization of Montmorillonite Clay

7.3.1. Thermal Gravimetric Analysis (TGA)

TGA results of pure MMT, silane surface modified MMT, Leucine-MMT and double modified MMT clays are illustrated in Figure 7.3. From this figure it is clear that the thermogram of pure MMT is quite different from that of Leucine-MMT and double modified MMT clays. It is also clear that the position of double modified clay decomposition curve is between the decomposition curves of Leucine-MMT and decomposition curve of pure MMT, whereas the silane surface MMT has higher thermal characteristic than pure MMT. This result can be accepted as an indication of successful insertion of both silane coupling agent and Leucine amino acid into MMT clay.

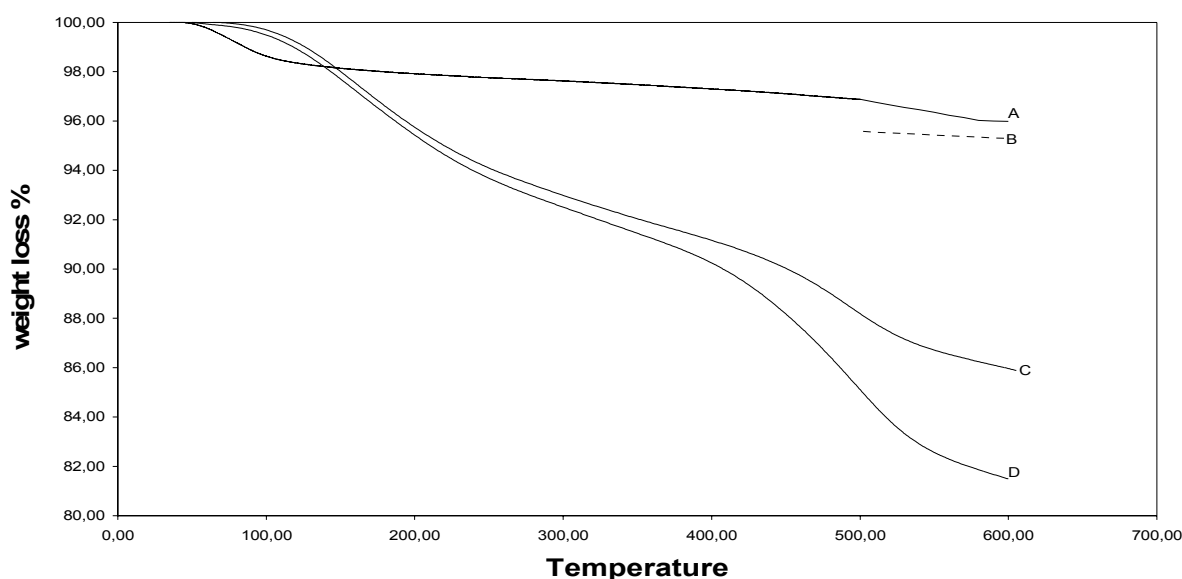
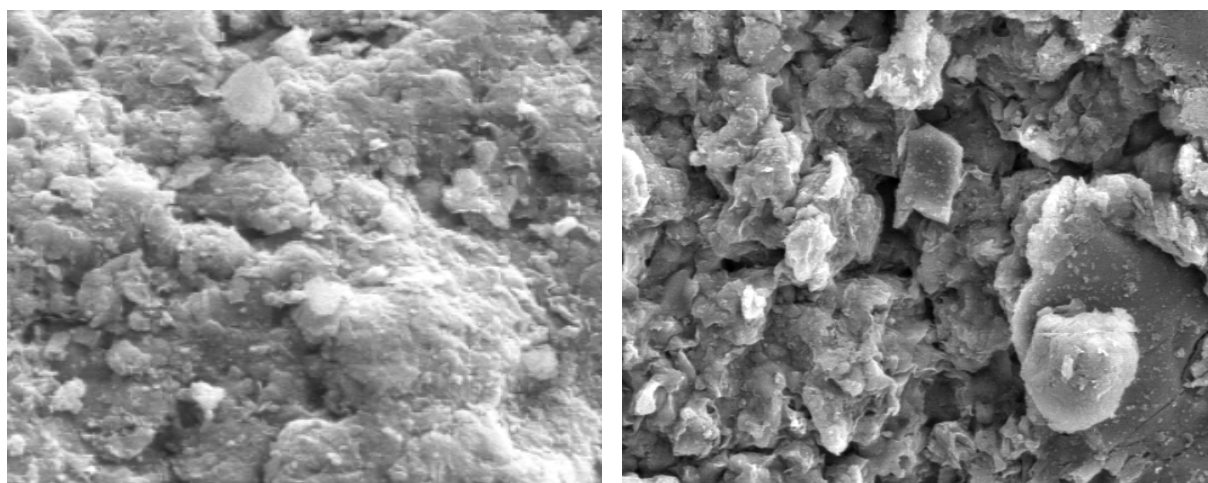


Figure 7.3: TGA thermograms of (A) Silane surface MMT, (B) Pure MMT, (C) double modified MMT and (D) Leucine-MMT.

7.3.2. Morphology of MMT Clay by Scanning Electron Microscope (SEM)

When the modification of the clay is completed, which is indicated when a colloid like suspension without any visible solid particles is obtained, a small portion of a stable suspension was dried to evaporate the water solvent and the residue was examined by scanning electron microscope (Figure 7.4-B). In order to investigate the effect of the modification, pristine Na-MMT was also deposited from water suspension free of any modifier and examined by scanning electron microscope (Figure 7.4-A). As shown in figure 7.4-A, Pristine MMT exhibits agglomeration morphology due to its poor dispersion in the solvent, where modified MMT displays a uniform distribution implying a good dispersion in the solvent which can be attributed to an effective organophilic transformation of the MMT surface after modification [270].



A

B

Figure 7.4: SEM of (A) Pristine MMT and (B) double modified MMT.

7.4. Applications of Montmorillonite Clay

7.4.1. The Swelling Degree

The swelling measurements of the modified and double modified clay in different solvents which is expressed as the amount of sorbed solvent per 100g of dry sample are illustrated in figure 7.5. From this figure it can be concluded that, the hydrophilic of mineral clay has been changed after modification to hydrophobic due to the intercalation of modified in the clay interlayer which led to: [401]

- I) A great affinity to an aprotic polar solvent as DMF and a nonpolar solvent as toluene.
- II) The protic polar solvents as methanol show a lower degree of swelling.

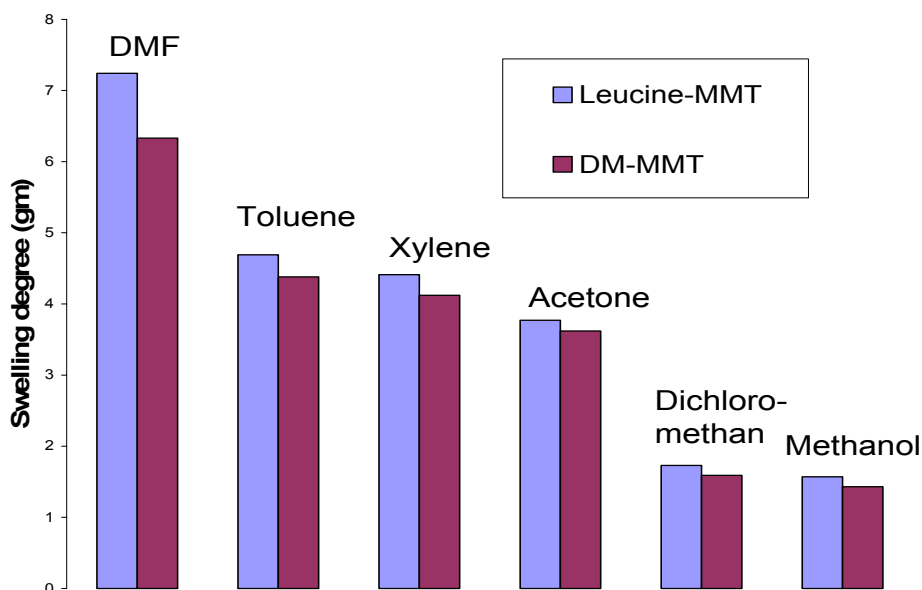


Figure 7.5: Swelling degree of Leucine-MMT and DM-MMT

From the data illustrated figure 7.5, it can be also noted that the swelling degree of Leucine-MMT is larger than that of DM-MMT due to the effect of the silane coupling agent which coats the surface of the MMT clay in case of DM-MMT and then the clay layers become closed for solvent penetration.

7.4.2. Sugar Absorption Study

In the bioprocess of converting starch to glucose and then to other saccharides through enzymatic reaction, the overall conversion is about 45%, of which 42% is fructose and 52% is glucose and the rest are oligosaccharides. Fructose contains less calories and higher degree of sweetness than glucose (1.7: 0.7 on sweetness scale). Fructose is high soluble especially at lower temperature and suitable for diabetic and light food production. [402, 403]

Tables 7.2 and 7.3 list the kinetic absorption degree of glucose and fructose mixture by Leucine-MMT and DM-MMT at different temperatures and different sugar concentrations. From the data listed in the tables it can be concluded that the absorption of glucose is much faster than that of fructose at all temperatures and concentrations due to the hydrophobic character of modified clay which led to an increase of the absorption of an aldose (Glucose) more than a ketose (Fructose). Furthermore, it can be seen that the absorption degree is directly proportional with time and sugar concentration, but it is inversely proportional with the temperature. The data show also that the absorption degree obtained from Leucine-MMT is larger than DM-MMT due to the effect of the silane coupling agent

which coats the surface of the MMT clay in case of DM-MMT and then the clay layer becomes closed for solvent penetration.

Table 7.2: Effect of temperature on the absorption degree of glucose and fructose at sugar concentration 25% W/V.

	Leucine-MMT						DM-MMT					
	30 °C		50 °C		70 °C		30 °C		50 °C		70 °C	
	G	F	G	F	G	F	G	F	G	F	G	F
	1 h	22,6	2,4	22,5	2,4	20,4	2,1	18,7	2,5	18,6	2,1	15,4
2 h	28,9	11,1	29,0	10,5	20,6	7,6	23,3	10,7	18,9	12,4	17,6	8,6
4 h	29,6	15,3	28,2	15,2	20,6	9,4	23,3	21,3	20,4	17,5	18,6	10,5
24h	25,9	27,3	20,4	18,6	20,9	14,7	20,5	29,2	20,1	23,6	18,7	14,6

Table7.3: Effect of sugar concentration on the absorption degree of glucose and fructose at t emperature 30 °C.

	Leucine-MMT						DM-MMT					
	10% W/V		25% W/V		50% W/V		10% W/V		25% W/V		50% W/V	
	G	F	G	F	G	F	G	F	G	F	G	F
1 h	13,5	1,4	22,6	2,4	33,6	12,6	11,2	1,5	18,7	2,5	24,3	13,2
2 h	14,4	7,1	28,9	11,1	41,3	23,7	11,6	6,4	23,3	10,7	30,9	18,6
4 h	13,3	10,3	29,6	15,3	45,6	27,6	11,9	11,7	23,3	21,3	36,4	34,8
24h	13,3	11,3	25,9	27,3	45,9	29,5	11,8	11,9	20,5	29,2	39,2	38,4

7.5. Conclusion:

- 1-** Montmorillonite clay (MMT) with interlayer spacing 7.74 nm and cation exchange capacity (CEC) 100 meq per 100g was successfully modified with different amino acids in the presence of hydrochloric acid. Alanine-MMT, Leucine-MMT and Phenylalanine-MMT display the biggest interlayer spacing of 11.1, 12.36 and 11.75 nm respectively when using 1x concentration of amino acid based on clay CEC and 11.55, 12.59 and 11.94 nm respectively when use 2x concentration of amino acid based on clay CEC.
- 2-** Surface modifier phenyl triethoxy silane coupling agent was used to modify the surface and edges of the MMT clay where the interlayer spacing of MMT clay after double modification by 2x concentration of Leucine amino acid and phenyl triethoxy silane was 11.94 nm.
- 3-** Pristine MMT exhibits agglomeration morphology due to its poor dispersion in xylene, whereas DM-MMT displays a uniform distribution implying a good dispersion in xylene.
- 4-** The hydrophilic character of mineral clay has been changed after modification with leucine to hydrophobic which led to:
 - I) A great affinity to an aprotic polar solvent as DMF and a nonpolar solvent as toluene.
 - II) The protic polar solvents as methanol show a lower degree of swelling.
- 5-** Swelling degree of leucine-MMT is larger than DM-MMT due to the effect of the silane coupling agent which coats the surface of the MMT clay and the clay layer becomes closed for solvent penetration.
- 6-** Hydrophobic character of modified clay led to an increase of the absorption of an aldose (Glucose) more than a ketose (Fructose)

CHAPTER 8

Synthesis and Characterization of some Polyacrylate / Montmorillonite Nanocomposites by In Situ Emulsion Polymerization using Redox Initiation System

8.1. Introduction

Polymer – Clay nanocomposites have attracted a great deal of attention with their improved physical and chemical properties due to the small size and large surface area of clay particles in nanoscale dimensions [25, 413]. These materials exhibit markedly improved mechanical [414], thermal [136, 415], optical [416] and barrier properties [417] in comparison with a pristine polymer or microscale composites.

The polymer / clay nanocomposites have been prepared by different methods as *in situ* polymerization which was the first method used to synthesis polymer / clay nanocomposites based on polyamide 6 [418]. In this technique the organoclay is swollen in the monomer for a certain time depending on the polarity of the monomer molecules, surface treatment of organoclay and the swelling temperature, then the reaction is initiated by addition of a curing agent in case of thermosets and by addition of a curing agent or by increasing the temperature in case of thermoplastics [30]. Then the polymer formation can occur in between the clay layers. It is known, depending on the organization of the clay layers , polymer / clay nanocomposites can be classified into two types: **Intercalated**, where the polymer chains intercalates between the silicate layers of the clay, and **Exfoliated**, where the silicate layers are completely delaminated in the polymer matrix [411]. Exfoliated clay platelets provide better contact and distribution within the polymer matrix, and thus enhance properties of the nanocomposites more effectively [415].

In this present study, the structure and properties of nanocomposites prepared by in situ emulsion polymerization of GMA and MMA with double modified clay were investigated.

8.2. Structures and Properties of Nanocomposites

8.2.1. Thermal Gravimetric Analysis (TGA)

The thermal stability of pure PMMA, pure PGMA and the prepared nanocomposites with different clay contents was determined by measuring the thermogravimetric analysis (TGA) within the temperature range 50-600 °C, as shown in figures 8.1 and 8.2. In general, it is clear that all weight loss temperatures for the nanocomposites samples are higher than that of pure polymer which can be attributed to the restriction of the motion of organic chains attached to MMT clay [270]. It is also obvious, that the increasing in the clay content plays an effective role in the increasing of thermal stability of these materials which can be explained by the increasing in homogenous dispersion between the individual layers which lead to increasing in the thermal stability. The TGA results of PGMA and PGMA-MMT are listed in table 8.1 which shows that the weight loss temperatures of nanocomposites are higher than that of pure PGMA. For example, T_{dc} (central weight loss) of PGMA-MMT is higher than that of pure PGMA (400 °C), and increases by increasing the double modified clay content by 22 °C, 38 °C, 56 °C and 63 °C when 2, 6, 10 and 20 weight % of double modified clay is added respectively. Table 8.2 contains the TGA results of pure PMMA and PMMA-MMT nanocomposites and shows that T_{dc} of pure PMMA is 472 °C and increased by 17 °C, 37 °C, 44 °C and 46 °C when 2, 6, 10 and 20 weight % double modified clay is added respectively. Table 8.3 shows a comparison in the weight loss % in different temperatures between PGMA-MMT and PMMA-MMT when 6 weight % of double modified clay is added. From the table, it can be concluded that, PMMA-MMT nanocomposites have more thermal resistance compared with PGMA-MMT nanocomposites when using the same weight % of clay content. PGMA-MMT nanocomposites lose the weight more rapidly and at lower temperature than PMMA-MMT nanocomposites.

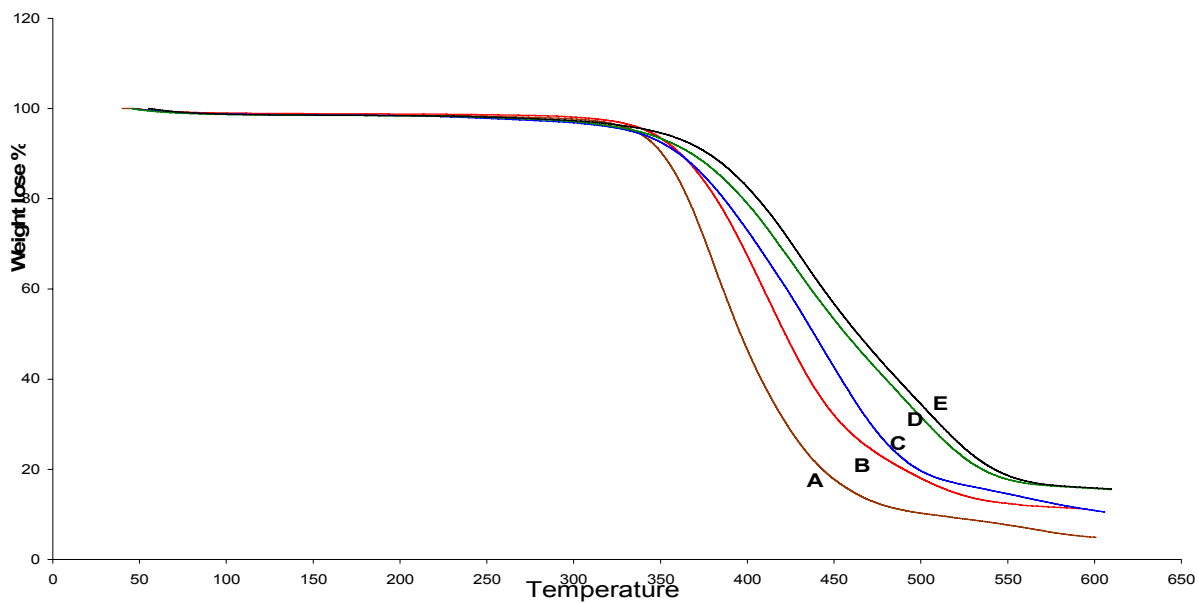


Figure 8.1: TGA thermograms of (A) Pure PGMA, (B)2%, (C)6%, (D)10% and (E)20% weight % MMT in PGMA-MMT nanocomposites.

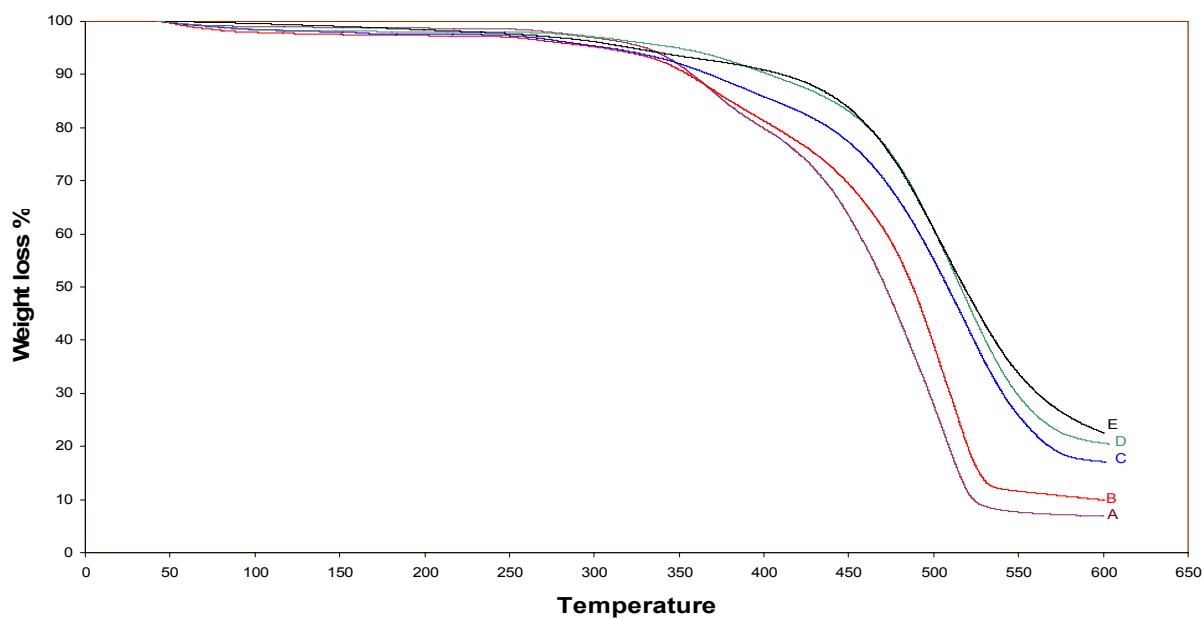


Figure 8.2: TGA thermograms of (A) Pure PMMA, (B)2%, (C)6%, (D)10% and (E)20% weight % MMT in PMMA-MMT nanocomposites.

Table 8.1: TGA data obtained for pure PGMA and PGMA-MMT nanocomposites

Degradation Temperature	Content of double modified clay %				
	0 %	2 %	6 %	10 %	20 %
T ₁₀	355	361	365	372	377
T ₂₀	370	382	386	397	406
T ₃₀	380	396	405	418	425
T ₅₀	400	422	438	456	463
T ₈₀	445	454	498	535	542

Table 8.2: TGA data obtained for pure PMMA and PMMA-MMT nanocomposites

Degradation Temperature	Content of double modified clay %				
	0 %	2 %	6 %	10 %	20 %
T ₁₀	347	360	367	402	410
T ₂₀	399	406	438	461	461
T ₃₀	433	448	471	485	484
T ₅₀	471	487	508	515	518
T ₈₀	508	519	568	-	-

Table 8.3: Comparison in the weight loss % between PGMA-MMT and PMMA-MMT when 6 weight % MMT is added in different temperatures

Temperature	Weight loss %	
	PGMA-MMT	PMMA-MMT
300	3,16	4,64
325	4,37	6,00
350	7,47	7,94
375	14,9	10,93
400	27,00	14,20
425	41,29	17,75
450	57,4	22,97
475	71,89	31,89
500	80,36	44,91
525	83,50	60,89
550	85,46	74,30
575	87,60	81,40
600	89,16	82,88

8.2.2. X-Ray Diffraction (XRD)

X-ray diffractograms of PGMA-MMT and PMMA-MMT nanocomposites when 6 weight % of double modified clay is used are illustrated in figure 8.3. It shows that there is no noticeable organoclay peak reflection appearing in the diffraction pattern for both PGMA-MMT and PMMA-MMT nanocomposites. This means that the silica layers were completely delaminated and led to production of exfoliated nanocomposites [400] with both PGMA and PMMA.

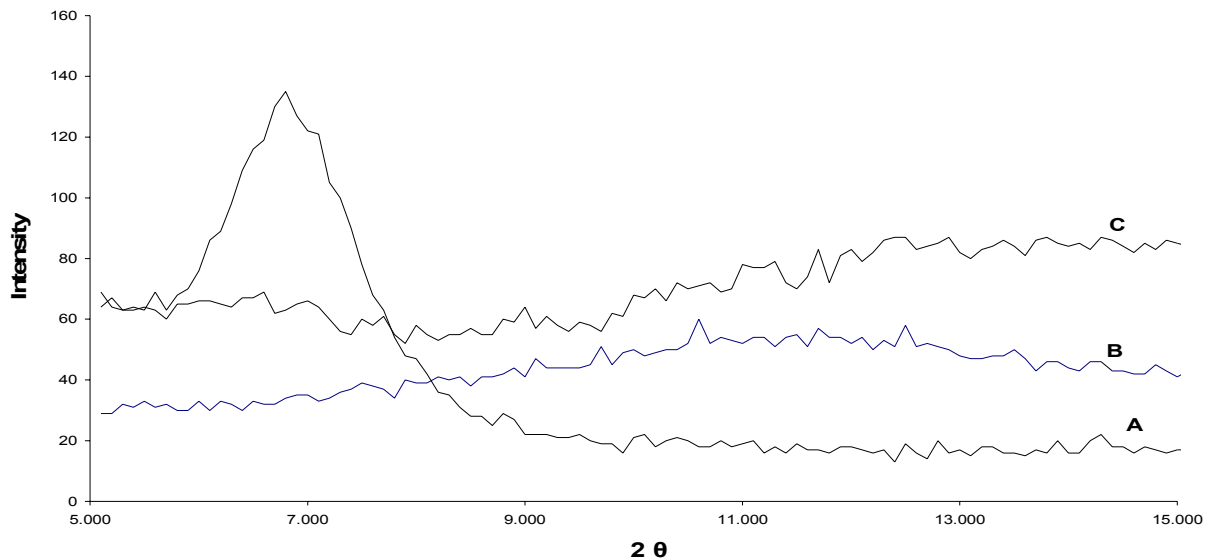


Figure 8.3: XRD patterns of (A) double modified MMT (B) PGMA-MMT nanocomposites (C) PMMA-MMT nanocomposites

8.2.3. Scanning Electron Microscope (SEM)

The examination of the surface of prepared samples was investigated by SEM. The SEM images indicate that the PGMA and PMMA are homogeneously intercalated in the interlayer of MMT clay to produce clay / polymer nanocomposites. Figure 8.4 shows SEM of pure PGMA and PGMA-MMT nanocomposites where small aggregates of around 5 μm in size together with few large aggregates are observed in the PGMA-MMT image, the presence of these aggregates indicate the poorly dispersed of MMT clay particles in the polymer matrix. On the other hand, figure 8.5 shows SEM of pure MMA and PMMA-MMT nanocomposites where MMT particles did not appear at micro level where the absence of MMT particles indicates, that the agglomerate did not reveal the inorganic domain. The particle size of MMT is not visible because it is well adherent to the polymer. This indicates that the mineral domains are submicron and homogeneously dispersion of MMT clay particles in the

polymer matrix and also indicates that the PMMA was intercalated in the interlayer of MMT clay in a homogenous matter [401].

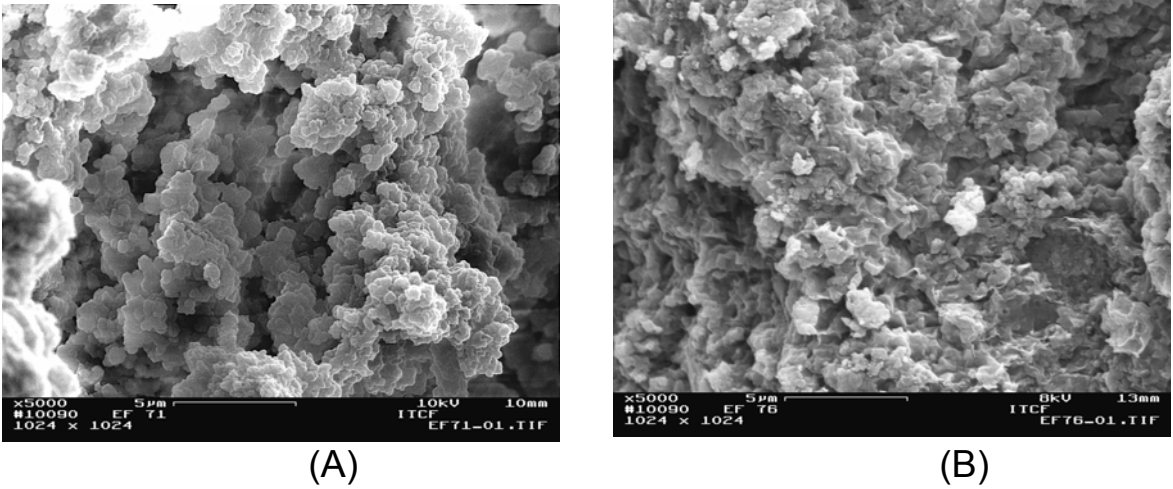


Figure 8.4: SEM images of (A) pure PGMA, (B) PGMA-MMT

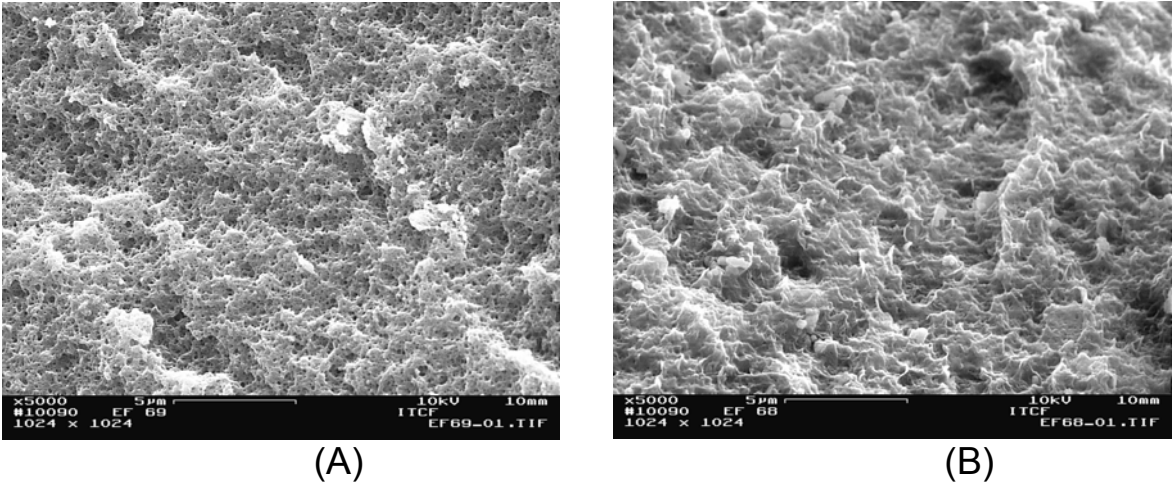


Figure 8.5: SEM images of (A) pure PMMA, (B) PMMA-MMT

8.3. Conclusion

- 1- Nanocomposites were successfully prepared by in situ emulsion polymerization of glycidyl methacrylate (GMA) and methyl methacrylate (MMA) monomers using redox initiation systems.
- 2- X-ray diffraction (XRD) investigation showed that exfoliated structures were formed during the preparation of polyglycidyl methacrylate – montmorillonite nanocomposites (PGMA-MMT) and polymethyl methacrylate – montmorillonite nanocomposites (PMMA-MMT).
- 3- Scanning electron microscope SEM shows that MMT clay is poorly dispersed in the polymer matrix in case of PGMA due to appearance of small aggregates of around 5um in size together with few large aggregates in the PGMA-MMT image while it is homogenously dispersed in case of PMMA.
- 4- Thermal gravimetric analysis (TGA) results show that all weight loses temperatures for the nanocomposite samples are higher than that of the pure polymers in both PGMA and PMMA which can be attributed to the restriction of the motion of organic chains attached to MMT clay. It is also obvious that, increasing the clay content plays an effective role in the increase of thermal stability of these materials which can be explained by the increasing in homogenous dispersion between the individual layers which lead to increasing in the thermal stability.

CHAPTER 9

Solution Preparation of Polyolefin / Montmorillonite Nanocomposites

9.1. Introduction

Polymer nanocomposites are commonly defined as the combination of a polymer matrix and nano-reinforcement additives that have at least one dimension in the nanometer range. The nano additives can be one dimensional (examples include nanotubes and fibres), two dimensional (which include layered mineral like clay), or three dimensional (including spherical particles) [108]. Over the past decades, polymer nanocomposites have attracted considerable interests in both academia and industry, owing to their outstanding mechanical properties [37,109-110] like elastic stiffness [111] and strength with only a small amount of additives. This is caused by the effect of large surface area to volume ratio of nano additives when compared to micro- and macro-additives [112]. Other superior properties of polymer nanocomposites include barrier resistance [113], gas permeability [114-115], thermal stability [116], flame retardancy [117], scratch/wear resistance [118] as well as optical [119], magnetic [120] and electrical properties [121].

Polyolefin are among the most interesting polymers that are deemed to benefit the most from the formation of nanocomposites [221,270,419-424] with clay, due to their wide spread application. Polypropylene exhibits an attractive combination of low cost, low weight, and extraordinary versatility in terms of properties, recycling and applications [425-426] Polypropylene is a commodity polymer used in a wide range of products ranging from automotive applications such as automotive bumpers and interior parts of automobile to packaging applications such as pouches for ready-to-eat meals and other food containers. Conventional fillers such as talc and mica are used at a rather high loading up to 40 wt% to improve mechanical properties and dimensional stability [220]. Polyethylene is probably the polymer which is seen most in daily life. This is the polymer that makes grocery bags, shampoo bottles, children's toys, and even bullet proof vests. Choices of surfactant, polymeric compatibilizer and other coupling agents are critical for optimizing the dispersion and properties of polyolefin clay nanocomposites. The interaction between the oxygen atoms on the

clay surface and the polymeric compatibilizer must be stronger than between the clay surface and the surfactant in order to obtain delamination of the silicates [427]. The polymeric compatibilizer must also be miscible with the bulk polypropylene [428]. Hence the structure of the surfactant and of the polymeric compatibilizer must be carefully engineered. In this work polyolefin / montmorillonite nanocomposites have been obtained by the solution method using xylene as solvent in case of polypropylene and using xylene – benzonitrile co-solvent in case of polyethylene.

9.2. Structure and Properties of Polyolefin Nanocomposites

9.2.1. Infra-Red (IR)

Figure 9.1 displays the FTIR of pure PE, DM-MMT and PE + 5% DMMMT nanocomposites, whereas figure 9.2 displays the FTIR of pure PP, DM-MMT and PP + 5% DMMMT nanocomposites. From the figures it can be concluded that, the appearance of the absorption band at 1092 cm^{-1} which is the characteristic band of Si-O group [18] in both DM-MMT clay and nanocomposite curves indicates the successfully preparation of polyolefin / montmorillonite nanocomposites.

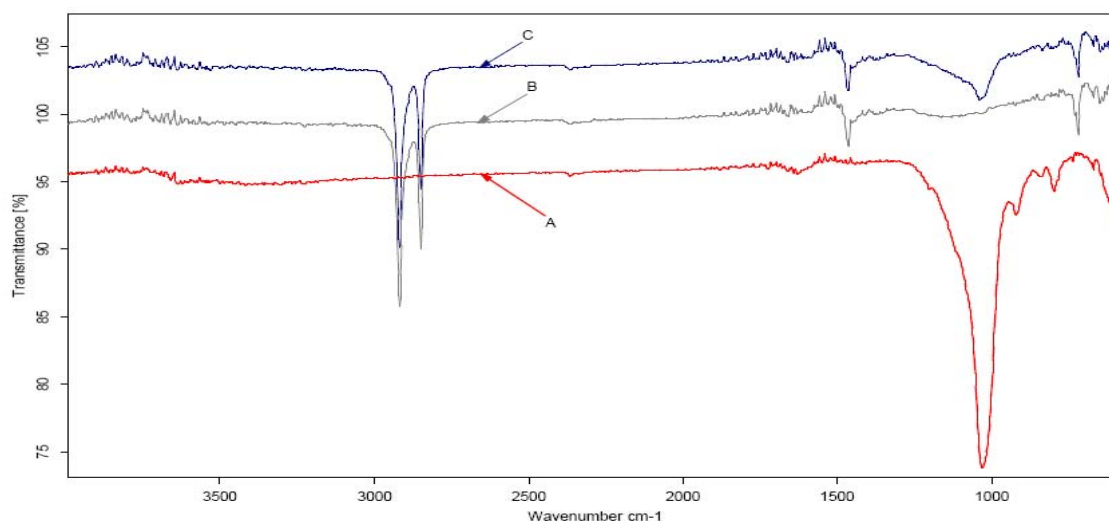


Figure 9.1: FTIR spectrum of A) DM-MMT, B) Pure PE and C) PE + 5% DM-MMT nanocomposite.

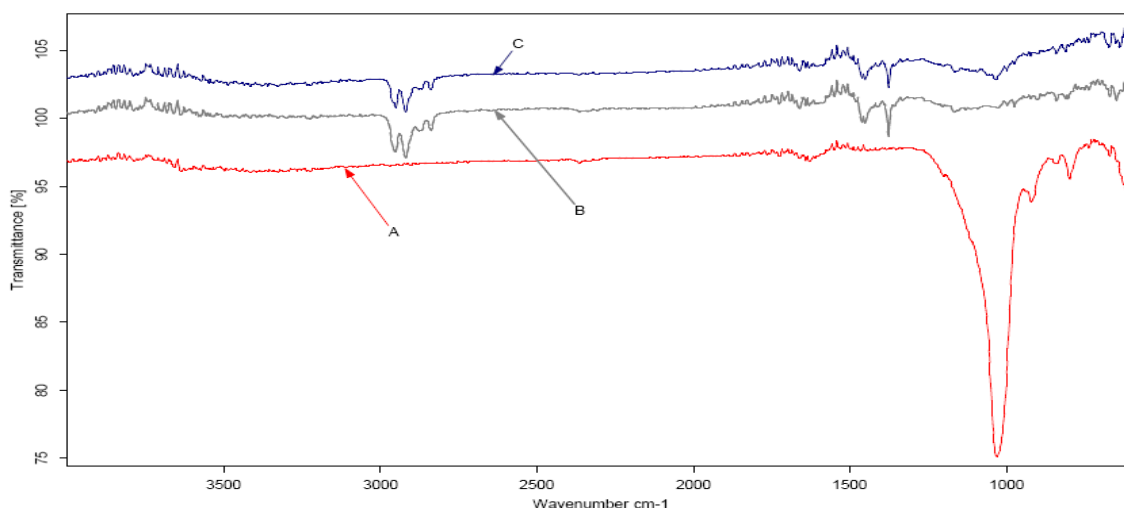


Figure 9.2: FTIR spectrum of A) DM-MMT, B) Pure PP and C) PP + 5% DM-MMT nanocomposite.

9.2.2. Thermal Gravimetric Analysis (TGA)

The thermal stability of the pure polyolefin and the prepared polyolefin nanocomposites with different modified montmorillonite clay was determined by thermogravimetric analysis (TGA) within the temperature range 50-600 °C, as illustrated in figures 9.3 and 9.4. The detailed data corresponding to the temperature point at which weight loss starting temperature (T_{start}), 25% weight loss temperature (T_{25}), 50% weight loss temperature (T_{50}) and 75% weight loss temperature (T_{75}) are listed in table 9.1. The temperature at which 25% degradation occurs (T_{25}) was found to increase by 65°C in case of polyethylene and increase by 132°C in case of polypropylene for the DM-MMT and by 62°C in case of polyethylene and increase by 126°C in case of polypropylene for the Leucine-MMT, whereas only 18°C in case of polyethylene and increase by 37°C in case of polypropylene for the Na-MMT. The mid-point degradation temperature (T_{50}) and the temperature at which 75% degradation occurs (T_{75}) were also found to be higher for the polymer nanocomposites than that of neat polyolefin. From the data illustrated in the figures 9.3, 9.4 and listed in table 9.1 it is clear that all weight loss temperatures for the nanocomposites samples are higher than that of pure polymer which can be attributed to the restriction of the motion of organic chains attached to MMT clay [270]. It can be also stated that the DM-MMT and Leucine-MMT nanocomposites seems to have the highest thermal stability relative to Na-MMT nanocomposites. This might be attributed to a maximized interaction between the clay and the polymer in the nanocomposites structure, due to the availability of a larger surface

area of clay in case of modified and double modified clay [85]. Finally, it is also clear that DM-MMT nanocomposites seems to have higher thermal stability than Leucine-MMT which may be due to the presence of silane coupling agent in case of DM-MMT nanocomposites.

Table 9.1: TGA data obtained for pure polyolefin and the prepared polyolefin nanocomposites

	Polyethylene				Polypropylene			
	Pure PE	PE + 5% Na-MMT	PE + 5% Leucine-MMT	PE + 5% DM-MMT	Pure PP	PP + 5% Na-MMT	PP + 5% Leucine-MMT	PP + 5% DM-MMT
T _{Start}	130	148	192	195	254	291	380	386
T ₂₅	192	212	233	239	353	370	400	407
T ₅₀	220	237	255	266	389	406	426	438
T ₇₅	244	263	275	295	413	432 </td <td>443</td> <td>464</td>	443	464

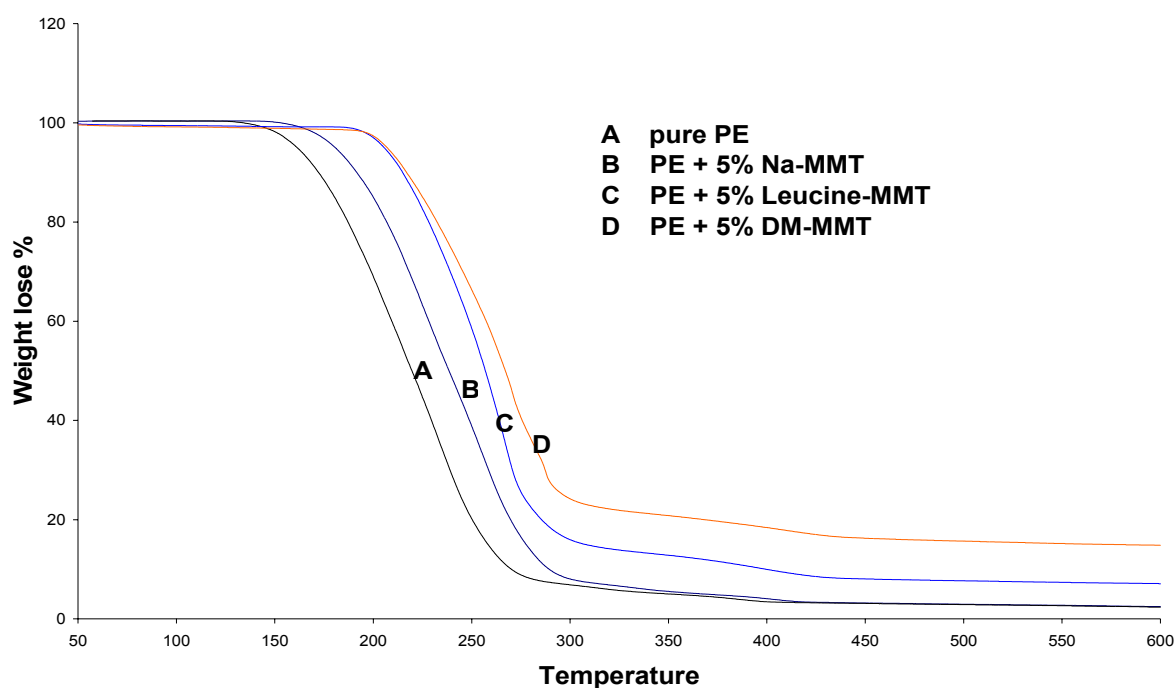


Figure 9.3: TGA thermograms of pure PE and the prepared PE nanocomposites with different modified montmorillonite clay

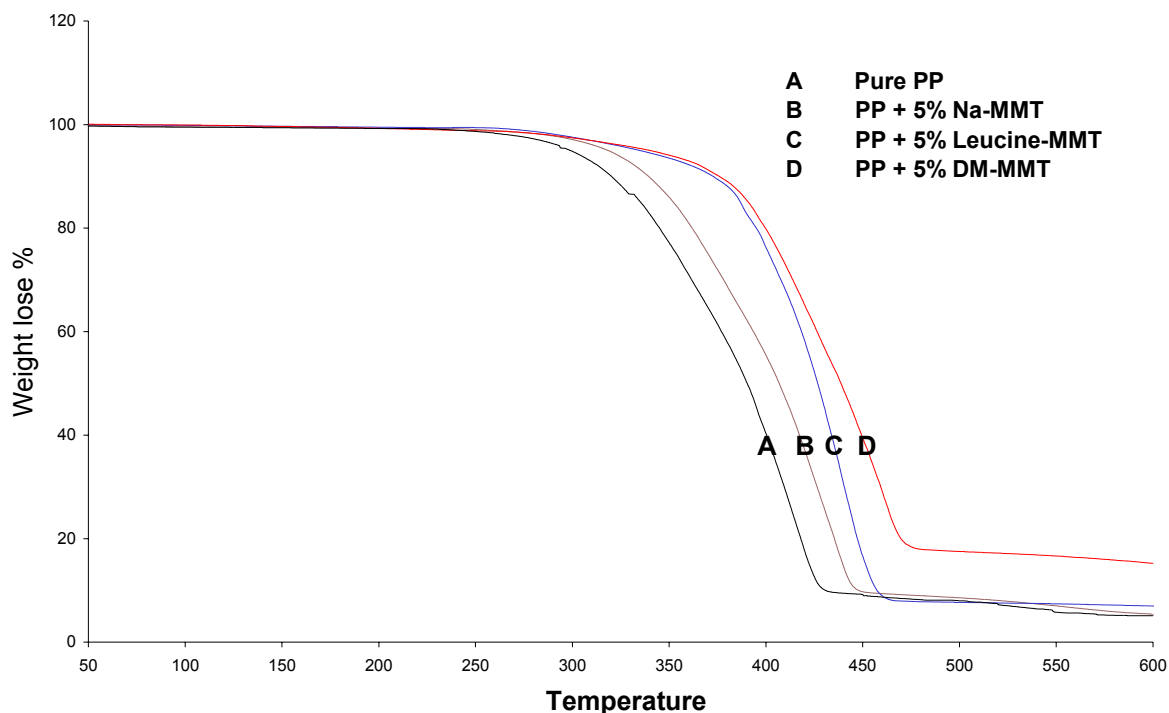


Figure 9.4: TGA thermograms of pure PP and the prepared PP nanocomposites with different modified montmorillonite clay

Effect of the percentage of double modified montmorillonite clay (DM-MMT) on the thermal stability of the prepared polyolefin / montmorillonite nanocomposites was studied by thermogravimetric analysis (TGA), within the temperature range 50-600 °C as illustrated in figures 9.5 and 9.6. From these figures and from the detailed data listed in table 9.2 it can be concluded, that the increasing in the clay content plays an effective role in the increasing of thermal stability of polyolefin / montmorillonite nanocomposites which can be attributed to the homogenous dispersion of the filler within the matrix [429-430].

Table 9.2: TGA data obtained for pure the prepared polyolefin nanocomposites with different percentage of DM-MMT.

	Polyethylene			Polypropylene		
	PE + 5% DM-MMT	PE + 10% DM-MMT	PE + 15% DM-MMT	PP + 5% DM-MMT	PP + 10% DM-MMT	PP + 15% DM-MMT
T _{Start}	195	211	259	386	398	418
T ₂₅	239	264	320	407	444	474
T ₅₀	266	297	346	438	466	495
T ₇₅	295	339	367	464	480	509

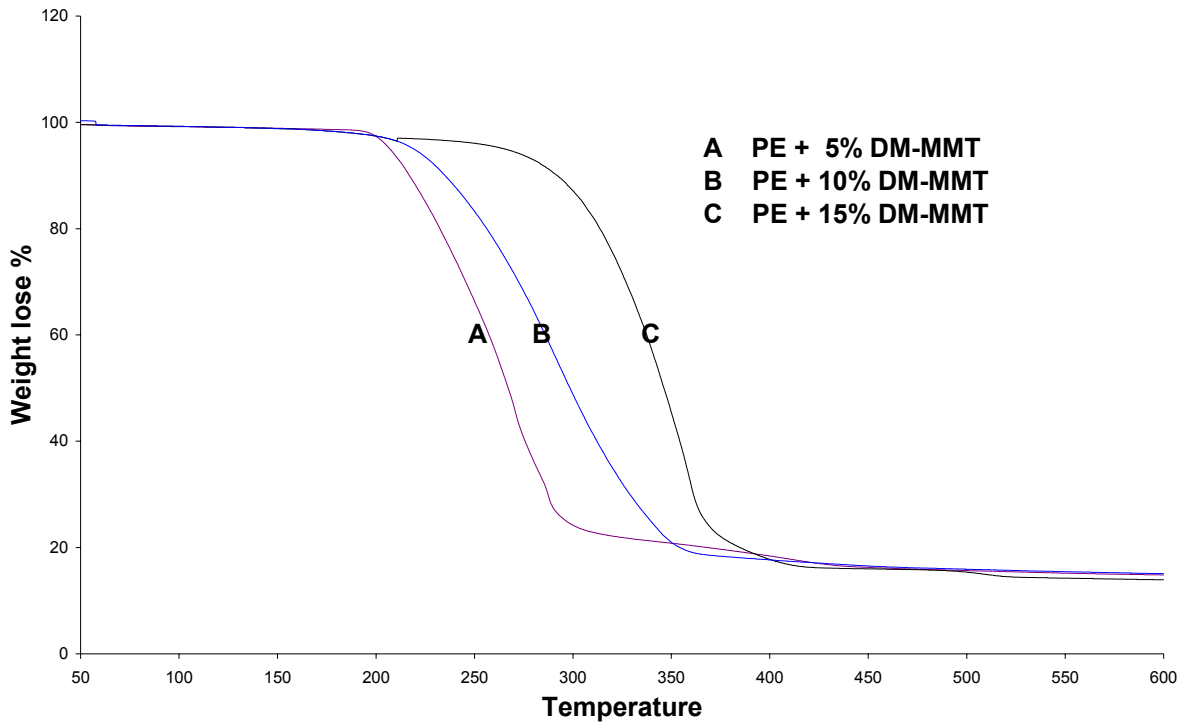


Figure 9.5: TGA thermograms of the prepared PE nanocomposites with different double modified montmorillonite clay percentage

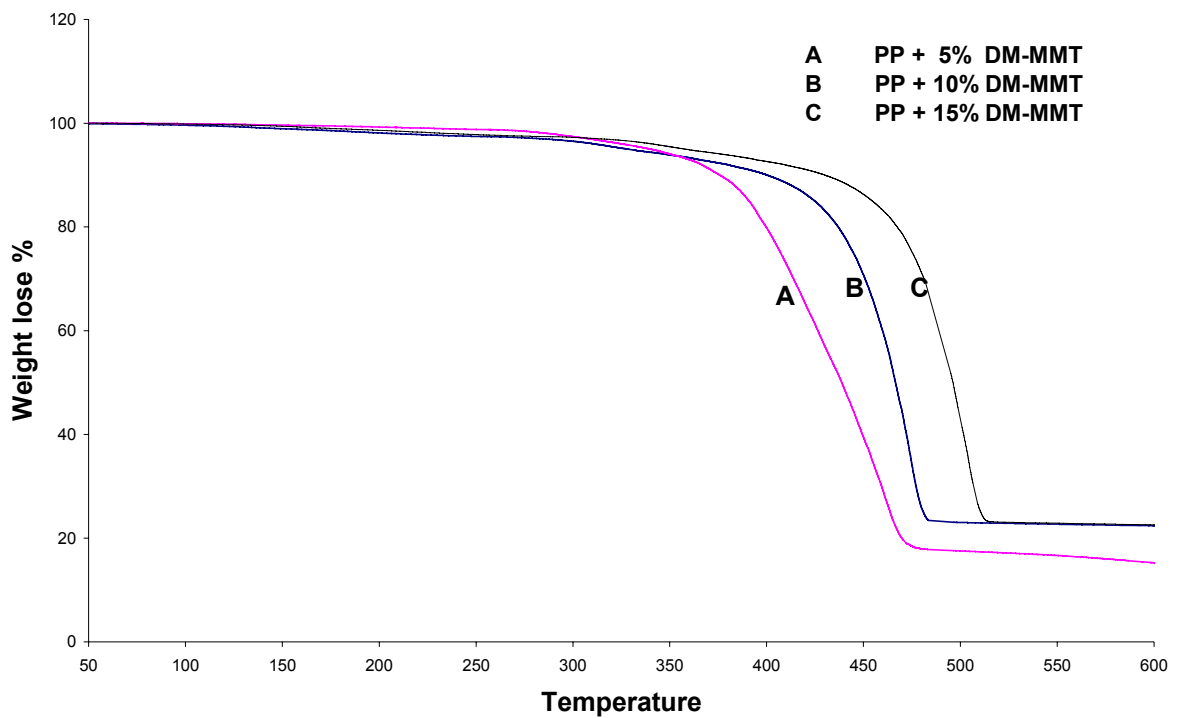


Figure 9.6: TGA thermograms of the prepared PP nanocomposites with different double modified montmorillonite clay percentage

9.2.3. Melting Point (MP)

The melting points of the pure polyolefin and the prepared polyolefin / montmorillonite nanocomposites were also measured. The measured melting temperatures are plotted in figure 9.7. From this figure and from the listed results in table 9.3, it is obvious, that the addition of 5%Na-MMT has no great effect in the melting temperature of polyolefin whereas the melt temperature of the pure polyolefin was approximately 2-3°C lower than polyolefin/5%Leucine-MMT nanocomposite and 5-7°C lower than polyolefin/5%DM-MMT nanocomposite. From the data it can be also concluded, that the increasing of the DM-MMT percentage is directly proportional with increasing melting points of the nanocomposite

Table 9.3: Melting points of pure polyolefin and the prepared polyolefin / montmorillonite nanocomposites

	PE	PP
Pure polyolefin	123,5	162
Polyolefin+5% Na-MMT	123,9	162,7
Polyolefin+5% Leucine-MMT	126,8	164,6
Polyolefin+ 5% DM-MMT	129,1	168,8
Polyolefin+10% DM-MMT	133,4	174,7
Polyolefin+ 15% DM-MMT	135,5	177,1

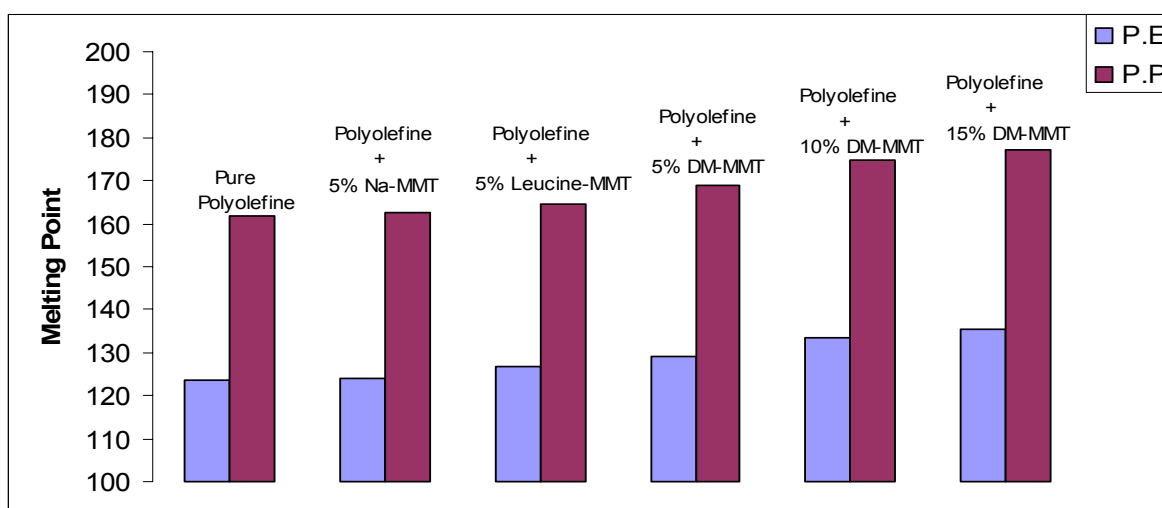


Figure 9.7: Melting points of pure polyolefin and the prepared polyolefin / montmorillonite nanocomposites

9.2.4. X-Ray Diffraction (XRD)

X-ray diffraction patterns of different PE nanocomposites with 5% of unmodified, modified and double modified MMT clay are displayed in figure 9.8. From this figure it can be concluded, that the clay is insoluble in the polymer matrix in case of Na-MMT clay whereas intercalated PE nanocomposites were formed with diffraction peak at 2θ value 7.2° in case of both Leucine-MMT and DM-MMT clay. Figure 9.9 shows XRD patterns of different PP nanocomposites with 5% of unmodified, modified and double modified MMT clay. From this figure it can be seen, that intercalated PP nanocomposites were formed in case of both Leucine-MMT and DM-MMT whereas the diffraction peak was present at 2θ value 7.0° in case of PP/5% Na-MMT nanocomposite and at 2θ value 6.5° in case of PP/5% Leucine-MMT nanocomposite. On the other hand, PP/5% DMT-MMT nanocomposite did not show any diffraction peak in the range of $2\theta = 5-15^\circ$, suggesting the formation of exfoliated structure in the formed nanocomposite [431]. Effects of the percentage of DM-MMT clay on the type of PP nanocomposite formed are studied by XRD and illustrated in figure 9.10. From this figure it is obvious that the diffraction peak did not present in case of both 5% DM-MMT and 10% DM-MMT clay whereas the diffraction peak was present at 2θ value 6.1° in case of 15% DM-MMT clay which indicates that exfoliated nanocomposite was formed in case of both PP/5% DM-MMT and PP/10% DM-MMT clay but only intercalated nanocomposite was formed in case of PP/15% DM-MMT.

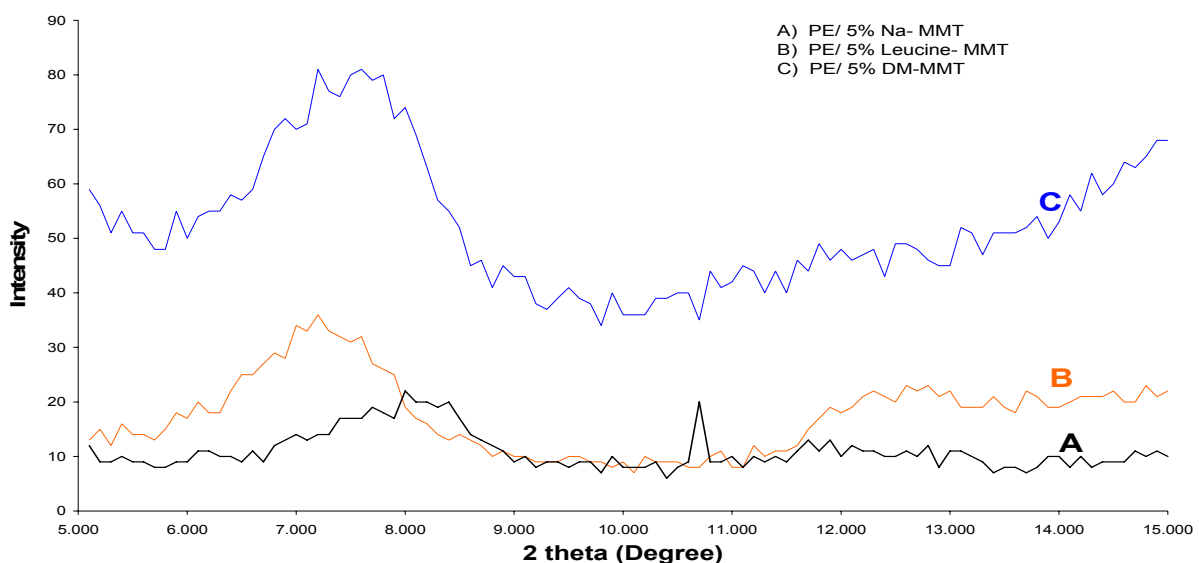


Figure 9.8: XRD patterns of (A) PE/5%Na-MMT, (B) PE/5%Leucine/MMT and (C) PE/5%DM-MMT nanocomposites.

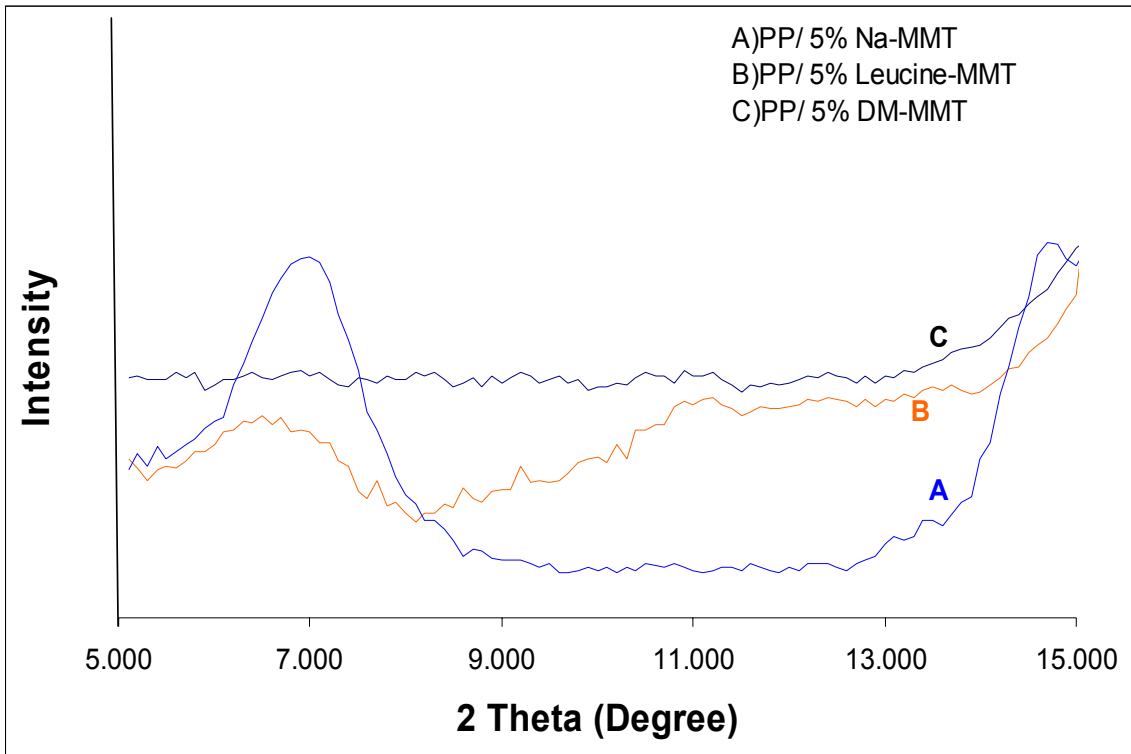


Figure 9.9: XRD patterns of (A) PP/5%Na-MMT, (B) PP/5%Leucine/MMT and (C) PP/5%DM-MMT nanocomposites.

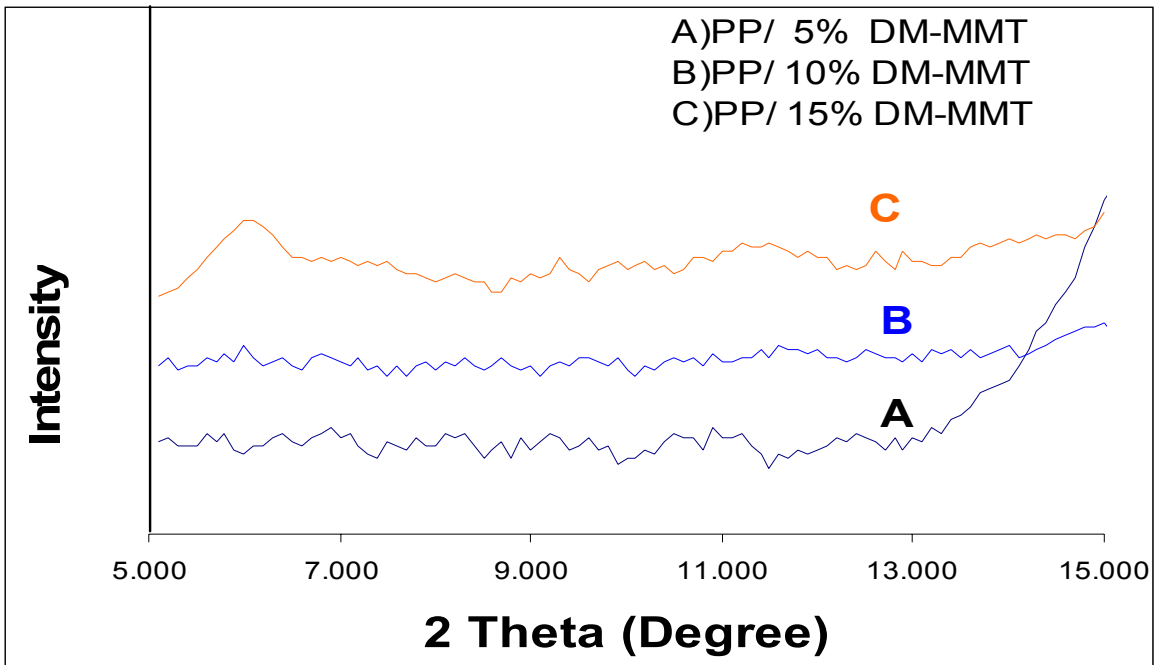


Figure 9.10: XRD patterns of (A) PP/5%DM-MMT, (B) PP/10%DM-MMT and (C) PP/15%DM-MMT nanocomposites.

9.2.5. Scanning Electron Microscope (SEM)

The surface morphology of the prepared samples was investigated by SEM at X1000 magnification. Figure 9.11 displays SEM micrographs of pure PE and the prepared PE nanocomposites with different modified montmorillonite clay. From the figure it is clear that, MMT clay is insoluble in the polymer matrix in case of PE/5%Na-MMT, where the clay particles are poorly dispersed in the polymer matrix in case of PE/5%Leucine-MMT and PE/5%DM-MMT. On the other hand figure 9.12 shows SEM of pure PP and the prepared PP nanocomposites with different modified montmorillonite clay. Where MMT clay particles are poorly dispersed in the polymer matrix in case of PP/5%Na-MMT and PE/5%Leucine-MMT but the homogenous intercalation between the clay particles and the polymer matrix is obtained in case of PP/5%DM-MMT.

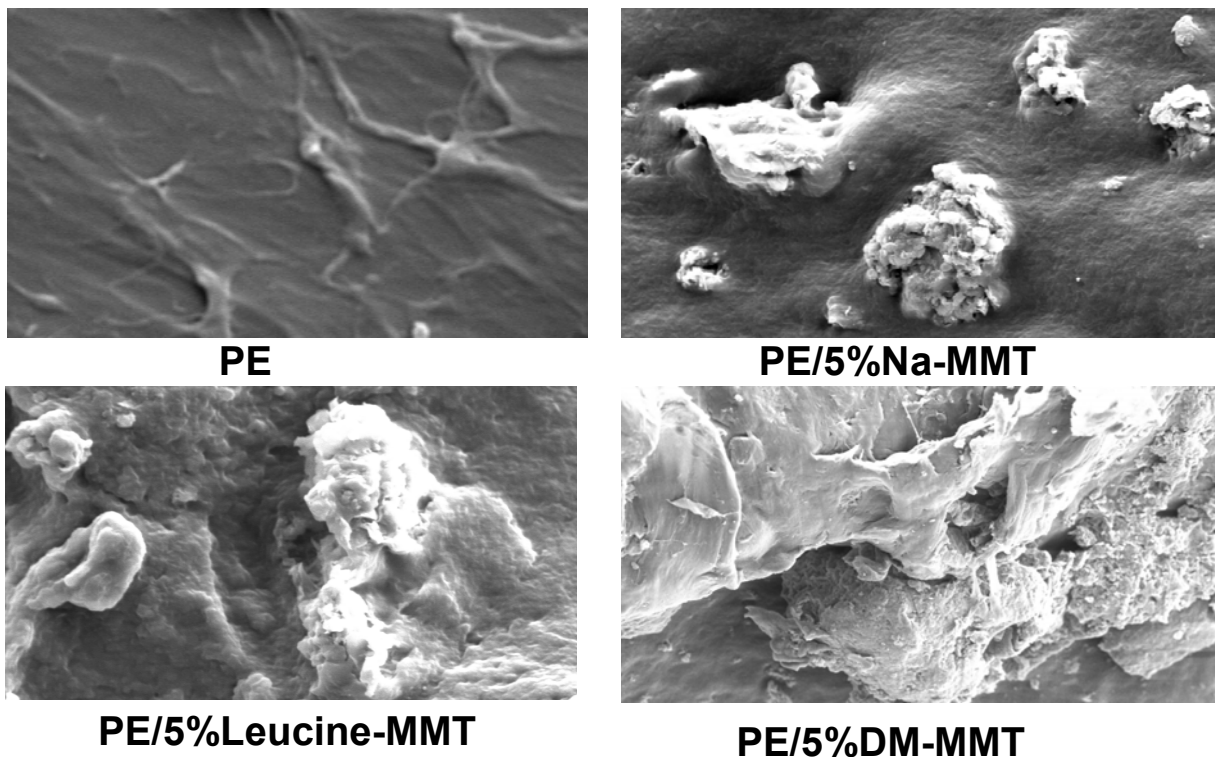
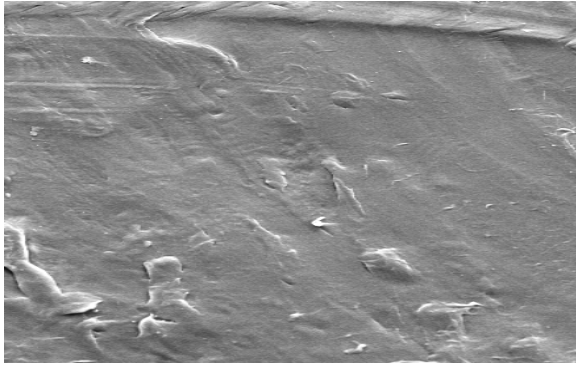
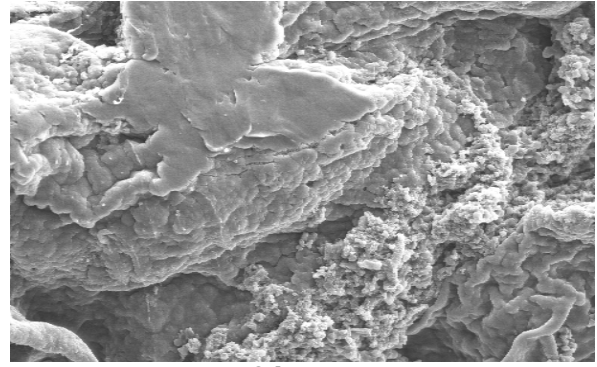


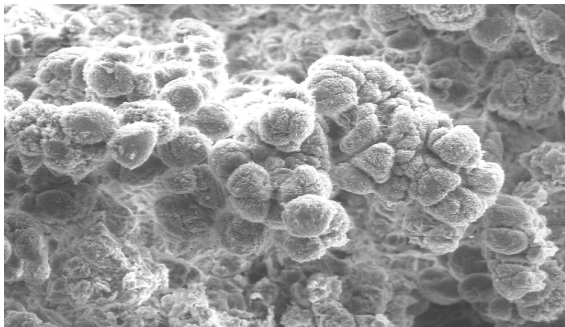
Figure 9.11: SEM of pure PE and the prepared PE nanocomposites with different modified montmorillonite clay



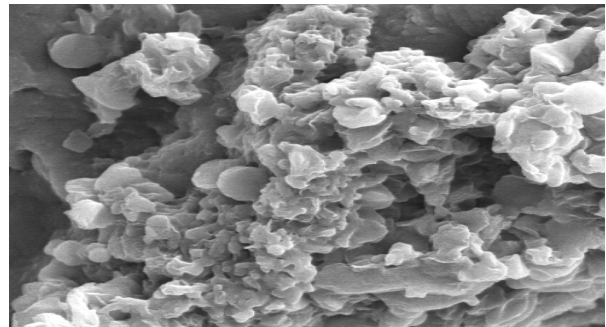
PP



PP/5%Na-MMT



PP/5%Leucine-MMT



PP/5%DM-MMT

Figure 9.12: SEM of pure PP and the prepared PP nanocomposites with different modified montmorillonite clay

9.3. Conclusion

- 1- Polyolefin montmorillonite nanocomposites were successfully prepared by solution polymerization using xylene in case of polypropylene (PP) and xylene – benzonitrile (80-20 %) in case of polyethylene (PE).
- 2- Thermal gravimetric analysis (TGA) results show, the weight loses temperatures for polypropylene and polyethylene nanocomposites depend on the type of clay modification and the thermal stability for the prepared nanocomposites was as follow:

Polyolefin/DM-MMT > Polyolefin/Leucine-MMT > Polyolefin/Na-MMT

It is also obvious, that increasing DM-MMT clay content plays an effective role in the increase of thermal stability of polyolefin nanocomposites.

- 3- X-ray diffraction (XRD) investigations show that good exfoliation nanocomposite was achieved in the preparation PP/ DM-MMT up to DM-MMT 10 Wt% and after this concentration of DM-MMT diffraction peak is observed again. Insoluble nanocomposites were obtained in case of PE/Na-MMT, whereas intercalated nanocomposites were achieved in the preparation of PP/Na-MMT, PP/ Leucine-MMT, PE/ Leucine-MMT and PE / DM-MMT.
- 4- Scanning electron microscope (SEM) shows, that homogenously dispersions of MMT clay in the polymer matrix were observed only in the case of PP/DM-MMT. MMT clay was insoluble in the polymer matrix in case of PE/Na-MMT whereas MMT was poorly dispersed in polyolefin matrix in all other cases.

CHAPTER 10

Elucidation of the Nanoparticles Effect in the Grafting of Vinyl Monomers onto Cotton Fabric

10.1. Introduction

Nanocomposite materials are widely used in various fields depending on the composite nature and structure [63]. Among these fields is the application in textiles where two principle ways can be considered for the use of nanocomposites in textile applications. Melt spinning of nanocomposite polymer [64] which can be subsequently woven or knitted, has been demonstrated as a promising approach for textile fire retardant applications [65-66]. Also coating of textile surfaces by nanocomposites formulation is another interesting way for the use of nanocomposites in textile application. In addition, the latter approach confers to textile surfaces other properties such as impermeability to water or gases for instance. Moreover, the incorporation of nanoparticles in polymers for fire retardant applications makes it possible to limit the toxicity of the degradation products compared with the more traditional additives such as halogenated products [67-69]. In addition, the use of nanocomposites allows a reduction in the weight content of additives [66]. Cotton is a widely used natural, healthy and cheap textile material. Nearly 94 % of its chemical structure consists of cellulose molecules. Where cotton is used to produce regenerated cellulose fibers, which have numerous textile applications. A major drawback of cotton is its inherent ability to burn. Many finishes have been developed to impart flame resistance to cotton. These finishes have limited use in textile for apparel because of problems with the finish remaining on the fabric after laundering or problems with the fabric holding up to water [2]. Most of these finishes have been developed for products that are not laundered, such as drapery and furnishing fabrics [164,432,433]. The textile industry has a high demand for cotton with improved physical and chemical properties [434]. Vinyl grafting polymerization onto cellulose has been successfully developed [405,435-440]. This work aims to elucidate the effect of nanoparticles in grafting emulsion polymerization of vinyl monomers onto cotton fabric by using redox initiation systems by comparing

the grafting percentage of cotton samples when the grafting takes place in presence and in absence of modified montmorillonite clay by studying the factors affecting grafting percentage as nanoparticles concentration, temperature, time, initiator concentration and monomer concentration.. And also study the effect of the treatment of the grafted cotton samples by different concentrations of dibutyl amine.

10.2. Factors Affecting Graft Polymerization of Vinyl Monomers onto Cotton Fabric

10.2.1. Effect of Double Modified Montmorillonite Clay Concentration

Graft polymerization onto cotton fibers was carried out with two types of vinyl monomers namely glycidyl methacrylate (GMA) and methyl methacrylate (MMA) in the presence of different weight % of double modified Montmorillonite clay (MMT) ranging between 2 and 20 Wt % using emulsion technique in presence of redox initiation system consisting potassium persulphate (PPS) as an oxidizing agent as well as sodium bisulphite (SBS) as a reducing agent and sodium dodecyl sulphate (SDS) as an emulsifier. The reaction was carried out at 70 °C for 60 min with 3 % monomer concentration. The results are illustrated in figure 10.1 which shows that, for both monomers used, the grafting yields initially increased with increasing the MMT clay Wt % and then decreased. From the data illustrated in this figure, it can be concluded that, GMA-MMT shows the highest rate of grafting in all clay concentrations. The difference in the grafting yield between GMA-MMT and MMA-MMT is due to the difference in behaviours of the monomers which depend on such factors as relative tendency to activation, polarization of the vinyl double bond, the ability of the monomer molecules to converted to free radicals, the ability of the monomer radicals to graft or homo-polymerized, the miscibility and diffusion of the monomer radicals from the aqueous phase to the fibre phase [405].

From the data illustrated in figure 10.1, it can be also noted that, in case of GMA-MMT, the graft yield increases gradually by increasing the MMT clay weight percentage to attain the maximum at 10 MMT clay concentrations, thereafter it falls. This could be interpreted in terms of coating of cotton fibre surfaces by MMT clay at high clay concentration and then the surface of cotton fibres becomes closed for GMA penetration.

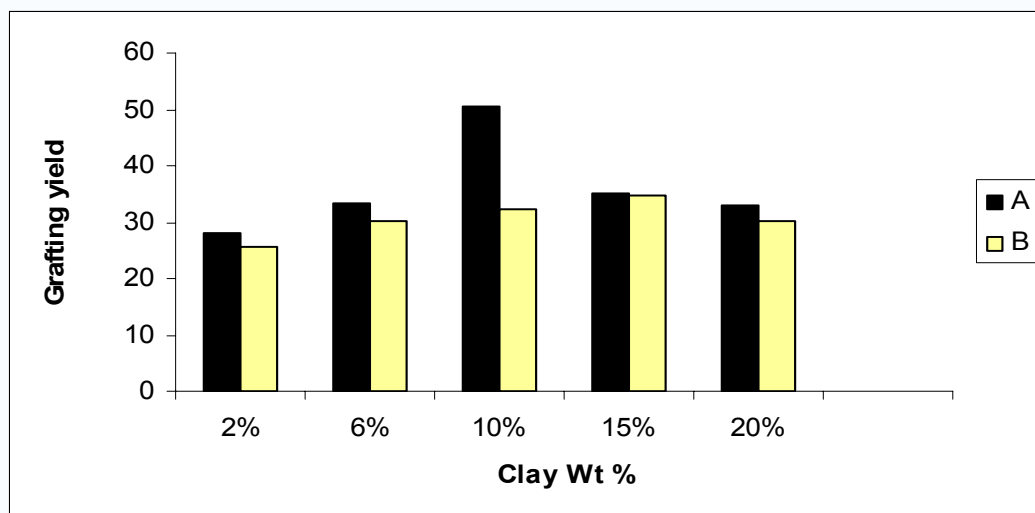


Figure 10.1: Effect of MMT concentration on the grafting yields of A) GMA and B) MMA monomers onto cotton

10.2.2. Effect of Temperature

The effect of temperature on the graft yield of GMA onto cotton fibers at constant concentration of initiator, emulsifier and monomer was studied within the range of 50 to 80 °C. The results are illustrated in figure 10.2. It is evident, regardless the presence of MMT clay (10 % concentration), as the temperature increased, the grafting yield also increased, reached a maximum value, and then decreased. The initial increase in the graft yield may be due to the raising in the temperature increases the efficiency of the redox initiation system. Maximum grafting yield was observed at 70 °C in the case of GMA-MMT and also in the absence of MMT clay. The grafting yield of GMA onto cotton in the presence of MMT clay was higher than in the absence of clay of all temperatures. The decrease in the grafting yield at higher temperatures in the two cases was due to the favoured chain termination reactions and the increase in the homopolymer formation at high temperature [434].

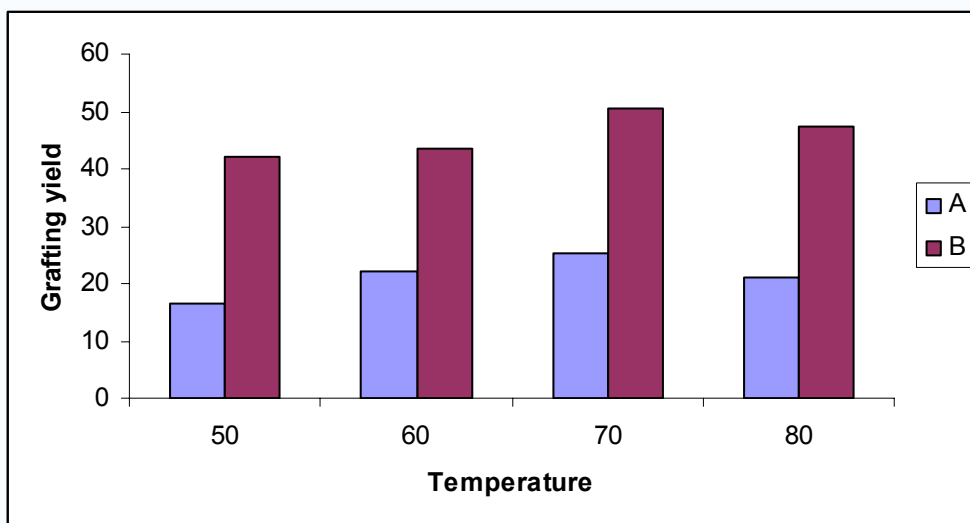


Figure 10.2: Effect of Temperature on the grafting yields of A) GMA and B) GMA-MMT onto cotton

10.2.3. Effect of Time

The effect of time on the graft yield was investigated by using different reaction time intervals which are 15, 30, 45, 60, 75, 90, 105 and 120 min. as shown in figure 10.3, in both two cases; the rate of the grafting starts very fast then tends to level-off after 60 min in case of GMA and after 90 min in case of GMA-MMT. This department could be attributed to depletion in both the monomer and initiator as well as the changes in the components of the system as the reaction proceeds [405]. It must be also noted that The grafting yield of GMA monomer onto cotton in the presence of MMT clay was higher than in the absence of clay of all time intervals

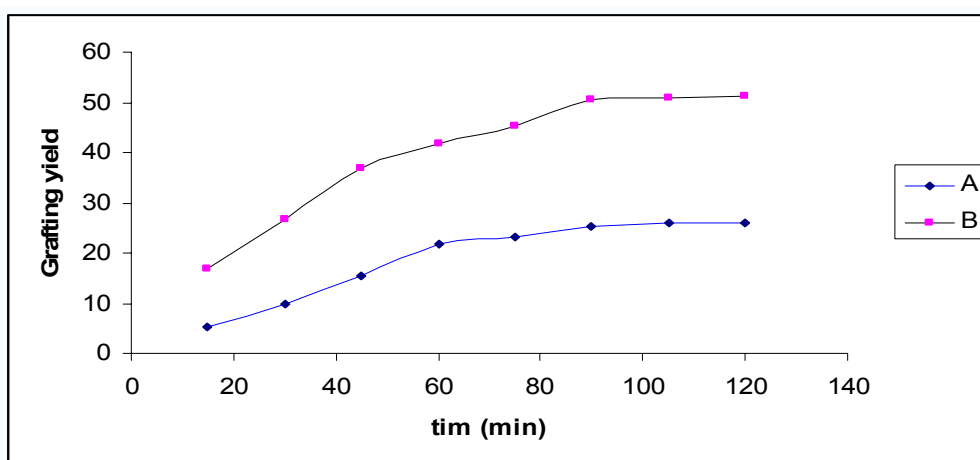


Figure 10.3: Effect of Time on the grafting yields of A) GMA and B) GMA-MMT onto cotton

10.2.4. Effect of Initiator Concentration

Effect of initiator concentration on the grafting of GMA and GMA-MMT onto cotton fibres is shown in figure 10.4. Grafting was carried out at initiator concentration ranging from 0,25 to 2,0 mmol /l. the data illustrated in figure 10.4 shows, that in case of GMA-MMT, the grafting yield is rapidly increased as the initiator concentration increased till an initiator concentration of 1,5 mmol/l. Above this concentration, the grafting continue increased but less rapidly. In case of GMA monomer, the graft yield increased significantly as the initiator concentration increases till an initiator concentration of 1.0 mmol/l. After this concentration, further increases in the initiator concentration decreased the grafting yield. This may be due to at high initiator concentration, the free radicals reacted with cellulose radical and growing polymer chains, which resulted in termination or combination reactions; consequently, the grafting yield decreased.

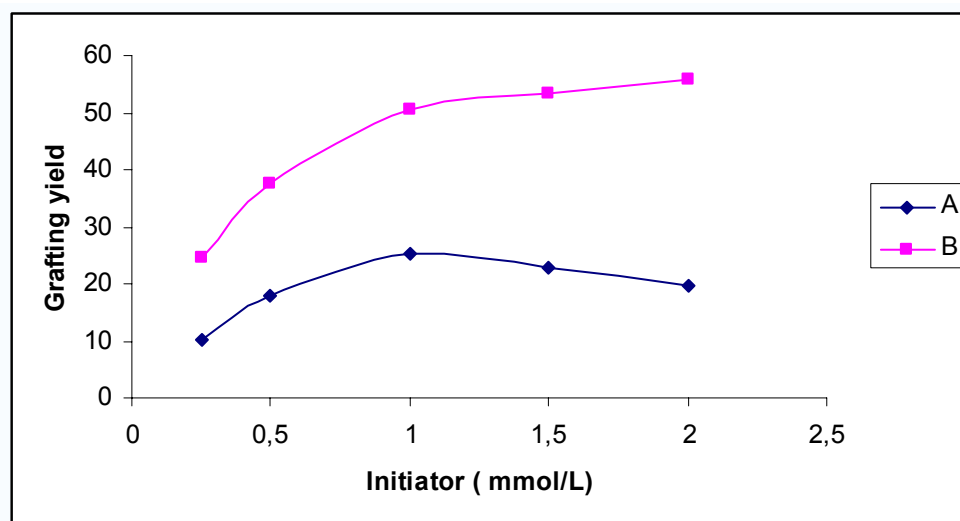


Figure 10.4: Effect of initiator concentration on the grafting yields of A) GMA and B) GMA-MMT onto cotton

10.2.5. Effect of Monomer Concentration

Figure 10.5 shows the effect of GMA monomer concentration in the range from 0,5 to 5,0 % on the grafting yield at constant initiator and emulsifier concentration. It is obvious, that regardless the presence of double modified MMT clay, the grafting yield increased with increasing the monomer concentration within the range studied. This may be due to the fact that at high monomer concentration, a higher number of growing polymer chains is available, which are mainly utilized for grafting

polymerization. Other probable explanation could be associated with greater availability of monomer molecules at higher monomer concentration in the proximity of cotton fibres. From figure 10.5 it can be noted, that the rate of grafting tends to level-off at monomer concentration 3 % in case of GMA monomer but no noticeable level-off for the grafting rate in case of GMA-MMT.

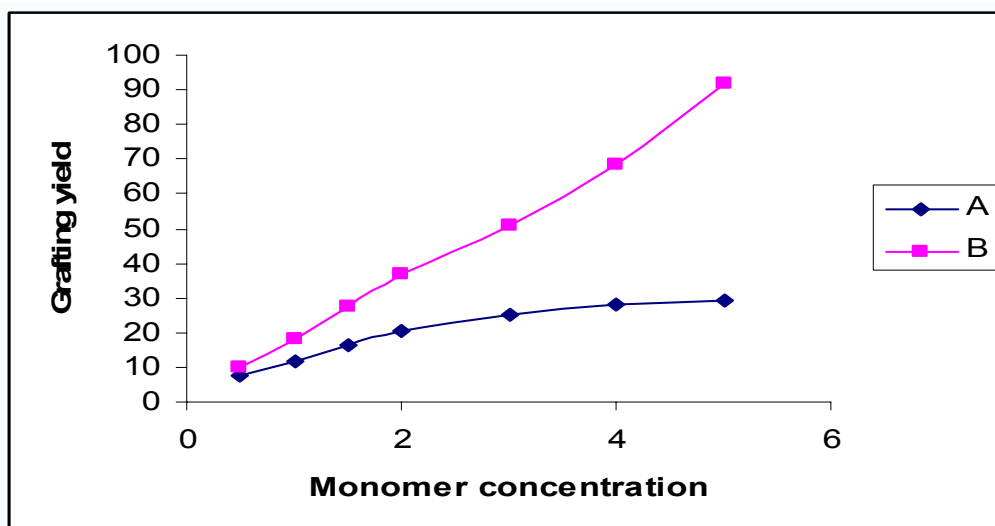


Figure 10.5: Effect of initiator concentration on the grafting yields of A) GMA and B) GMA-MMT onto cotton

From the results above from all factors studied, it is obvious that, there is a great effect of the addition of double modified Montmorillonite clay on the grafting yield of glycidyl methacrylate monomer onto cotton fibres by emulsion polymerization technique in the presence of redox initiation system.

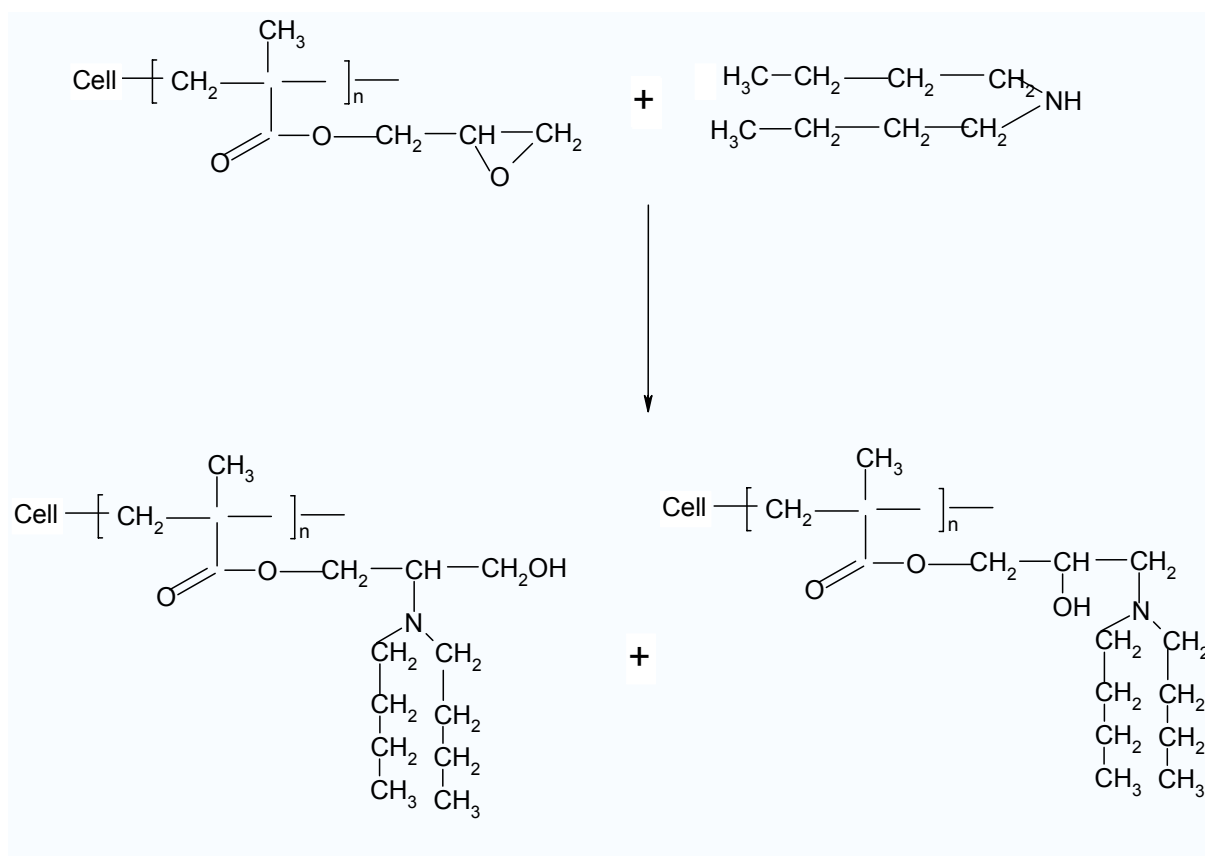
10.3. Characterization of Cotton Fibres Grafted with GMA Monomer in the Presence of Double Modified MMT Clay and Treated with Dibutyl Amine

Chemical modification of cotton fibres is mainly carried out to improve its properties to be satisfied for end-user application. The desirable properties for cotton fibres are its thermal stability, mechanical properties and dye uptake. In this study, glycidyl methacrylate monomer (3 %) was grafted onto cotton fibres in the presence of double modified Montmorillonite clay (10 Wt %) using emulsion polymerization technique in the presence of redox initiation system (1,5 mmol/l) at 70 °C for 90 min to obtain grafted cotton with graft yield about 50 % . The grafted cotton fibres were treated with four different concentrations of dibutylamines (DBA) ranging from 1 to 4 % and with liquor ratio 1:20 for 3 hours at 80°C. The treated cotton samples were

thoroughly washed with deionized water and dried at 50 °C. Unmodified cotton (B), grafted cotton with GMA (G), grafted cotton with GMA-MMT (GM) as well as the four mentioned grafted cotton with DBA (GMAm₁, GMAm₂, GMAm₃ and GMAm₄) were subjected to different tools of characterization and evaluation. It is well known that imparting tert-amino group to polymeric material such as starch, cellulose and polyester would certainly affect their hydrophobic character to some extent [441]. The magnitude of the hydrophilic-hydrophobic property of the modified polymer is greatly depending on the number and the type of alkyl group attached to nitrogen atom of tert-amino group.

10.3.1. Nitrogen Content

Figure 10.6 shows the relation between the nitrogen contents in the grafted cotton samples and DBA concentrations used in treatment of these samples. It is obvious that the nitrogen content increased by increasing the DBA concentrations from 1 % (GMAm₁) up to 3 % (GMAm₃), after which, the nitrogen content become to decrease at 4 % (GMAm₄). The increment of amine concentration leads to more interaction via opening the epoxy functional group of GMA according to the next Equation:



After DBA concentration of 3 %, the nitrogen content was decreased which may be due to the fact that, the highly amine concentration confers suitable basic medium, which affect the solubility of amino acids existing between the MMT clay interlayer.

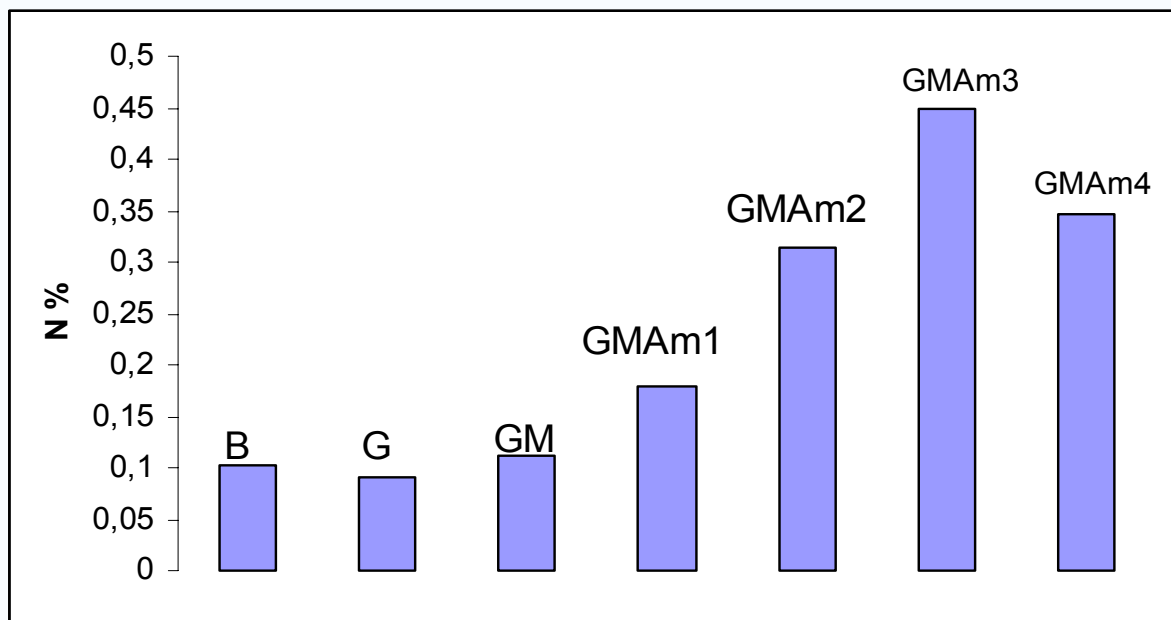


Figure 10.6: Nitrogen percentages of unmodified cotton sample and treated samples

10.3.2. Thermal Stability

Thermal gravimetric analysis (TGA) is a simple and accurate method for studying the decomposition pattern and the thermal stability of the polymer. Figure 10.7 compares TGA curves for B, G, GM and GMAm₃ within the temperature range 50: 500 °C. The TGA results of the samples are listed in table 10.1 which shows that the degradation temperatures of GM sample are higher than that of G sample due to the effective role of MMT clay in increasing of thermal stability of the fibres. From the table it can be also noted, that the degradation temperatures of G sample was higher than that of B sample which could be mainly related to the deposition of polyglycidyl methacrylate on the cotton fibres. On the other hand it is obvious that GMAm₃ sample has lower degradation temperature than G and GM samples which could be explained due to the degradation effect caused by the action of PH medium, either for grafting bath for acidic GMA or alkaline DBA solution.

Table 10.1: Degradation temperatures of unmodified cotton sample and treated samples.

Degradation Temperature	B	GMAm ₃	G	GM
T 10%	237	275	294	315
T 30%	295	304	325	346
T 50%	311	316	333	354
T 70%	325	327	341	361
T 90%	377	404	421	440

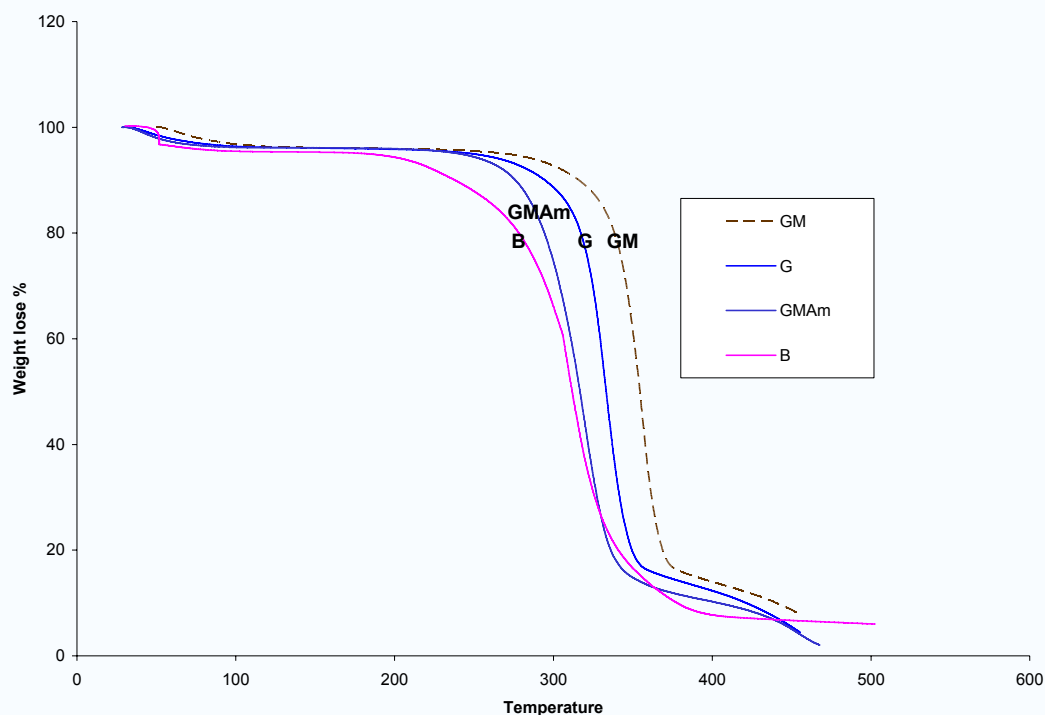


Figure 10.7: TGA thermograves of unmodified cotton sample and treated samples

10.3.3. Mechanical Properties

Table 10.2 shows the mechanical properties expressed as the tensile strength (N), elongation (%) at F_{max} and elongation (%) at break of the modified and unmodified cotton samples. From the table it can be noted, that the tensile strength and the elongation were increased after grafting with GMA which may be due to the plasticizing effect of GMA grafted in the matrix of the cotton. And increased again in the presence of MMT clay. Meanwhile, the tensile strength and the elongation of the grafted cotton sample treated by DBA solution were decreased at 1 % DBA concentration which could be due to the opening up of the cotton structure after interaction between the epoxy group of the GMA monomer and the amino group of

the DBA. Increasing the DBA concentration over 1 % induces an observed increment in the tensile strength and elongation due to substantial improvement in the uniformity of the inter-fibre structure via more deposition of the reacted amine compound inside the fibre matrix.

10.3.4. Water Absorption:

The S% values calculated are listed in table 10.2, it is evident that S % was decreased after grafting with GMA-MMT. Treatment of grafted cotton samples with different DBA concentration was accompanied by increasing the water absorption property till a certain DBA concentration after which S% decreased again. Increasing the water absorption by increasing DBA concentration could be ascribed to the pronounced effect of the created tertiary amino group with its superior hydrophilic character in the molecular structure of cotton fibers. As the nitrogen content increases the magnitude of the butyl alkyl group also increased causing creation of hydrophobic centers at the cotton surfaces preventing more water absorption.

10.3.5. Scanning Electron Microscope (SEM)

Figures 10.8a -10.8d show the scanning electron microscope of untreated cotton sample (B), sample grafted with GMA (G), sample grafted with GMA-MMT (GM) and grafted sample treated with DBA (GMa) at X 1000 magnification. From the micrographs it is clear, that the untreated fibres are completely separated from each other, whereas in case of grafted sample, full fibres can be noticed which may be due to the formation of the fibre bundles between cotton and polymer during the polymerization process. Also some aggregates of MMT clay can be noticed on cotton fibres in GM sample which is a good evidence for the success of the grafting process. For the micrograph related to the grafted cotton treated with DBA, it can be observed, that the cotton surface showed smooth fibres, soft grain and the fibres interfered with each other.

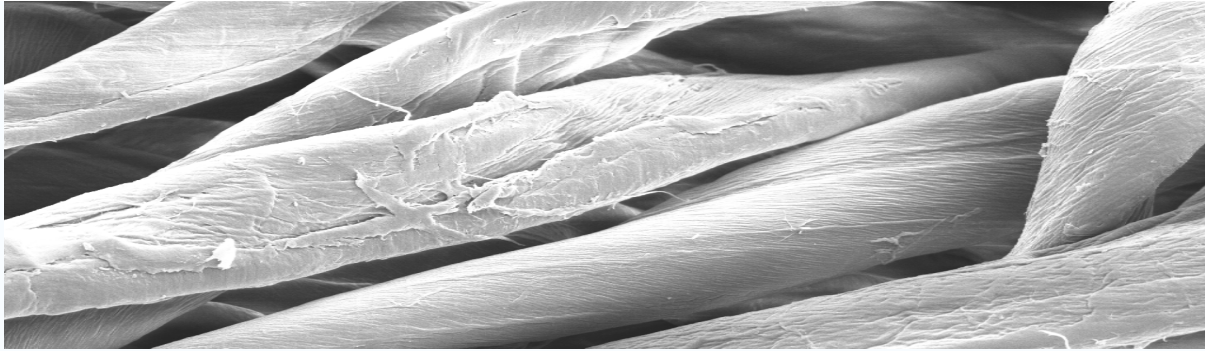


Figure 10.8a: SEM of unmodified cotton sample

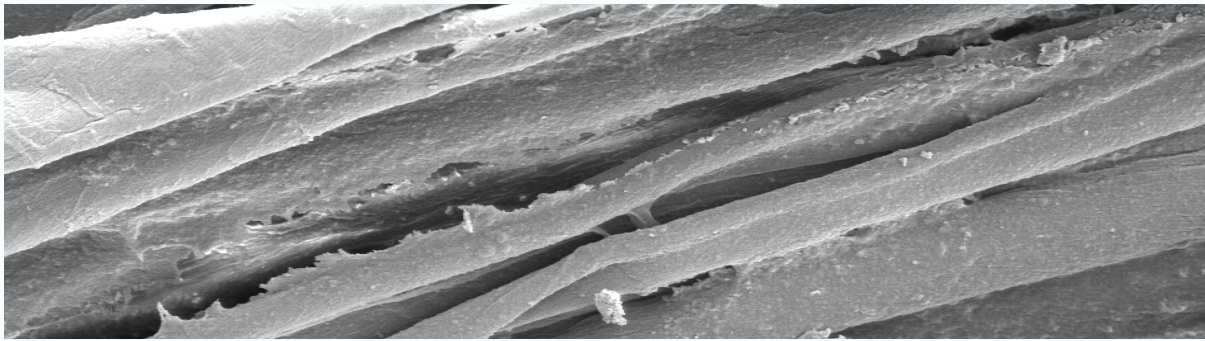


Figure 10.8b: SEM of cotton sample grafted with GMA

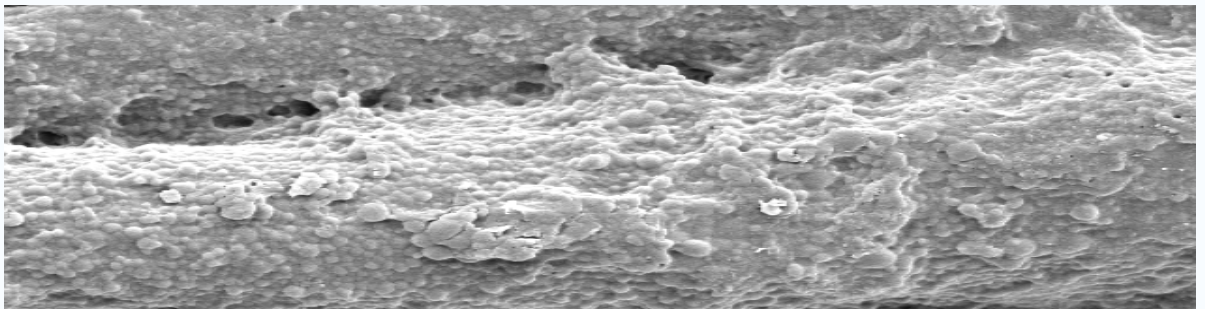


Figure 10.8c: SEM of cotton sample grafted with GMA-MMT

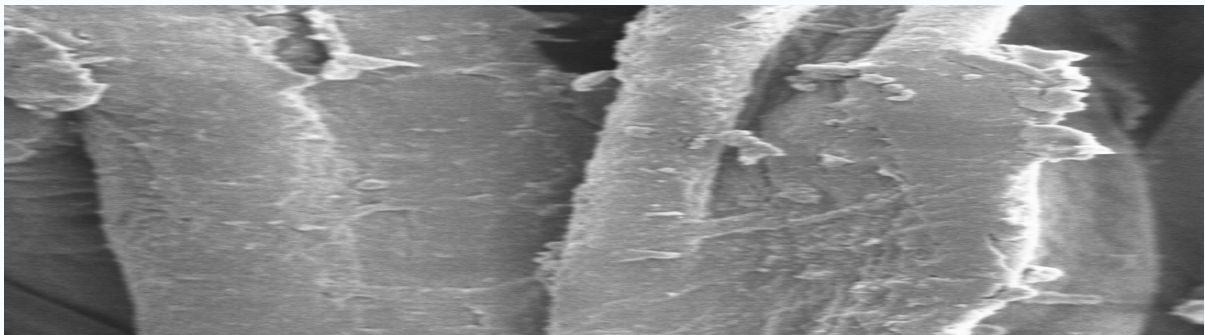


Figure 10.8d: SEM of cotton sample grafted with GMA-MMT and treated by DBA

10.3.6. Colour Measurement

Seven sets of cotton, ungrafted sample (B), cotton sample grafted with GMA (G), cotton sample grafted with GMA in the presence of MMT clay (GM) and cotton sample grafted with GMA in the presence of MMT clay and treated with different concentrations of dibutyl amine (GMAM₁ – GMAM₄) were independently dyed with three types of dyes namely acid, basic and reactive dyes. The dyeing properties expressed as colour strength (K/S) are illustrated in figures 10.9 -10.11 and listed in table 10.2.

For acid dye, it is evident that GM sample acquires an improvement in the K/S value compared with G sample and both are greater than that of unmodified cotton. Moreover, imparting tertiary amino group in the molecular structure of cotton fibres via the reaction of GM sample with DBA – up to 2% DBA concentration - brings a considerable increase in the K/S value. The colour strength for the acid dyed cotton samples follows the following descending order

$$\text{GMAM}_2 > \text{GMAM}_1 > \text{GMAM}_3 > \text{GMAM}_4 > \text{GM} > \text{G} > \text{B}$$

The noticeable increment of the colour strength values for G, GM and GMAM samples compared with that for unmodified cotton could be due to the following aspects: a) opening up the structure of cellulose through grafting and/or DBA treatment, b) direct interaction between the acid dye and GMA containing cotton via ring opening of epoxy groups, and c) increasing the magnitude of the acid dye accumulation and penetration through GMAM samples due to hydrogen bonding between the acid dye and additional basic tertiary amino functional groups [442]. The gradual increase of the dyeing behaviour from GMAM₁ to GMAM₂ could be recognized due to the relatively higher nitrogen content for GMAM₂ (Table 10.2), which in turn brings a significant increase in the dye hydrogen bond interaction. On the other hand, the observed decrease in the colour strength values for GMAM₃ and GMAM₄ could be explained due to the blocking of the fibres porosity by dibutyl amine causing a limitation of dye penetration.

In case of basic dye, it is known that cellulose fibres have no affinity for basic dyes. For adsorption, the fibre must possess acidic group [406]. From the K/S values, it is obvious that the unmodified sample has quite poor colour strength, the higher colour

strength observed after using GMA which has acidic group. The samples which are treated by DBA have low K/S values which are due to the repulsion forces between the alkali character of DBA and the basic dye. The colour strength for the acid dyed cotton samples follows the descending order

$$GM > G > GMAM_1 > GMAM_2 > GMAM_3 > GMAM_4 > B$$

For reactive dye, it is known that reactive dye have good affinity towards cotton fabrics, in which dyeing proceeds through chemical bonding between the hydroxyl groups of the cellulose and the dye [406]. The colour strength for the reactive dyed cotton samples follows the descending order

$$GMAM_4 > GMAM_3 > GMAM_2 > GMAM_1 > B > G > GM$$

From the values of K/S it is clear that GMAM samples have higher colour strength values than that of untreated cotton then the grafted samples which have the lowest colour strength values which can be attributed to the repulsion force between the anionic epoxy content of cotton and the anionic nature of the reactive dye. Enhancement in the colour strength by increasing the nitrogen content could be simply recognized to the higher basicity of cotton fabrics which leads to increase of the extent of the nucleophilic substitution reaction between the dye molecules and cotton fabrics [443].

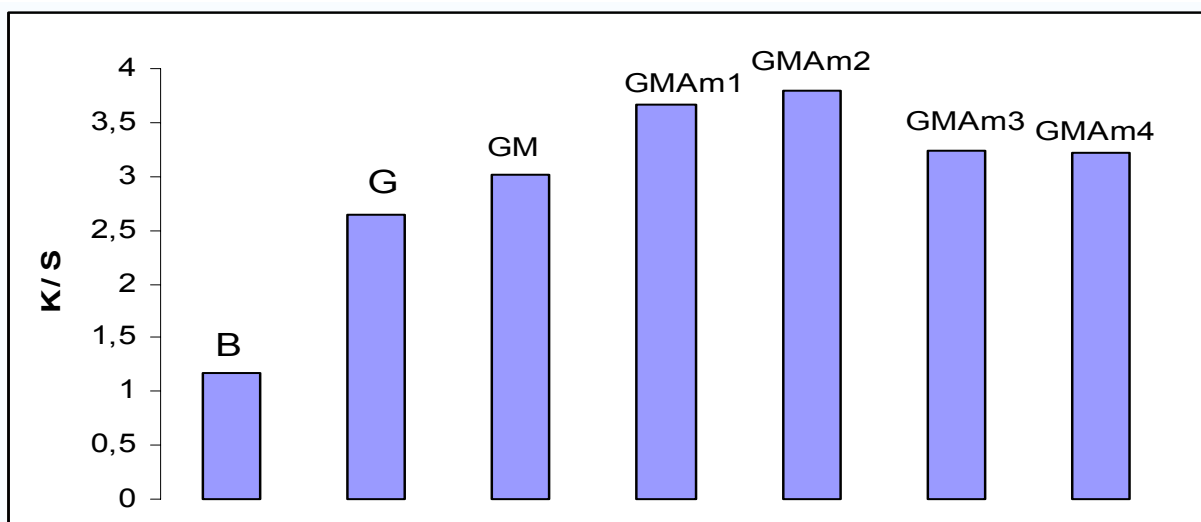


Figure 10.9: Effect of acid dyes on colour strength of unmodified cotton and treated samples.

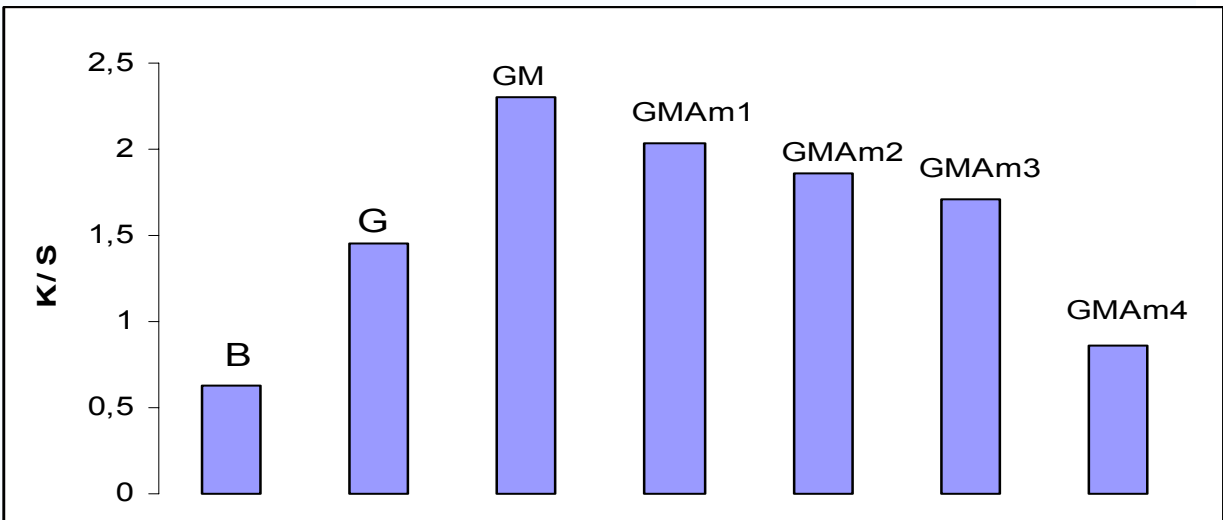


Figure 10.10: Effect of basic dyes on colour strength of unmodified cotton and treated samples.

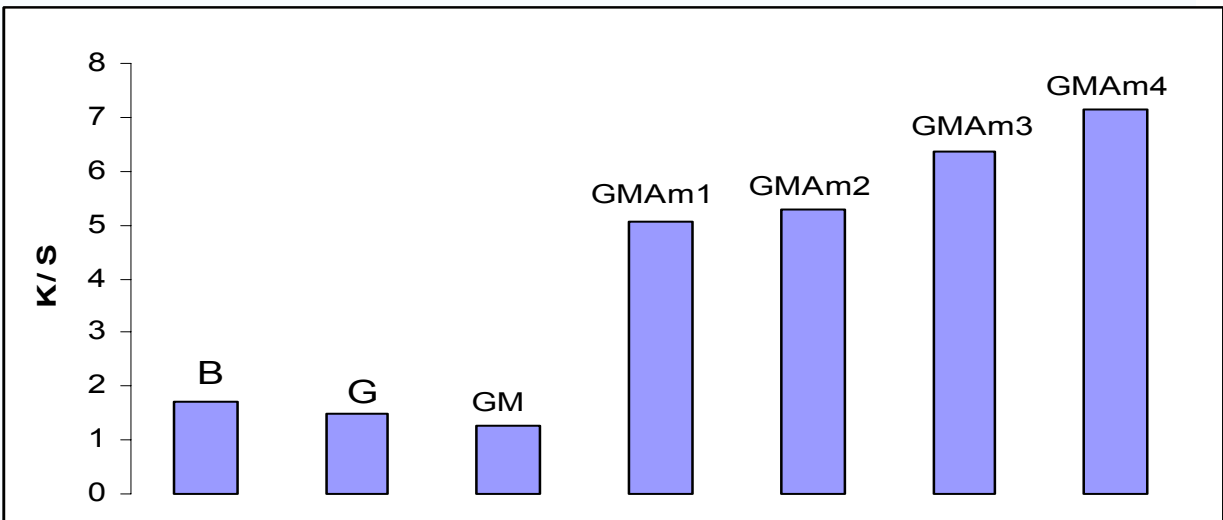


Figure 10.11: Effect of reactive dyes on colour strength of unmodified cotton and treated samples

Table 10.2: Variation of mechanical properties, colour strength and water absorption of unmodified cotton sample with treated samples

Sample Code	DBA Concentration	Mechanical properties			Colour strength (K/S)			Water absorption		
		Tensile Strength (T.S)	Elongation at break (E)	Elongation at F_{max} (E^*)	Acid dye	Basic dye	Reactive dye	30 min [%]	60 min [%]	120 min [%]
B	-	230	24,7	25,7	1,18	0,63	1,71	92,43	109,98	126,50
G	-	252,9	26,4	26,3	2,65	1,45	1,47	81,84	88,15	98,70
GM	-	258,4	26,9	27,2	3,01	2,30	1,27	52,81	58,44	76,60
GMAm ₁	1 %	246,4	25,6	25,9	3,66	1,39	5,05	57,24	70,65	79,30
GMAm ₂	2 %	263,5	28,2	28,4	3,80	1,70	5,27	60,17	76,83	82,04
GMAm ₃	3 %	267,1	29,9	30,1	3,24	1,09	6,37	52,80	73,18	79,70
GMAm ₄	4 %	273,2	31,2	33,5	3,21	0,86	7,13	48,90	68,80	70,80

10.4. Conclusion

A) Factors affecting grafting polymerization of vinyl monomers onto cotton fibers:

- 1- Grafting yield of GMA-MMT onto cotton increases gradually by increasing the MMT clay concentration to attain a maximum at 10 wt % MMT clay and then falls down again.
- 2- GMA-MMT shows a higher rate of grafting than MMA-MMT of all clay concentrations.
- 3- The grafting yield of GMA monomer onto cotton in the presence of MMT clay was higher value than in the absence of clay of all factors studied as follow:
 - a) **Temperature:** the maximum grafting yield was observed at 70 °C.
 - b) **Time:** The rate of grafting starts very fast and then tends to level-off after 90 min.
 - c) **Initiator concentration:** The grafting percentage is rapidly increased as the initiator concentration increased till a concentration of 1.5 mmol/l. Above this concentration, the grafting continue increased but less rapidly
 - d) **Monomer concentration:** the grafting yield increased with increasing the monomer concentration within the range studied with no noticeable level-off for the grafting.

B) Characterization of cotton fibres grafted with GMA monomer in the presence of double modified MMT clay and treated with dibutyl amine:

- 1- **Nitrogen content:** The nitrogen content increased by increasing DBA concentrations from 1 % (GMAM₁) up to 3 % (GMAM₃), after which, the nitrogen content become to decrease at 4 % DBA concentration (GMAM₄).
- 2- **Thermal Stability:** The degradation temperatures of GM samples are higher than that of G samples where the degradation temperatures of G samples were higher than that of B sample. On the other hand it is obvious that GMAM₃ samples were lower degradation temperature than G and GM samples.
- 3- **Mechanical properties:** the tensile strength and the elongation were increased after grafting with GMA and increased again in the presence of MMT clay where increasing the DBA concentration over 1 % induces an observed increment in the tensile strength and elongation.

4- Water absorption: S % decreased after grafting with GMA-MMT. Treatment of grafted cotton samples with different DBA concentrations was accompanied by increasing the water absorption property till 2% DBA concentration after which S% decreased again.

5- Scanning Electron Microscope (SEM): the untreated fibres are completely separated from each other, where full fibres can be noticed in grafted samples. Also some aggregates of MMT clay can be noticed on cotton fibres in GM samples and cotton surface showed smooth fibres in case of grafted cotton treated with DBA solution.

6- Colour Measurement: Three types of dyes were used and the K/S values for the studied samples were as follow

Acid dye: $GMAM_2 > GMAM_1 > GMAM_3 > GMAM_4 > GM > G > B$

Basic dye: $GM > G > GMAM_1 > GMAM_2 > GMAM_3 > GMAM_4 > B$

Reactive dye: $GMAM_4 > GMAM_3 > GMAM_2 > GMAM_1 > B > G > GM$

CHAPTER 11

Effect of Montmorillonite Clay Nanoparticles on the Properties of Polypropylene Fibres

11.1. Introduction

Synthetic fibers are mostly made from polyamides, polyesters, polyacrylonitrile, polyolefins, polyurethane and polyvinyl alcohol [398]. They are widely used for producing household textiles, but they are also used in diverse applications such as filters, protective clothing or reinforcement for tyres, rubber goods and composites. Two principal routes are used to convert fibre-forming polymers into filaments. These are (i) melt spinning, and (ii) solution spinning, which involves the extrusion of a solution to form the fibers. In both cases, after the spinning process, the fibers are generally subjected to drawing followed by heat-setting to increase their dimensional stability [444-447].

Polypropylene fibres have several advantages over other fibres, including low cost, high flexibility and abrasion resistance as well as light weight. They are used in many industrial fields and are particularly promising in the textile industry.

The primary aim of the work described in this chapter has been to produce melt spun PP and PP/MMT filaments for use in hybrid yarns. A further aim is to understand the influence of the melt spinning process on the morphology of the nanocomposites and the resulting physical properties. During melt spinning and subsequent drawing operations, the polymer is subjected to high shear forces that tend to align the polymer chains along the filament axis. This raises the question of the influence of these forces on the intercalation and dispersion of the MMT platelets. The limitations and constraints on the melt spinning of PP/MMT filaments compared with pure PP have been studied in order to assess the extent to which PP/MMT can be produced on an industrial level. Attention is given to how the MMT platelets influence the physical properties of the filaments, in order to understand the characteristics of the final hybrid composite part.

11.2. Structure and Properties of Polypropylene / Montmorillonite Fibres

Addition of montmorillonite nanoparticles in the production of polypropylene fibres is mainly carried out to improve its properties to be satisfied for the end-user application.

The desirable properties for the polypropylene fibres are its thermal stability, mechanical properties, water absorption, morphology and dye uptake.

11.2.1. Thermal Gravimetric Analysis (TGA)

The thermal stability of the pure polypropylene fibre and the nanocomposites polypropylene fibres prepared Na-MMT and DM-MMT clays was determined by thermogravimetric analysis (TGA) within the temperature range 50-600 °C, as illustrated in figure 11.1. The detailed data corresponding to the temperature point at which weight loss starting temperature (T_{start}), 25% weight loss temperature (T_{25}), 50% weight loss temperature (T_{50}) and 75% weight loss temperature (T_{75}) are listed in table 11.1. The temperature at which 25% degradation occurs (T_{25}) was found to increase by 44°C in case of using Na-MMT and by 75°C in case of using DM-MMT in the fibre production. Also, the mid-point degradation temperature (T_{50}) and the temperature at which 75% degradation occurs (T_{75}) were also found to be higher for the nanocomposites polypropylene fibres than that of pure polypropylene fibres.

From the data illustrated in the figure 11.1 and listed in table 11.1 it is clear that all weight loss temperatures for the nanocomposites polypropylene fibres are higher than that of pure polypropylene fibre which can be attributed to the restriction of the motion of organic chains attached to MMT clay [448]. It can be also stated that the polypropylene/DM-MMT fibre seems to have the highest thermal stability relative to polypropylene/Na-MMT fibre. This might be attributed to a maximized interaction between the clay and the polypropylene in the fibre structure, due to the availability of a larger surface area of clay in case of double modified clay [85].

Table 11.1: Degradation temperatures of polypropylene and nanocomposites polypropylene fibres

Degradation Temperature	Polypropylene	Polypropylene +Na-MMT	Polypropylene +DM-MMT
T_{start}	342	390	445
T₂₅	395	439	470
T₅₀	424	463	490
T₇₅	465	477	503

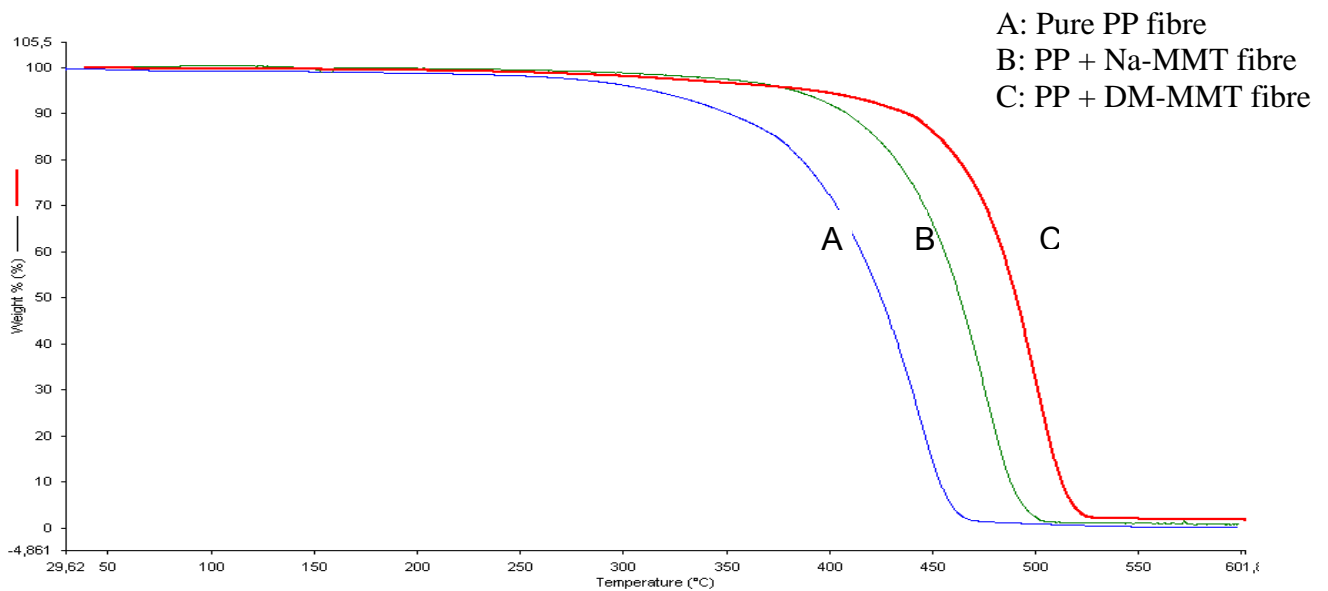


Figure 11.1: TGA thermograms of polypropylene and nanocomposites polypropylene fibres

11.2.2. Melting Point (MP)

The melting points of the pure polypropylene fibre and the nanocomposites polypropylene fibres were determined. The measured melting temperatures are plotted in figure 11.2. From this figure and from the listed results in table 11.2, it is obvious, that the addition of Na-MMT has no great effect in the melting temperature of polypropylene fibre whereas the melt temperature of the pure polypropylene fibre was approximately 1.5°C lower than DM-MMT polypropylene fibre.

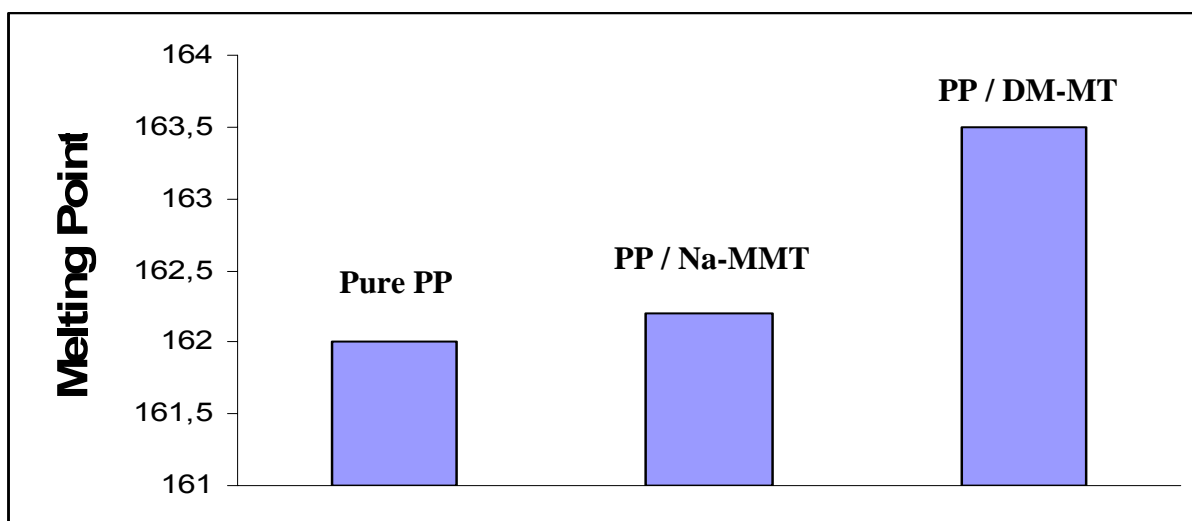


Figure 11.2: Melting point of polypropylene and nanocomposites polypropylene fibres

11.2.3. Mechanical Properties

This part of study was carried out to investigate the effect of MMT clay on the mechanical properties of the polypropylene fibre. Table 11.2 shows the mechanical properties expressed as tensile strength (T.S), elongation at break (E) and elongation at maximum force (E^*) of pure polypropylene fibre, polypropylene fibre intercalated with 1% Na-MMT and polypropylene fibre intercalated with 1% DM-MMT.

From the table it can be concluded, that both tensile strength and elongation are increased by the addition of Na-MMT clay and increased further by using DM-MMT clay. This increase in the mechanical properties can be an indication of nanodispersion [449].

11.2.4. Water Absorption

Polypropylene fibre has to be more resistance to water absorption and various methods have been developed to impart increased water resistance.

Using of MMT clay is beneficial to increase the polypropylene fibre water repellence. S% was calculated for pure polypropylene fibre, polypropylene fibre intercalated with 1% Na-MMT and polypropylene fibre intercalated with 1% DM-MMT. The results are listed in table 11.2. From the results it can be concluded, that using Na-MMT clay in the polypropylene fibre leads to less water absorption and also remarkable decrease in the water absorption is observed by using DM-MMT clay.

11.2.5. Scanning Electron Microscope (SEM)

Morphology studied was carried out for pure polypropylene fibre, polypropylene fibre intercalated with 1% Na-MMT and polypropylene fibre intercalated with 1% DM-MMT. From figures 11.3(a):11.3(c) it is clear that, the pure polypropylene fibres are completely smooth while a small aggregate appears in the fibre surface in case of polypropylene – Na-MMT fibres. Increasing of nanodispersion in case of polypropylene – DM-MMT fibres leads to more homogeneity between the polypropylene and the clay. In general it can be noted that fibres are particularly difficult to observe under SEM because of their generally featureless circular shape and transparency [449].

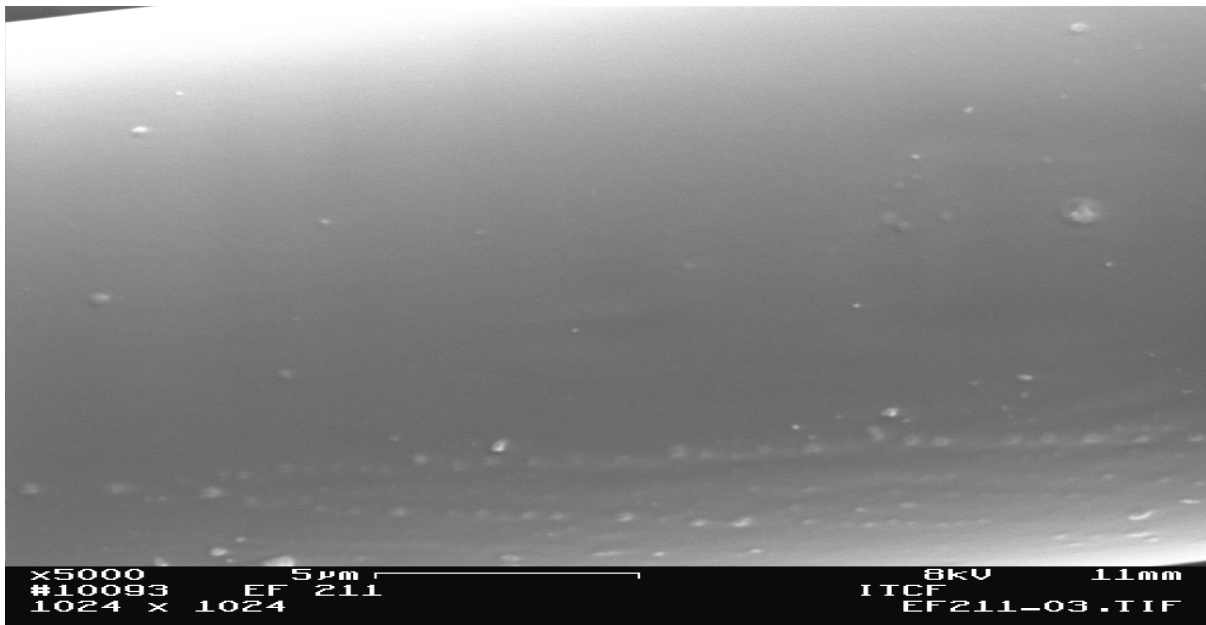


Figure 11.3(a): SEM of pure polypropylene fibre

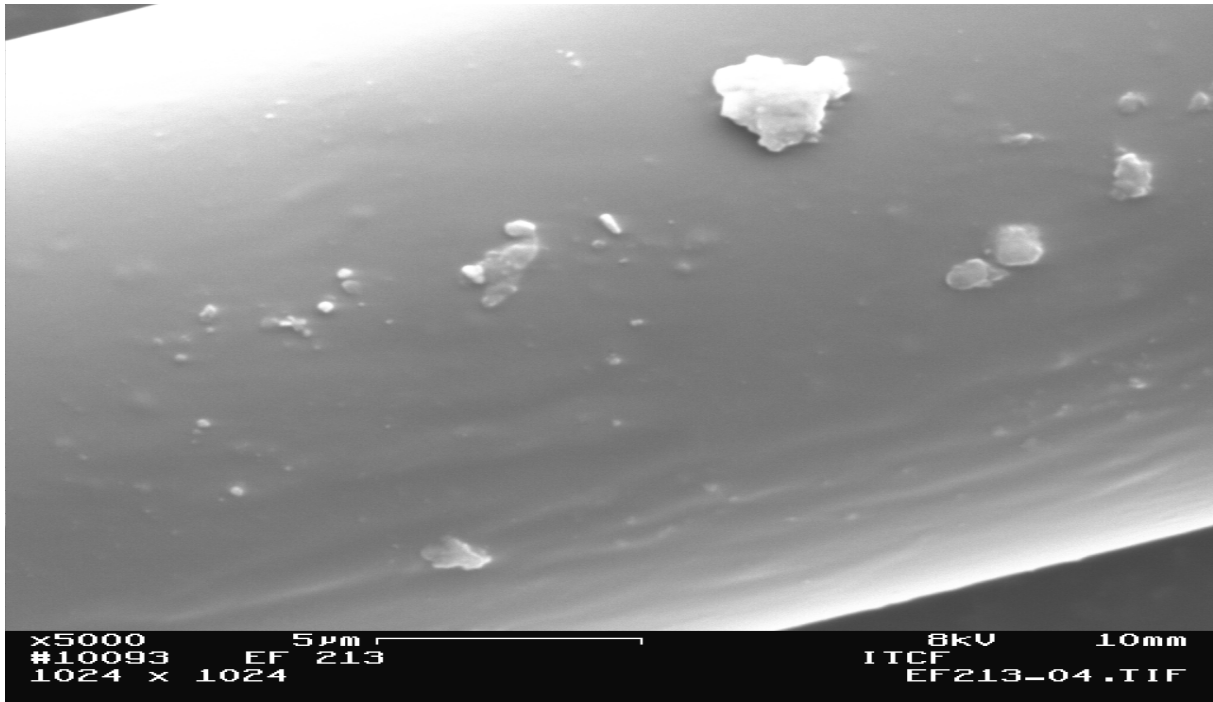


Figure 11.3(b): SEM of polypropylene /Na-MMT fibre

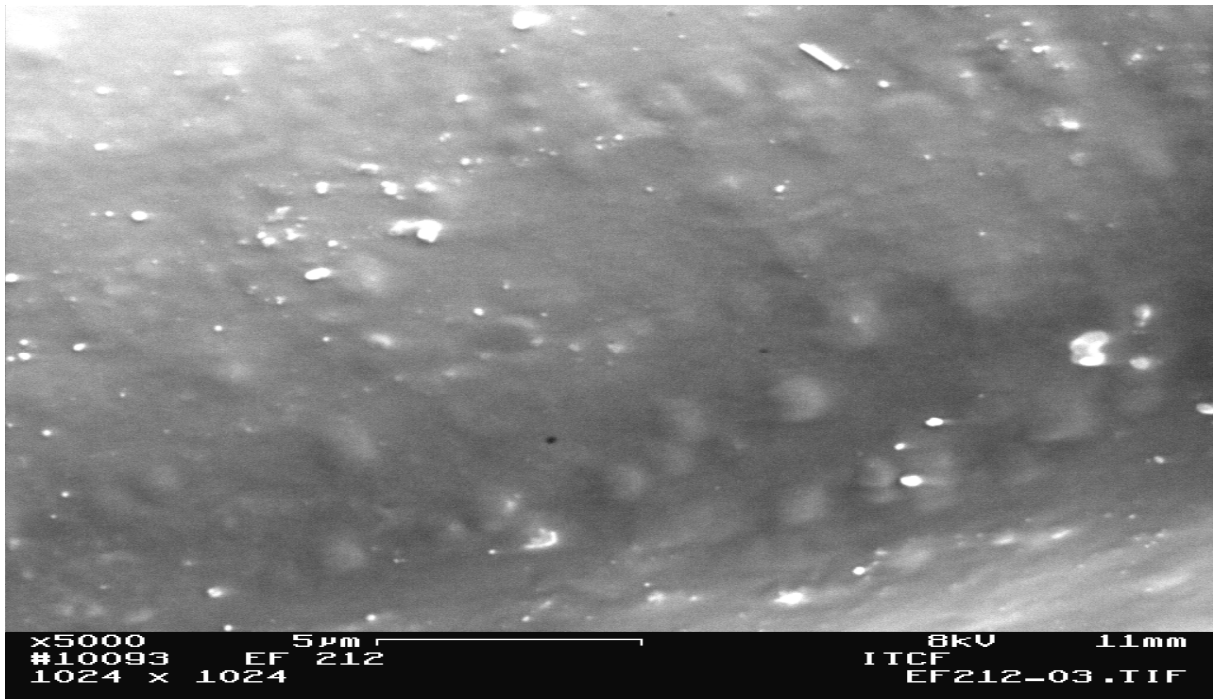


Figure 11.3(c): SEM of polypropylene /DM-MMT fibre

11.2.6. Colour Measurement

The dyeing behaviour of a fibre depends on both its physical and chemical structure. As regard to the chemical structure, dyeability is governed by the presence, firstly, of polar groups which interact with water molecules and allow fibre swelling and, secondly, by functional groups which attract dye molecules [450, 451]. The use of conventional direct dyeing techniques to colour PP fibres is limited by their lack of substantivity. PP is a non-polar, hydrophobic polymer. In contrast, in nanocomposites polypropylene, the quaternary ammonium salts act as effective dye sites for acid dyes as a result of ionic interactions.

With regard to the physical structure, the fibre must be accessible to water, dyes and other reagents. It must have a certain permeability, particularly to permit the dye molecules to diffuse into the fibre matrix. In nanocomposites polypropylene, the accessibility of the fibre can be improved by the introduction of particles [452]. According to the study of Fan et al. [452, 453], dyeing was possible because of the pathways created by oriented nanoclay layers in the polymer system. Pure polypropylene fibre, polypropylene fibre intercalated with 1% Na-MMT and polypropylene fibre intercalated with 1% DM-MMT were independently dyed with acid dyes. The dyeing properties expressed as colour strength (K/S) are illustrated in figures 11.4 and 11.5 and listed in table 11.2.

It is evident that the presences of DM-MMT clay in the polypropylene fibres improve the K/S value better than polypropylene-Na-MMT fibres and both are greater than that of pure polypropylene fibres. The lowest value obtained in the pure polypropylene fibres was expected because no sites are available for dye interaction with pure polypropylene. Moreover, the best result was obtained with DM-MMT because it has a higher interlayer spacing than Na-MMT clay.

On the other hand, disperse dyes gave better results than acid dyes where the difference between acid and disperse dye sorption has already been described by Fan et al. [453] in the case of nanocomposite polypropylene dyeing. Fan also studied the sorption ability of nanoclay to commonly used dyes [454]. The author concluded that nanoclay had very strong sorption ability due to its high surface area and strong Van der Waals forces, as well as hydrophobic and ionic interactions with dyes. The Van der Waals forces and hydrophobic interactions were the two major forces for dye sorption onto clay and is the reason why dye sorption is better with disperse dyes than with acid dyes [407].

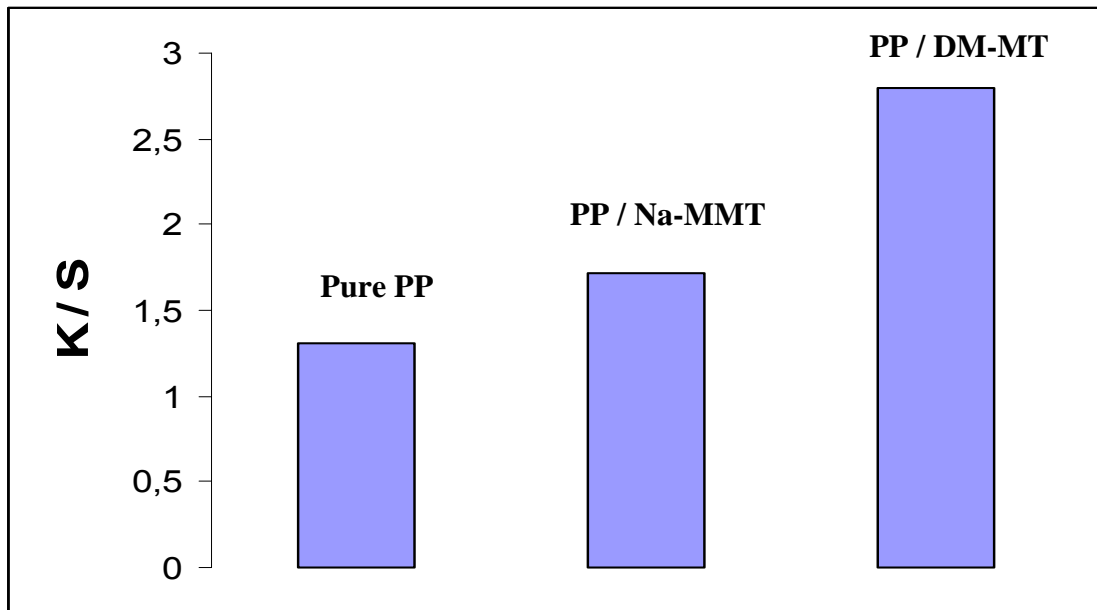


Figure 11.4: Effect of acid dyes on the colour strength of polypropylene fibres

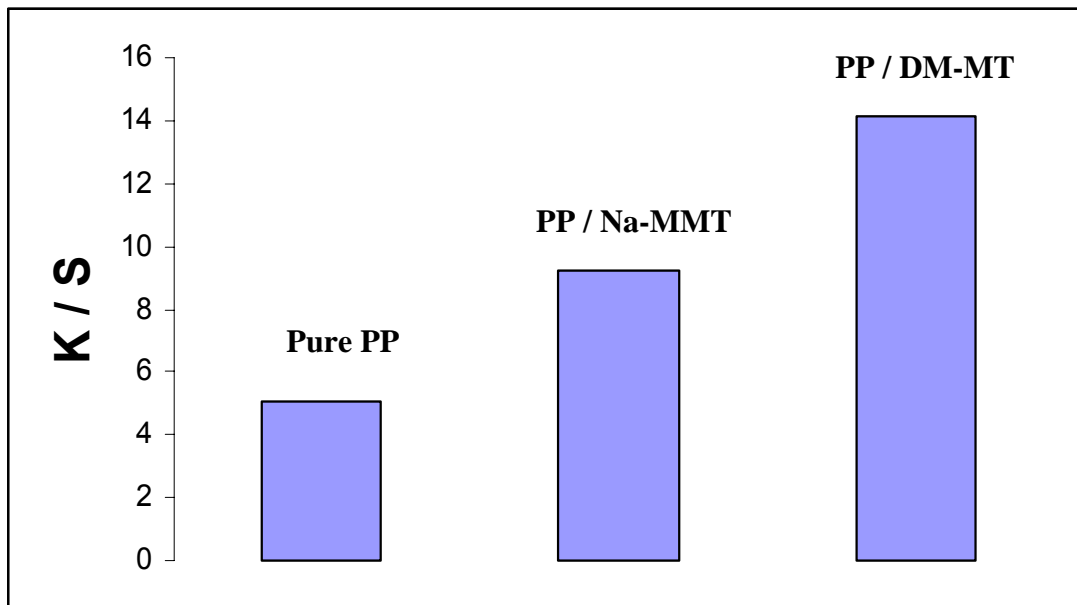


Figure 11.5: Effect of disperse dyes on the colour strength of polypropylene fibres

Table 11.2: Variation of mechanical properties, colour strength and water absorption of polypropylene fibres

Sample	Mechanical properties			Colour strength (K/S)		Water absorption		
	Tensile Strength (T.S)	Elongation at break (E)	Elongation at F_{max} (E^*)	Acid dye	Disperse dye	30 min [%]	60 min [%]	120 min [%]
Polypropylene	143.9	25.3	26.3	1.31	5.08	107.5	128.0	147.3
Polypropylene + Na-MMT	171.0	25.6	26.8	1.72	9.24	95.1	101.2	115.0
Polypropylene + DM-MMT	184.5	26.1	27.0	2.80	14.12	61.4	68.7	89.8

11.3. Conclusion

- 1- Polypropylene and nanocomposites polypropylene fibres were successfully prepared via melt spinning process.
- 2- The prepared fibres were characterized by TGA and SEM; the results obtained show that the addition of MMT clay in the fibre production induces a higher thermal stability.
- 3- Water absorption and mechanical properties of the fibres were also studied and it can be concluded that there were improved by the introduction of MMT clay nanoparticles in the fibre production.
- 4- Dyeing studies underlined the effect of the clay on the dyeability of the fibre which improved the accessibility of the fibre for both acid and disperse dyes. Moreover, it was observed, that polypropylene and nanocomposites polypropylene fibres were satisfactorily dyed with disperse dye more than with acid dyes.

Summary

Montmorillonite (MMT) clay with interlayer spacing 7.74 nm and cation exchange capacity (CEC) 100 meq per 100g was successfully modified with different amino acids in the presence of hydrochloric acid. Alanine-MMT, Leucine-MMT and Phenylalanine-MMT display the biggest interlayer spacing of 11.1, 12.36 and 11.75 nm respectively when using 1x concentration of amino acid based on clay CEC and 11.55, 12.59 and 11.94 nm respectively when using 2x concentration of amino acid based on clay CEC. Surface modifier phenyl triethoxy silane coupling agent was used to modify the surface and edges of the MMT clay where the interlayer spacing of MMT clay after double modification by 2x concentration of Leucine amino acid and phenyl triethoxy silane was 11.94 nm. The hydrophilic character of mineral clay has been changed after modification to hydrophobic which led to a great affinity to an aprotic polar solvent as DMF and a nonpolar solvent as toluene and it leads to an increase of the absorption of an aldose (Glucose) in comparison to a ketose (Fructose).

Exfoliated Polyacrylate / montmorillonite nanocomposites were successfully prepared by in situ emulsion polymerization of glycidyl methacrylate (GMA) and methyl methacrylate (MMA) monomers using redox initiation system. MMT clay was poorly dispersed in the polymer matrix in case of polyglycidyl methacrylate (PGMA) while it was homogeneously dispersed in polymer matrix in case of polymethyl methacrylate (PMMA). Thermal gravimetric analysis (TGA) results show that all weight loss temperature for the nanocomposites samples were higher than that of pure polymer in both PGMA and PMMA. And it is also obvious that, the increasing in the clay content plays an effective role in the increasing of thermal stability of these materials.

Polyolefin montmorillonite nanocomposites were successfully prepared by solution polymerization method using xylene in case of polypropylene (PP) and xylene – benzonitrile (80-20 %) in case of polyethylene (PE). Good exfoliation nanocomposite was achieved in the preparation PP/ DM-MMT up to DM-MMT 10 Wt% and after that diffraction peak is observed again. Insoluble nanocomposite was obtained in case of PE/Na-MMT, whereas intercalated nanocomposites are achieved in the preparation

of PP/Na-MMT, PP/ Leucine-MMT, PE/ Leucine-MMT and PE / DM-MMT. The homogenously dispersion of MMT clay in polymer matrix is observed only in the case of PP/DM-MMT. MMT clay is insoluble in the polymer matrix in case of PE/Na-MMT whereas MMT is poorly dispersed in polyolefin matrix in all other cases. The weight loses temperatures for polypropylene and polyethylene nanocomposites depend on the type of clay modification and the thermal stability for the prepared nanocomposites was as follow:

Polyolefin/DM-MMT > Polyolefin/Leucine-MMT > Polyolefin/Na-MMT

It is also obvious, that increasing DM-MMT clay content plays an effective role in the increasing of thermal stability of polyolefin/DM-MMT nanocomposites.

The grafting emulsion polymerization of vinyl monomers onto cotton was carried out in the presence of double-modified montmorillonite clay. The obtained results show that grafting with glycidyl methacrylate/montmorillonite gave a higher rate of grafting than grafting with methyl methacrylate/montmorillonite with all clay percentages, and also, the grafting yield of glycidyl methacrylate monomer onto cotton in the presence of montmorillonite clay had a higher yield than that in the absence of the clay for all factors studied. The results were as follow:

- a) Temperature:** the maximum grafting yield was observed at 70 oC.
- b) Time:** The rate of grafting starts very fast and then tends to level-off after 90 min.
- c) Initiator concentration:** The grafting percentage is rapidly increased as the initiator concentration increased till initiator concentration 1,5 mmol/l. above this concentration, the grafting continue increased but less rapidly
- d) Monomer concentration:** the grafting yield increased with increasing the monomer concentration within the range studied with no noticeable level-off for the grafting.

Cotton grafted with glycidyl methacrylate/ montmorillonite with a graft yield of about 50% was prepared according to the emulsion polymerization technique and was treated with different concentrations of dibutylamine solutions ranging from 1 to 4%.

The obtained samples were characterized according to the nitrogen content which increased by increasing the DBA concentrations from 1 % (GMAM₁) up to 3 % (GMAM₃), after which, the nitrogen content becomes to decrease at 4 % (GMAM₄). Thermal Stability which conclude that the degradation temperatures of cotton sample grafted with GMA in presence of MMT clay (GM) sample are higher than that of cotton sample grafted with GMA (G) sample where the degradation temperatures of G sample was higher than that of ungrafted cotton sample (B) sample. On the other hand it is obvious that cotton sample grafted with GMA in presence of MMT clay and treated with 3% dibutyl amine (GMAM₃) sample has lower degradation temperature than G and GM samples.

Mechanical properties were studied and the results indicating that the tensile strength and the elongation were increased after grafting with GMA and increased further in presence of MMT clay where Increasing the DBA concentration over 1 % induces an observed increment in the tensile strength and elongation.

Water absorption was also studied and it was observed that the water absorption percentage was decreased after grafting with GMA-MMT. Treatment of grafted cotton samples with different dibutyl amine concentrations (DBA) was accompanied by increasing the water absorption property till 2% DBA concentration after which water absorption decreased again.

Scanning Electron Microscope (SEM) for the untreated fibres are completely separated from each other. Full fibres can be noticed in case in grafted sample also some aggregates of MMT clay can be noticed on cotton fibres in GM sample and cotton surface showed smooth fibres in case of grafted cotton treated with DBA solution.

Colour Measurement was studied for three types of dyes and the K/S values for the studied samples were as follow

Acid dye: GMAM₂ > GMAM₁ > GMAM₃ > GMAM₄ > GM > G > B

Basic dye: GM > G > GMAM₁ > GMAM₂ > GMAM₃ > GMAM₄ > B

Reactive dye: GMAM₄ > GMAM₃ > GMAM₂ > GMAM₁ > B > G > GM

Polypropylene and nanocomposites polypropylene fibres were successfully prepared via a melt spinning process. The prepared fibres were characterized by TGA and SEM. The results obtained show that the addition of MMT clay in the fibre induces a higher thermal stability. Water absorption and mechanical properties of the fibres

were improved by the introduction of MMT clay nanoparticles in the fibre. Dyeing studies underlined the effect of the clay on the dyeability of the fibres which improved the accessibility of the fibre for both acid and disperse dyes. Moreover, it was observed, that polypropylene and nanocomposites polypropylene fibres were satisfactorily dyed with disperse dyes more than with acid dyes.

Zusammenfassung

Ton (Montmorillonit (MMT)) mit einem Zwischenschichtabstand von 7,74 nm und einer Kationenaustauschkapazität (CEC) von 100meq pro 100g wurde erfolgreich mit verschiedenen Aminosäuren bei Anwesenheit von Salzsäure modifiziert. Alanin-MMT, Leucin-MMT und Phenylalanin-MMT zeigten mit 11,10nm, 12,36nm und 11,75nm die größten Zwischenschichtabstände, jeweils bei Verwendung der einfachen Konzentration an Aminosäure auf der Ton CEC und 11,55nm, 12,59nm und 11,94nm bei Verwendung der zweifachen Konzentration an Aminosäure. Dort, wo der Zwischenschichtabstand nach zweifacher Behandlung mit doppelter Konzentration an Leucin-Aminosäure und Phenyltriethoxysilan 11,94nm betrug, wurde der Oberflächenmodifizierer Phenyltriethoxysilan-Kopplungsmittel zur Modifizierung der Oberfläche und der Kanten eingesetzt. Der hydrophile Charakter der Mineralerde wechselte nach der Behandlung zu einem hydrophoben, was zu einer großen Affinität für aprotische polare Lösemittel wie DMF und nichtpolare Lösemittel wie Toluol führte und es führte zu einem Anwachsen der Absorption von Aldose (Glukose) im Vergleich zu Ketose (Fruktose).

Delaminierte Polyacrylat / Montmorillonit Nanokomposite wurden erfolgreich hergestellt durch in-situ-Emulsionspolymerisation von Glycidyl-Methacrylat- (GMA) und Methyl-Methacrylat- (MMA) –Monomeren, unter Verwendung eines Redox-Initiationssystems. Die MMT-Ton war schlecht verteilt in der Polymermatrix des Polyglycidyl-Methacrylat (PGMA) und homogen verteilt in der Matrix des Polymethylmethacrylats (PMMA). Die Ergebnisse der Thermogravimetrischen Analyse (TGA) zeigen, dass die Temperaturen, bei der die Masse abnimmt, sowohl bei PGMA, als auch bei PMMA, bei den Nanokompositen höher war, als bei den reinen Polymeren. Ebenfalls deutlich ist, dass der anwachsende Gehalt an Ton eine effektive Rolle spielt beim Anwachsen der thermischen Stabilität dieser Materialien.

Polyolefin-Ton-Nanokomposite wurden erfolgreich durch Lösungs-Polymerisation hergestellt, im Fall des Polypropylens (PP) mit Xylol, im Fall des Polyethylen (PE) mit Xylol/Benzonitril (80%/20%). Gut delaminierte Nanokomposite wurden erreicht in einer PP/DM-MMT-Bereitung mit bis zu 10 Gew.% DM/MMT, wobei der

Beugungspeak wieder beobachtet wurde. Unlösliche Nanokomposite wurden beobachtet im Fall des PE/Na-MMT, wobei eingefügte Nanokomposite erhalten wurden in den Präparaten aus PP/Na-MMT, PP/Leucin-MMT, PE/Leucin-MMT und PE/DM-MMT. Eine homogene Dispersion von MMT-Ton in einer Polymermatrix wurde nur im Fall des PP/DM-MMT beobachtet. MMT-Ton ist unlöslich in der Polymermatrix im Fall des PE/Na-MMT, wobei MMT in allen anderen Fällen schlecht in der Polyolefinmatrix dispergiert ist. Die Gewichtsverlusttemperatur für Polypropylen- und Polyethylen-Nanokompositen hängt ab von der Ton-Modifikation. Die thermische Stabilität der hergestellten Nanokomposite war wie folgt:

Polyolefin/DM-MMT > Polyolefin/Leucin-MMT > Polyolefin/Na-MMT

Ebenso ist ersichtlich, dass das Anwachsen des DM-MMT-Ton-Gehalts eine effektive Rolle spielt beim Anwachsen der thermischen Stabilität der Polyolefin/DM-MMT Nanokomposite.

Die Pfröpf-Emulsions-Polymerisation von Vinylmonomeren auf Baumwolle wurde in Anwesenheit von doppelt modifiziertem Montmorillonit-Ton. Das erhaltene Resultat zeigt, dass Pfröpfung mit Glycidyl-Methacrylat/Montmorillonit eine höhere Pfröpfungsrates ergibt, als Pfröpfung mit Methyl-Methacrylat/Montmorillonit bei allen Prozentgehalten. Ebenso ist die Pfröpfungsausbeute von Glycidyl-Methacrylat-Monomer auf Baumwolle in Anwesenheit von Montmorillonit-Ton größer als bei Abwesenheit der Ton bei allen untersuchten Faktoren. Die Resultate waren wie folgt:

- a) **Temperatur:** Die maximale Pfröpfungsausbeute wurde bei 70°C erhalten.
- b) **Zeit:** Die Pfröpfungsrates startet sehr schnell und tendierte nach 90 min zum Gleichbleiben.
- c) **Initiator-Konzentration:** Der Pfröpfung-Prozentgehalt steigt schnell mit der Konzentration des Initiators bis zur Initiator-Konzentration von 1,5mmol/l. Oberhalb dieser Konzentration steigt der Pfröpfungsforgang weiter, aber nicht mehr so schnell.
- d) **Monomer-Konzentration:** Die Pfröpfungsausbeute wächst mit wachsender Monomer-Konzentration innerhalb des untersuchten Bereichs mit keinem erkennbaren Gleichgewicht für die Pfröpfung.

Baumwolle, gepfropft mit Glycidyl-Methacrylat/Montmorillonit mit einer Pfropf-Ausbeute von ca. 50%, wurde, in Anlehnung an Emulsionspolymerisations-Techniken, behandelt mit verschiedenen konzentrierten Dibutylamin-Lösungen mit Konzentrationen zwischen 1-4%. Die erhaltenen Proben wurden anhand ihres Stickstoffgehalts charakterisiert, der mit ansteigender DBA-Konzentration (von 1% (GMAm₁) bis 3% (GMAm₃) ansteigt, danach wieder absinkt bei 4% (GMAm₄).

Die thermische Stabilität lässt folgern, dass die Zersetzungstemperatur der Baumwollprobe, die mit GMA in Anwesenheit von MMT Ton gepfropft wurde, höher ist als die der Baumwollprobe, die mit GMA (G) gepfropft wurde, wobei die Zersetzungstemperatur der Probe G höher war, als die der ungepfropften Baumwollprobe (B). Auf der anderen Seite ist ersichtlich, dass die Baumwollprobe, die mit GMA in Anwesenheit von MMT Ton gepfropft und mit 3%iger Dibutylamin-Lösung behandelt wurde, eine niedrigere Zersetzungstemperatur hat als die Proben G und GM.

Die mechanischen Eigenschaften wurden untersucht und die Ergebnisse indizieren, dass die Bruchfestigkeit und die Bruchdehnung angewachsen sind nach Pfropfung mit GMA und weiter angewachsen in Anwesenheit von MMT-Ton, wobei eine DBA-Konzentration über 1% eine beobachtete Erhöhung der Bruchfestigkeit und Bruchdehnung bewirkt.

Die Wasserabsorption wurde ebenfalls untersucht und es wurde beobachtet, dass sich die Absorption verringert nach der Pfropfung mit GMA-MMT. Eine Behandlung gepfropfter Baumwollproben mit unterschiedlichen Dibutylamin-Konzentrationen (DBA) war begleitet von einem Anstieg des Wasserabsorptionsvermögens bis zu einer DBA-Konzentration von 2%, nach der die Wasserabsorption wieder abgenommen hat.

Elektronmikroskopische Aufnahmen der unausgerüsteten Fasern zeigen, dass diese komplett separiert sind. Ganze Fasern konnten im Fall gepfropfter Proben beobachtet werden, ebenso wie MMT-Anhäufungen auf Baumwollfasern in GM-Proben. Die Baumwolloberfläche zeigte feine Fasern im Fall von gepfropfter Baumwolle, die mit DBA-Lösung behandelt wurde.

Die Farbmessungen wurden mit drei verschiedenen Farbstofftypen durchgeführt. Die K/S-Werte der Proben nehmen in folgender Reihenfolge ab:

Säure-Farbstoff: GMam₂ > GMam₁ > GMAm₃ > GMAm₄ > GM > G > B

Substantiv-Farbstoff: GM > G > GMAm₁ > GMAm₂ > GMAm₃ > GMAm₄ > B

Reaktiv-Farbstoff: GMAm₄ > GNAm₃ > GMAm₂ > GMAm₁ > B > G > GM

Polypropylen- sowie Polypropylen-Nanokomposit-Fasern wurden erfolgreich durch Schmelzspinnen hergestellt. Diese hergestellten Fasern wurden durch TGA und SEM charakterisiert. Die Ergebnisse der TGA zeigen, dass die mit MMT-Ton-Komposit-Fasern eine höhere thermische Stabilität aufweisen. Die Wasserabsorption und die mechanischen Eigenschaften werden durch die Einlagerung der MMT-Ton-Nanopartikel in die Fasern verbessert. Färbeuntersuchungen bestätigen einen Effekt des Tons auf die Anfärbbarkeit der Fasern. Durch die Modifizierung wird die Farbstoffaufnahme bei der Verwendung von Säure- und Dispersionsfarbstoffen verbessert. Des Weiteren wurde festgestellt, dass Polypropylen- und Polypropylen-Nanokomposit-Fasern mit Dispersionsfarbstoffen tiefer angefärbt werden als mit Säurefarbstoffen.

References

- [1] Gary Stix, *Little Big Science*, 285 Sci. Am. 32, 34 (Sept. 2001) (quoting Steven Block).
- [2] See Foresight FAQ General Nanotechnology Information, <http://www.foresight.org/NanoRev/FIFFAQ1.html#FAQ1>.
- [3] National Nanotechnology Initiative (“NNI”), what is Nanotechnology? <http://www.nano.gov/html/facts/whatIsNano.html>.
- [4] D.Mihailovic, Prog. Mater.Sci. 54(2009)309.
- [5] S.Kynchoi, S.Lee, Current Application physics. 9(2009)658.
- [6] M.Tories-Cisneros, C.Velasquez-Ordonez, J.Sanchez-Mondragon, A.Campero, O.G.Ibara-Manzano, D.A.May-Arriolja, H.Plascencia-Mora, A.Espinoza-Calderon and I.Sukhoivanov, Microelectronic journal 40(2009)618.
- [7] T.X.Phuok, B.H.Howard, D.V.Martello, Y.Soong and M.K.Chyu, Optics and Laser in Engineering 46(2008)829.
- [8] Y.Zou, Y.Hu, H.Gu and Y.Wang, Mater.Chem&Phys.115(2009)151.
- [9] J.F.Conley, L.Stecker and Y.Ono, J.Electronics Materials 35(2006)795.
- [10]G.Y.Akimov and V.M.Timchenko, Refractories and Industrial Ceramics 45(2004)1573
- [11] L.S.Vasilev and O.V.Karban, Glass & Ceramics 64(2007)193.
- [12]J.Konnert, P.Dantonio, J.M.Cowley, A.Higgs and H.J.Ou, Ultramicroscopy 30(1989)371.
- [13] T.Wang and L.Joseph, Advances in Colloid Interface Science 147(2009)319.
- [14] S.K.Amin, R.H.Mahmoud and N.Jalili, Composites Sci.&Tech.69(2009)545.
- [15] S.Yu, H.Hu, J.Ma and J.Yin, Tribology International 41(2008)1205.
- [16] Z.L.Wang, E-Book, Characterization of nanophase materials.
- [17] L.D. Zhang, Q. M. Mo, Nanomaterial Science, Press of Liaoning Science and Technology, Shenyang, 1994.
- [18] Y.C. Ke, Polymer-Inorganic Nanocomposites, Chemical Industry Press, Beijing, 2003.
- [19] Y.X. Zhao, Clay Minerals, Geological Press of China, Beijing, 1980.
- [20] Y. Wang, N. Herron, Science, 273, (1996) 632.

- [21] Q. Li, Postdoctoral Dissertation, Inst. Chem., China Academy of Science, Beijing, 1997.
- [22] L.D. Zhang, Y. Sheng, D.Q. Zhu, J.D. Chen, *Polym. Bull. (Chin.)* 4, (2001) 9.
- [23] Y. Kojima, A. Usuki, M. Kawasumi, A. Okada, Y. Fukushima, T. Kurauchi, O. Kamigaito, *J. Mater. Res.* 8(1993)1185.
- [24] M. Zanetti, S. Lomakin, G. Camino, *Macromol. Mater. Eng.* 279(2000)1.
- [25] S.S. Ray, M. Okamoto, *Prog. Polym. Sci.* 28(2003)1539.
- [26] Y. Ke, C. Long, Z. Qi, *J. Appl. Polym. Sci.* 71(1999)1139.
- [27] Y. Wang, J. Gao, Y. Ma, U.S. Agarwal, *Composites: Part B* 37(2006)399.
- [28] K. Wang, S. Liang, R. Du, Q. Zhang, Q. Fu, *Polym. J.* 45(2004)7953.
- [29] K.P. Pramoda, T. Liu, Z. Liu, C. He, H.-J. Sue, *Polym. Degrad. Stab.* 81(2003)47.
- [30] P.B. Messersmith, E.P. Giannelis, *J. Polym. Sci., Part A: Polym. Chem.* 33(1995) 1047.
- [31] T. Liu, K.P. Lim, W.C. Tjiu, K.P. Pramoda, Z. Chen, *Polym. J.* 44(2003)3529.
- [32] K. Masenilli-Varlot, E. Reynaud, G. Vigier, J. Varlet, *J. Polym. Sci., Part B: Polym. Phys.* 40(2002)272.
- [33] X. Liu, Q. Wu, *Eur. Polym. J.* 38(2002)1383.
- [34] X. Liu, Q. Wu, *Polym. J.* 43(2002)1933.
- [35] F.J. Medellin-Rodriguez, C. Burger, B.S. Hsiao, B. Chu, R.A. Vaia, S. Phillips, *Polym. J.* 42(2001)9015.
- [36] D.M. Lincoln, R.A. Vaia, Z.G. Wang, B.S. Hsiao, *Polym. J.* 42(2001)1621.
- [37] T.D. Fornes, P.J. Yoon, H. Keskkula, D.R. Paul, *Polym. J.* 42(2001)9929.
- [38] J.W. Cho, D.R. Paul, *Polym. J.* 42(2001)1083.
- [39] T. Liu, W.C. Tjiu, C. He, S.S. Na, T.-S. Chung, *Polymer International* 53(2004) 392.
- [40] Z. Liu, D. Yan, *Polymer Engineering and Science* 44(2004)861.
- [41] A. Usuki, M. Kato, A. Okada, T. Kurauchi, *Appl. Polym. Sci.* 63(1997)794.
- [42] P. Peltola, E. Valipakka, J. Vuorinen, S. Syrjala, K. Hanhi, *Polym. Eng. Sci.* (2006)995.
- [43] J. Li, C. Zhou, G. Wang, D. Zhao, *J. Appl. Polym. Sci.* 89(2003)3609.
- [44] D. Marchant, K. Jayaraman, *Ind. Eng. Chem. Res.* 41(2002)6402.
- [45] A. Lele, M. Mackley, G. Galgali, C. Ramesh, *J. Rheol.* 46(2002)1091.

- [46] M.J. Solomon, A.S. Almusallam, K.F. Seefeldt, A. Somwangthanaroj, P. Varadan, *Macromolecules* 34(2001)1864.
- [47] P.H. Nam, P. Maiti, M. Okamoto, T. Kotaka, N. Hasegawa, A. Usuki, *Polym. J.* 42(2001)9633.
- [48] M. Kato, A. Usuki, A. Okada, *J. Appl. Polym. Sci.* 66(1997)1781.
- [49] D. Wu, C. Zhou, W. Yu, X. Fan, *J. Polym. Sci., Part B: Polym. Phys.* 43(2005) 2807.
- [50] C.H. Davis, L.J. Mathias, J.W. Gilman, D.A. Schiraldi, J.R. Shields, P. Trulove, T.E. Sutto, H.C. Delong, *J. Polym. Sci., Part B: Polym. Phys.* 40(2002)2661.
- [51] X. Huang, S. Lewis, W.J. Brittain, *Macromolecules* 33(2000)2000.
- [52] Y. Imai, S. Nishimura, E. Abe, H. Tateyama, A. Abiko, A. Yamaguchi, T. Aoyama, H. Taguchi, *Chem. Mater.* 14(2002)477.
- [53] H.R. Dennis, D.L. Hunter, D. Chang, S. Kim, J.L. White, J.W. Cho, D.R. Paul, *Polym. J.* 42(2001)9513.
- [54] H. Shi, T. Lan, T.J. Pinnavaia, *Chem. Mater.* 8(1996)1584.
- [55] E.P. Giannelis, R. Krishnamoorti, *Adv. Polym. Sci.* 138(1999)107.
- [56] N. Sheng, M.C. Boyce, D.M. Parks, G.C. Rutledge, J.I. Abes, R.E. Cohen, *Polymer* 45(2004)487.
- [57] W.J. Boo, L. Sun, J. Liu, E. Moghbelli, A. Clearfield, H.-J. Sue, H. Pham, N. Verghese, *J. Polym. Sci., Part B: Polym. Phys.* 45(2007)1459.
- [58] S.S. Ray and M. Okamoto, *Macromolecules* 36(2003)2355.
- [59] J.-T. Xu, Q. Wang, Z.-Q. Fan, *Eur. Polym. J.* 41(2005)3011.
- [60] R. Krishnamoorti, J. Ren, A.S. Silva, *J. Chem. Phys.* 114(2001)4968.
- [61] V.E. Yudin, G.M. Divoux, J.U. Otaigbe, V.M. Svetlichnyi, *Polym. J.* 46(2005) 10866.
- [62] M. Modesti, A. Lorenzetti, D. Bon, S. Besco, *Polym. J.* 46(2005)10237.
- [63] A. Usuki, *Adv. Polym. Sci.*, 179(2005)135.
- [64] A.W. Leslie, *J. Appl. Polym. Sci.*, 92(2004)2025.
- [65] S. Bourbigot, E. Devaux and X. Flambard, *Polym. Deg. Stab.*, 75(2002)397.
- [66] E. Devaux, M. Rochery and S. Bourbigot, *Fire Mater.*, 26(2002)149.
- [67] J. Gilman and T. Kashiwagi, *Sample J.33* (1997)40.
- [68] J. Gilman, *Appl. Clay. Sci.* 15 (1999)31.
- [69] J. Gilman, C. Jackson and A. Morgan, *Chem. Mat.* 12 (2000)1866.
- [70] Z. Wang, T. Lan and T.J. Pinnavaia, *Chem. Mater.* 8(1996)2200.

- [71] C.D. Munzy, B.D. Butler, H.J.M. Hanley, F. Tsvetkov and D.G. Pfeiffer, *Material Letters*, 28(1996)379.
- [72] T. Lan and T.J. Pinnavaia, *Mat.Res.Soc.Symp.Proc.* 435(1996)79.
- [73] A.A. Damour and D. Salvetat, *Ann.Chim.Phys.Ser.* 21(1847)376.
- [74] W.A. Deer and R.A. Howie, *Rock-Forming Minerals* 3(1962)240.
- [75] J.W. Earley, B.B. Osthaus and I.H. Milne, *Am. Miner.* 38(1953)707.
- [76] G.W. Brindley and G. Grown, eds. *Crystal Structure of Clay Minerals and Their X-Ray Identification*. 3rd ed. 1980, The Mineralogical Society:London.
- [77] R.E. Grim, *Clay Mineralogy*, 1953, McGraw Hill: New York.
- [78] S. Brindley, G. Brown, "Crystal Structure of Clay Minerals and Their X-ray Diffraction", Mineralogical Society, London (1980)
- [79] T. Pinnavaia, *Science* 220(1983)365.
- [80] N. Guven, in *Hydrous Phyllosilicates*, Bailey, S.W., Editor.1988, Mineralogical Society of America: Washington, D.C.
- [81] R.A. Vaia, *Structural Characterization of Polymer-Layered Silicate Nanocomposites*, in *Polymer-Clay Nanocomposites*, T.J.Pinnavaia and G.W.Beaall, Editors. 2000, Johnson Wiley & Sons: New York.
- [82] S.R. Suprakas and O.Masami, *Progress in Polymer Science* 28(2003)854.
- [83] T. Pinnavaia and G. Beall, "Polymer-Clay Nanocomposites," John Wiley & Sons, Ltd., New York (2000)
- [84] J. Lulis, R.T. Woodhams, M. Xanthos, *Polym. Eng.Sci.*13(1973)139.
- [85] F.Effenberger, M.Schweizer and W.S.Mohamed, *J.Appl.Polym.Sci.* 112(2009)1572.
- [86] B.K.G. Theng, *the Chemistry of Clay-Organic Reactions*, 1974, John Wiley & Sons: New York.
- [87] E.P. Giannelis, *Adv.Mater.* 8(1996)29.
- [88] E.D. Magauran, M.D. Kieke, W.W. Reichert and A. Chiavoni, *NGLI Spokeman* 50(1987)453.
- [89] W.S. Mardis, *J. Am.Oil Chemists Soc.*61(1984)382.
- [90] X. Kornmann, L.A. Berglund, J. Sterte and E.P. Giannelis, *Polym.Eng.& Sci.*38(1998)1351.
- [91] K. Isoda, K. Kuroda and M. Ogawa, *Chemistry of Materials*,12(2000)1702.
- [92] H.V. Olphen, *An Introduction to Clay Colloid Chemistry*, John Wiley & Sons: New York.

- [93] A. Usuki, Y. Kojima, M. Kawasumi, A. Okada, Y. Fukushima, T. Kurauchi, O. Kamigaito, *J. Mater. Res.* 8(1993)1179.
- [94] Southern Clay Products, Technical Data Sheets, http://www.nanoclay.com/product_bulletins.asp, 2006.
- [95] E. Busenberg and C.V. Clemency, *Clays and clay minerals*, 21(1973)213.
- [96] M.M. Mortland and J.L. Mellor, *Soil Sci. Soc.Proc.* 18(1954)363.
- [97] J.L.Mfcatee, *Am. Miner.* 44C1959)1230.
- [98] M. Stul and W.J. Mortier, *Clays and clay minerals*, 22(1974)391.
- [99] A.Usuki, M.Kawasumi, Y.Kojima A.Okada, T.Karauchi and O.Kamigaito, *J.Mater.Res.*8(1993)1174.
- [100] J.W. Jordan, *J.Phys.Colloid Chem.* 53(1949)294.
- [101] A. Weiss, *Angew. Chem. internat. Edit.* 2(1963)134.
- [102] T. Lan, P.D. Kaviratna and T. J. Pinnavaia, *Chem. Mater.* 7(1995)2144.
- [103] Z. Wang and T. J. Pinnavaia, *Chem. Mater.* 10(1998)1820.
- [104] G. Lagaly, *Solis State Ionics*, 22(1986)43.
- [105] Z. Klapyta, T. Fujita and N. Lyi, *Appl. Clay Sci.*19(2001)5.
- [106] A. Krysztafkiewicz, R. Werner, LK. Lipska and T. Jesionowski, *Colloids Surf A: Physicochem Eng. Aspects*, 182(2001)65.
- [107] N. Alkadas, UR. Kapadi and DG Hundiwale, *.Appl.POLym.Sci.* 93(2004)1299.
- [108]L.A. Utrack and M.R. Kamal, *Arabian J.Sci.Eng.*27 (2002)44.
- [109] P.Reichert, H. Nitz, S. Klinke, R.Brandsch, R.Thomann and R.Mülhaupt, *Macromol.Mater.Eng.*275(2000)8.
- [110] S.Y.Gu, J.Ren and Q.F.Wang, *J.Appl.Polym.Sci.*91(2004)2427.
- [111]T.G.Gopakumar, J.A.Lee, M.Kontopoulou and J.S.Parent, *Polymer* 43(2002)5483.
- [112] M.T.Ton-That, F.Perrin-Sarazin, K.C.Cole, M.N.Bureau and J.Denault, *Polym.Eng. &Sci.*44(2004)1212.
- [113] M.J.Dumont, A.Reyna-Valencia, J.P.Emond and M.Bousmina, *J.Appl.Polym.Sci.*103 (2007)618.
- [114] J.M. Lagaron, R. Catala and R. Gavara, *Mater.Sci.Technol.*20 (2004)1.
- [115] J.H. Chang and Y.U. An, *J.Polym.Sci. Polym.Phys.*40 (2002)670.
- [116] J. Ma, Z. Qi and Y.Hu, *J.Appl.Polym.Sci.*82 (2001)3611.
- [117] G. Beyer, *J.Fire Sci.*23 (2005)75.

- [118] H. Alimadadi, M. Ahmadi, M. Aliofkhazraei and S.R. Younesi, *Material and Design* 30(2009)1356.
- [119] A.C. Esteves, M.C. Olinda, M.V. Barros-Timmons, C. Boemare, M.J. Soares, T. Montiero and T. Trindada, *J.Nanoscience&Nanotechnol.*2 (2002)177.
- [120] K.G. Anit, M. Krishna and A.M. Sara, *Mater. Phys. &Mech.*1 (2000)1.
- [121] V.F. Madhavi, P.V. Adhyapak, U.P. Mulik, D.P. Amalnerkar and R.C. Aiver, *Talanta*78 (2009)590.
- [122] J.M. Yeh, K.C. Chang, C.W. Peng, M.C. Lai, C.B. Hung, S. C. Hsu, S.S. Hwang and H.R. Lin, *Mater. Chem. & Phys.* 115(2009)744.
- [123] C.M. Nshuti, J.M. Hossenlopp and C.A. Wilkie, *Polym. Deg. &Stab.* 93(2008)1855.
- [124] T. Yu, J. Lin, J. Xu, T. Chin, S. Lin and X. Tian, *Compos. Sci. & Technol.* 67(2007)3219.
- [125] M. Tanoglu and Y. Ergün, *Composites Part A* 38(2007)318.
- [126] P.K. Sahoo and R. Samal, *Polym. Deg. & Stab.* 92(2007)1700.
- [127] A. Tabtiang, S. Lumlong and R.A. Venables, *Eur. Polym. J.* 36(2000)2559.
- [128] K.R. Ratinac, R.G. Gilbert, L. Ye, A. S. Jones and S.P. Ringer, *Polymer* 47(2006)6337.
- [129] M. Okamoto, S. Morita, H. Taguchi, Y.H. Kim, T. Kotaka and H.Tateyama, *Polymer J.* 41(2000)3887.
- [130] S. Bandyopadhyay and E.P. Giannelis, *Polym Mater. Sci. & Eng.* 82(2000)208.
- [131] X. Huang and W.J. Brittain, *Macromolecules* 34(2001)3255.
- [132] C. Zeng and L.J. Lee, *Macromolecules* 34(2001)4098.
- [133] N. Salahuddin and M. Shehata, *Polymer* 42(2001)8379.
- [134] H. Bottcher, M.L. Hallensleben, S. Nu, H. Wurm, J. Bauer and P.Behrens, *J Mater. Chem.*12(2002)1351.
- [135] A.S. Zerda, T.C. Caskey TC and A.J. Lesser, *Macromolecules* 36(2003)1603.
- [136] S. Su and C.A. Wilkie, *J Polym Sci, Part B: Polym Phys* 41(2003)1124.
- [137] J. Y. Jang, M.S. Kim, H.M. Jeong and C.M. Shin, *Compos. Sci. & Technol.* 69(2009)186.
- [138] S.Y. Lee, H. Chen and M.A. Hanna, *Industrial Crops & Products* 28(2008)95.
- [139] M.S. Kim, J. k. Jun and H.M. Jeong, *Compos. Sci. & Technol.* 68(2008)1919.
- [140] M. Okamoto, S. Morita, Y.H. Kim, T. Kotaka and Tateyama, *Polymer J.* 42(2001)1201.

- [141] Y. Someya and M. Shibata, *Polymer* 46(2005)4891.
- [142] J. Kajutuna and U. Sebnik, *J. Adhesion & Adhesives* 29(2009)543.
- [143] Z. Chen, C. Huang, S. Liu, Y. Zhang and K.Gong, *J. Appl. Polym. Sci.* 75(2000)796.
- [144] J. Billingham, C. Breen and J. Yarwood, *J. Vibration Spectroscopy*, 14(1997)19.
- [145] J. Lin, J. Wu, Z. Yang and M. Pu, *Macromol. Rapid Commun.* 22(2001)422.
- [146] R. Blumstein, A. Blumstein and K.K. Parikh, *Appl. Polym. Symp.* 25(1994):81.
- [147] Y.Sugahara, S. Satakawa, K. Kuroda and C. Kato, *Clay Miner* 36(1988)343.
- [148] F. Bergaya and F. Kooli, *Clay Miner* 33(1991)33.
- [149] Y.S. Choi, K.H. Wang, M. Xu and I.J. Chung, *Chem Mater* 14(2002)2936.
- [150] D.B. Zax , D.K. Yang, R.A. Santos, H. Hegmann, E.P. Giannelis and E.Manias, *J Chem. Phys.*112(2000)2945.
- [151] R.A. Vaia, H. Ishii and E.P. Giannelis, *Chem. Mater.*5 (1993)1694.
- [152] H. Li, Y. Ya and Y. Yong, *Europ. Polym. J.* 41(2005)2016.
- [153] A. Akelah, *Emerging technologies and business opportunities.*
New York: Plenum Press; 30(1995)625.
- [154] C. Ding, B. Guo, H. He, D. Jia and H. Hong, *Europ. Polym. J.* 41(2005)1781.
- [155] C.L. Park, O. Park, J.G. Lim and H.J. Kim. *Polymer* 42(2001)7465.
- [156] G.H. Wang and L.M. Zhang, *App. Clay Sci.* 38(2007)17.
- [157] M. Sikka, L.N. Cerini, S.S. Ghosh and K.I. Winey, *J. Polym. Sci. Part B: Polym. Phys.* 34(1996)1443.
- [158] M. Laus, M. Camerani, M. Lelli, K. Sparnacci and F. Sandrolini, *J Mater Sci* 33(1998)2883.
- [159] J.G. Doh and I. Cho, *Polym. Bull.* 41(1998)511.
- [160] T.L. Porter, M.E. Hagerman, B.P. Reynolds and M.E. Eastman, *J. Polym. Sci. Part B: Polym. Phys.* 36(1998)673.
- [161] N. Hasegawa, H. Okamoto, M. Kawasumi and A. Usuki, *J. Appl. Polym. Sci.* 74(1999)3359.
- [162] M.W. Noh and D.C. Lee, *Polym. Bull.* 42(1999)619.
- [163] M.W. Weimer, H. Chen, E.P. Giannelis and D. Y. Sogah, *J. Am. Chem. Soc.* 121(1999)1615.
- [164] X. Fu and S. Qutubuddin, *Polymer* 42(2001)807.
- [165] G. Chen, S. Liu, s. Zhang and Z. Qi, *Rapid Commun.* 21(2000)746.
- [166] Y.T. Lim and O. Park, *Macromol Rapid Commun.* 21(2000)231.

- [167] B. Hoffman, C. Dietrich, R. Thomann, C. Friedrich and R. Mulhaupt, *Macromol. Rapid. Commun.* 21 (2000)57.
- [168] C. Zilg, R. Thomann, M. Baumert, J. Finter and R. Mulhaupt, *Macromol. Rapid Commun.* 21(2000)1214.
- [169] H.D. Wu, C.R. Tseng and F.C. Chang, *Macromolecules* 34(2001)2992.
- [170] P. Xiao, M. Xiao and K. Gong, 42(2001)4813.
- [171] C.R. Tseng, J.Y. Wu, H.Y. Lee and F.C. Chang, *Polymer* 42(2001)10063.
- [172] J. Zhu, A.B. Morgan, F.J. Lamelas and C.A. Wilkie, *Chem. Mater.* 13(2001) 3774.
- [173] Q.H. Zeng, D.Z. Wang, A.B. Yu and G.Q. Lu, *Nanotechnology* 13(2002)549.
- [174] F.L. Beyer, N.C.B. Tan, A. Dasgupta and M.E. Galvin, *Chem. Mater.* 14(2002)2983.
- [175] J.W. Gilman, W.H. Awad, R.D. Davis, J. Shields, R.H. Harris, C. Davis, A.B. Morgan, T.E. Sutto, J. Callahan, P.C. Trulove and H.C. Delong, *Chem. Mater.* 14(2002)3776.
- [176] S.D. Argoti, S. Reeder, H. Zhao and D.A. Shipp, *Polym Prepr. (USA)* 43(2002)267.
- [177] M.Y. Gelfer, H.S. Hyun, L. Liu, B.S. Hsiao, B. Chu, M. Rafailovich, M. Si and V. Zaitsev, *J Polym Sci, Part B: Polym. Phys.* 41(2003)44.
- [178] H.Z. Friedlander and C.R. Frink, *J Polym Sci, Part B*, 2(1964)475.
- [179] N.A. Churochkina, S.G. Starodoubtsev and A.R. Khokhlov, *Polym. Gels Networks* 6(1998)205.
- [180] D. Gao, R.B. Heimann, M.C. Williams, L.T. Wardhaugh and M. Muhammad, *J. Mater.Sci.* 34(1999)1543.
- [181] X. Xia, J. Yih, N.A. D'Souza and Z. Hu, *Polymer* 44(2003) 3389.
- [182] A. Wheeler, *US Pat.* 2(1958)847.
- [183] D.J. Greenland. *J Colloid Sci.* 18 (1963)647.
- [184] N. Ogata, S. Kawakage and T. Ogihara, *J. Appl. Polym. Sci.* 81(1997)573.
- [185] H. Matsuyama, and J.F Young, *Chem. Mater.* 11(1999)16.
- [186] K.E. Strawhecker, and E. Manias, *Chem. Mater.* 12(2000)2943.
- [187] Y. Wang and Yan D, *Polym. Prepr (USA)*. 44(2003)1102.
- [188] C.W. Francis, *Soil. Sci.* 115(1973):40.
- [189] K.A. Carrado and Xu L, *Chem. Mater.* 10(1998) 1440.

- [190] A. Gultek, T. Seckin, Y. Onal and G. Icduygu, *J. Appl. Polym. Sci.* 81(2001) 512.
- [191] R. Levy and C.W. Francis, *J. Colloid Interface Sci.* 50(1975) 442.
- [192] C.W. Koo, H.T. Ham, M.H. Choi, Kim and I.J.Chung, *Polymer* 44(2003)681.
- [193] Y. Komori, Y. Sugahara and K. Kuroda, *Chem. Mater.* 11(1999)3.
- [194] A. Nisha, M.K. Rajeswari and R. Dhamodharan, *J. Appl.Polym.Sci.*76 (2000) 1825.
- [195] K.G. Fournaris, M.A. Karakassides, D. Petridis, K. Yiannakopoulou, *Chem. Mater.* 11(1999)2372.
- [196] R.L. Parfitt and D.J. Greenland, *Clay Miner.* 8(1970)305.
- [197] X. Zhao, K. Urano and S. Ogasawara, *Colloid Polym. Sci.* 276(1989) 899.
- [198] L. Priya and J.P. Jog, *J. Polym. Sci. Part B: Polym. Phys.* 41(2003)31.
- [199] C.O. Oriakhi, X. Zhang and M.M. Lerner, *Appl. Clay Sci.* 15(1999) 109.
- [200] S.L. Hsu and K.C. Chang, *Polymer* 43(2002) 4097.
- [201] S.W. Kim, W.H. Jo, M.S. Lee, M.B. Ko and J.Y. Jho, *Polymer* 42(2001)9837.
- [202] N. Artzi, Y. Nir, M. Nakris and A. Seigmann, *J. Polym. Sci. Part B: Polym. Phys.* 40(2002)1741.
- [203] J. Ren, A.S. Silva and R. Krishnamoorti, *Macromolecules* 33(2000) 3739.
- [204] C.A. Mitchell and R. Krishnamoorti, *J. Polym. Sci, Part B: Polym. Phys.* 40(2002)1434.
- [205] J.E. Mark, *Polym. Eng. Sci.* 36(1996)2905.
- [206] L.B. Pavia, A.R. Morales and T.R. Guimaraes, *Mater. Sci. & Eng.* 447(2007)261.
- [207] A. Ardanuy, J.I. Verlasco, VF.Relainho, D. Arencon and A.B. Mortinez, *Thermochemica Acta* 479(2008)45.
- [208] A. Hedayati and A. Arefarzar, *Polym. Testing* 28(2009)128.
- [209] Y. Dong, D. Bhattacharyya and P.J. Hunter, *Composites Part A* 68(2008)2864.
- [210] C.O. Rohlmann, M.F. Horst, L.M. Quinzani and M.D. Failla, *Europ. Polym. J.* 44(2008)2749.
- [211]J. Golebiewski and A. Galeski, *Compos. Sci. & Techno.* 67(2007)3492.
- [212] J. Ma, E. Biolotti, T. Peijs and J.A. Darr, *Europ. Polym. J.* 43(2007)4931.
- [213] Y. Tang and M. Lewin, *Polym. Deg. & Stab.* 92(2007)53.
- [214] A. Monhard and J. Varga, *Europ. Polym. J.* 42(2006)3257.

- [215] A. Oya, T.J. Pinnavaia and G.W. Beall, *Polymer–clay nanocomposites*. London: Wiley; 2000. p. 151.
- [216] N. Hasegawa, H. Okamoto, M. Kato and A. Usuki, *J. Appl. Polym. Sci.* 78(2000)1918.
- [217] A. Oya, Y. Kurokawa H. Yasuda, *J. Mater. Sci.* 35(2000)1045.
- [218] J.W. Lee, Y.T. Lim and O. Park, *Polym. Bull.* 45(2000) 191.
- [219] Q. Zhang, Q. Fu, L. Jiang and Y. Lei, *Polym. Int.* 49(2000)1561.
- [220] J.M. Garces, D.J. Moll, J. Bicerano, R. Fibiger and D.G. McLeod, *Adv. Mater.* 12(2000)1835.
- [221] N. Hasegawa, H. Okamoto, M. Kawasumi and M. Kato, A. Tsukigase and A.Usuki, *Macromol. Mater. Engng.*280 (2000)76.
- [222] S. Hambir, N. Bulakh, P. Kodgire and R. Kalgaonkar, *J. Polym. Sci, Part B: Polym. Phys.* 39(2001)446.
- [223] M. Zanetti, G. Camino, P. Reichert and R. Mulhaupt, *Macromol. Rapid Commun.* 22(2001)176.
- [224] G. Galgali, C. Ramesh and A. Lele, *Macromolecules* 34(2001)852.
- [225] J.M. Gloaguen and J.M. Lefebvre, *Polymer* 42(2001) 5841.
- [226] J.M. Garcia-Martinez, O. Laguna, S. Areso, and E.P. Collar, *J. Appl. Polym. Sci.* 81(2001)625.
- [227] D. Schmidt, D. Shah E.P. Giannelis, *Solid State Mater. Sci.* 6(2002)205.
- [228] P. Reichert, B. Hoffman, T. Bock, R. Thomann, R. Mulhaupt, and C. Friedrich, *Macromol. Rapid Commun.* 22(2001)519.
- [229] P.H. Nam, P. Maiti, M. Okamoto and T. Kotaka, June 25–27, 2001, Chicago, Illinois, USA: ECM Publication; 2001.
- [230] E. Manias, *Mater. Res. Soc. Bull.* 26(2001)862.
- [231] M. Okamoto, P.M. Nam, P. Maiti , T. Kotaka, N. Hasegawa and A.Usuki, *Nano Lett.*1(2001) 295.
- [232] M. Okamoto, P.H. Nam, M. Maiti, T. Kotaka, T. Nakayama, M.Takada, M. Ohshima, A. Usuki, N. Hasegawa and H. Okamoto, *Nano Lett.* 1(2001)503.
- [233] T. Sun and J.M. Garces, *Adv. Mater.* 14(2002)128.
- [234] P. Maiti, P.H. Nam, M. Okamoto, T. Kotaka, N. Hasegawa A. Usuki, *Macromolecules* 35(2002)2042.
- [235] P. Maiti, P.M. Nam, M. Okamoto, T. Kotaka, N. Hasegawa and A. Usuki, *Polym. Eng. Sci.* 42(2002)1864.

- [236] P.M. Nam, P. Maiti, M. Okamoto, T. Kotaka, T. Nakayama, M. Takada, M. Ohshima, A. Usuki, N. Hasegawa and H. Okamoto, *Polym. Eng. Sci.* 42(2002)1907.
- [237] S. Hambir, N. Bulakh and J.P. Jog, *Polym. Engng. Sci.* 42(2002)1800.
- [238] D. Kaempfer, R. Thoman and R. Mulhaupt, *Polymer* 43(2002)2909.
- [239] Q. Zhang, Y. Wang and Q. Fu, *J. Polym. Sci, Part B: Polym. Phys.* 41(2003) 41.
- [240] A. Somwangthanaroj, E.C. Lee and M.J. Solomon, *Macromolecules* 36(2003)2333.
- [241] A.B. Morgan and J.D. Harris, *Polymer* 44(2003)2113.
- [242] V. Pettarin, P.M. Frontini, V.J.R. Pita, M.L. Dias and F.V. Diaz, *Composites Part A* 39(2008)1822.
- [243] A.D. Drozdov, E.A. Jensen and J.D. Christianis, *Comput. Mater. Sci.* 43(2008)1027.
- [244] Y. Cai, L. song, Q. He, D. Yang and Y. Hu, *Energy Conver. & MAneg.* 49(2008)2055.
- [245] J. Zhang, D.D. Jiang and C.A. Wilkie, *Thermachemica Acta* 430(2005)107.
- [246] J. Rong, J. Jing, H. Li and M. Sheng, *Macromol. Rapid Commun.* 22(2001)329.
- [247] K.H. Wang, M.H. Choi, C.M. Koo, Y.S. Choi and I.J. Chung, *Polymer* 42(2001)9819.
- [248] M. Alexandre, P. Dubois, T. Sun, J. M. Graces and R. Jerome, *Polymer* 43(2002)2123.
- [249] Y.H. Jin, H.J. Park, S.S. Im, S.Y. Kwak and S. Kwak, *Macromol. Rapid Commun.* 23(2002)135.
- [250] A. Bafna, G. Beaucage, F. Mirabella and S. Mehta, *Polymer* 44(2003)1103.
- [251] M.A. Osman, G. Seyfang and U.W. Suter, *J. Phys. Chem.* 104 (2000)4433.
- [252] A. Usuki, A. Tukigase and M. Kato, *Polymer* 43(2002)2185.
- [253] S.D. Wanjale and J.P. Jog, *J. Polym. Sci, Part B: Polym. Phys.* 41(2003)1014.
- [254] T.J. Pinnavaia, T. Lan. Z.Wang, H. Shi and P.D. Kaviratna, *ACS Symposium Series*, 622(1996)250.
- [255] R.A. Vaia and E.P. Giannelis, *MRS Bulletin*, 26(2001)394.
- [256] R.A. Vaia, K.D. Jandt, E.J. Kramer and E.P. Giannelis, *Macromolecules* 28(1995) 8080.
- [257] K. Hbaieb, Q.X. Wang, Y.H.J. Chia and B. Cotterell, *Polym. J.* 48(2007)901.

- [258] G. Jimenez, N. Ogata, H. Kawai and T. Ogihara, *J Polym Sci: Part B: Polym. Phys.* 35(1997)389.
- [259] A. Blumstein, *J. Appl. Polym. Sci.* 3(1965)2653.
- [260] D.H. Salmon and M. J. Rosser, *J. Appl. Polym. Sci.* 9(1965)1261.
- [261] D.H. Salmon and J. D. Swift, *J. Appl. Polym. Sci.* 11(1967)2567.
- [262] D.H. Salmon and B. B. Loft, *J. Appl. Polym. Sci.* 12(1968)1253.
- [263] P. Reichert, J. Kressler, J. Thomann, R. Muelhaupt and G. Stoepelmann, *Acta Polymerica* 49(1998)116.
- [264] D.C. Lee and L.W. Jang, *J. Appl. Polym. Sci.* 61(1996)1117.
- [265] L. Biasci, M. Aietto, M. Ruggeri and F. Ciadelli, *Polymer* 35(1994)3296.
- [266] M. Okamoto, S. Morita, H. Taguchi, Y. H. Kim, T. Kotaka and H. Tateyama, *Polymer* 41(2000)3887.
- [267] F. Dietsche, Y. Thomann, R. Thomann and R. Mulhaupt, *J. Appl. Polym. Sci.* 75(2000)396.
- [268] A. Akelah and A. Moet, *J. Mater. Sci.* 31(1996)3589.
- [269] G. Chen, Y. Ma and Z. Qi, *Scripta Materiala* 44(2001)125.
- [270] Y. Ding, C. Guo, J. Dong and Z. Wang, *J. Appl. Polym. Sci.* 102 (2006)4314.
- [271] H.G. Jeon, H.T. Jung, S.W. Lee and S.D. Hudson, *Polym. Bull.* 41(1998)107.
- [272] R. A. Vaia, B. B. Sauer, O. K. Tse and E.P. Giannelis, *J. Polym. Sci. Part B Polym. Phys.* 35(1997)59.
- [273] E. Ruiz-Hitzky, P. Arenda, B. Casal and J. C. Galvan, *Adv. Mater.* 7(1995)180.
- [274] J. Bujdak, E. Hackett and E. P. Giannelis, *Chemistry of materials*, 12 (2000)2168.
- [275] Y. H. Hyun, S.T. Lim, H. J. Choi and M. Jho, *Macromolecules*, 34(2001)8084.
- [276] D. Campbell, R.A. Pethrick and J.R. White, *Polymer Characterization: Physical Techniques*, Stanley Thornes Ltd, Cheltenham, UK, 2000.
- [277] V. Singh, T. Singh, A. Chandra, S.K. Bandyopadhyay, P. Sen, K. Witte and A. Srivastava, *Nucl. Instrum. Methods Phys. Res., Sect. B* 244 (2006)243.
- [278] G. Galgali, S. Agarwal and A. Lele, *Polym. J.* 45(2004)6059.
- [279] A. Guinier, *X-ray Diffraction in Crystals, Imperfect Crystals and Amorphous Bodies*, Dover, New York, 1994.
- [280] D.M. Moore, J. R. C. Reynolds, *X-ray Diffraction and the Identification and Analysis of Clay Minerals*, Second ed., Oxford University Press, New York, 1997.

- [281] R. Krishnamoorti, R.A. Vaia and E.P. Giannelis, *Chem. Mater.* 8(1996)1728.
- [282] Y.T. Lim and O. Park, *Rheol. Acta* 40(2001)220.
- [283] W. Letwimolnun, B. Vergnes, G. Ausias and P.J. Carreau, *J. Non-Newtonian Fluid Mech.* 141(2007)167.
- [284] R.A. Vaia, G. Price, P.N. Ruth, H.T. Nguyen and J. Lichtenhan, *Appl. Clay Sci.* 15(1999)67.
- [285] K. Sall and *Eur. Plas. News* (2002).
- [286] A.K. Bledzki and J. Gassan. *Prog. Polym. Sci.* 24(1999)221.
- [287] A.K. Bledzki, S. Reihmane and J. Gassan, *J. Polym. Plast. & Technol. Eng.* 37(1998)451.
- [288] M. Ratajski and S. Boryniec, *Polym. Adv. Technol.* 10(1999)625.
- [289] B. Wielage, T. Lampke, G. Marx, K. Nestler and D. Starke, *Thermochemica Acta* 337(1999)169.
- [290] J. George, S.S. Bhagawan and S. Thomas, *J. Therm. Anal.* 47(1996)1121.
- [291] D. Plackett, T.A. Logstrup, W.P. Batsberg and L. Nielsen, *Comp. Sci. & Technol.* 63(2003)1287.
- [292] N.R. McDill, Commercial Standardization of Instrument Testing of Cotton, Proceeding of EFS system Conference ⁷PP. 2004.
- [293] F.G. Goldwaith and J.D. Guthrie, (1954). *Matthew's Textile Fibers*, H. R. Mauersberger, ed., Wiley Interscience, New York.
- [294] Y.L. Hsieh and A. Wang, *Textile Research Journal* 70(2000)495.
- [295] A.J. Michell, *Carbohydr. Res.* 197 (1990)53.
- [296] D.A. Goring and T.E. Timell, (1962), *TAPPI*, 45(1962)454.
- [297] M. Figini, (1982). 243–271, Plenum Press, New York.
- [298] J.D. Timpa and B.A. Triplett, 189(1993)101.
- [299] M.L. Nelson and T. Mares, *Textile Res. J.*, 35(1965), 592–603.
- [300] R. Freytag and J. Donze, *Handbook of Fibre Science and Technology: Volume 1* (1993), Chemical Processing of Fibers and Fabrics, Fundamentals and Preparation, Part A Marcel Dekker, NY, pp. 94.
- [301] A. Heredia, R. Guillen, A. Jimenez and J. Fernandez-Bolanos, *Revista Espanola de Ciencia y Tecnologia de Alimentos*, 33(1993),113.
- [302] A. Darvill, M. McNeil, P. Albersheim and D.P. Delmer, *The Biochemistry of Plants*, Vol. 1(1980)91, Academic Press, New York.
- [303] M.C. Meinert and D.P. Delmer, *Plant Physiol.* 59(1977)1088.

- [304] M.L. Hartzell and Y.L. Hsieh, *Textile Research Journal* 70(2000)810.
- [305] G.V. Hornuff and H. Richter, *Faserforsch. Textiltechnol.* 15(1964)115.
- [306] M.A. Rouselle, *Textile Res J*, 72(2002)131.
- [307] J.D. Timpa and H.H. Ramey, *Textile Res. J.* 64(1994)537.
- [308] K.H. Meyer and L. Misch, *Chim. Acta*, 20(1937)232.
- [309] A. Sarko and R. Muggli, *Macromolecules*, 7(1974)4.
- [310] A.D. French, (1985) 'Physical and theoretical methods for determining the supramolecular structure of cellulose', in T.P. Nevell and S.H. Zeronian, *Cellulose chemistry and its applications*, Chichester, Ellis Horwood Ltd.
- [311] N.M. Bikales and L. Segal, Eds, *High Polymers, Vol. V (1971), Part V, Cellulose and Cellulose Derivatives*, Wiley Interscience, New York, NY.
- [312] M.A. Pepenzhik, A.D. Virnik and Z.A. Rogovin, *Vysokomol. Soedin. Ser B* 11(1969)245.
- [313] B.N. Misra, R. Dogra and I.K. Mehta, *J. Polym. Sci. Polym. Chem.* 118(1980)749.
- [314] B.N. Misra, I.K. Mehta and R.C. Khetrapal, *J. Polym. Sci. Polym. Chem.* 22(1984) 2767.
- [315] K.V. Prasanth and R.N. Tharanathan, *Carbohydr. Polym.* 54(2003)43.
- [316] W. Xie, P. Xu, W. Wang and Q. Liu, *Carbohydr. Polym.* 50(2002)35.
- [317] U.D. Bajpai, A. Jain and S. Ray, *J. Appl. Polym. Sci.* 39(1990)2187.
- [318] M. Szwarc, *J. Polym. Sci. Part A: Polym. Chem.* 57(1998)36.
- [319] K.E. Russell, *Prog. Polym. Sci.* 27(2002)1007.
- [320] U.M. Stehling, E.E. Malmstrom, R.M. Waymouth and C.J. Hawker, *Macromolecules* 31(1998)4396.
- [321] V. Percec and B. Barboiu, *Macromolecules* 28(1995)7970.
- [322] J.S. Wang and K. Matyjaszewski, *J. Am. Chem. Soc.* 117(1995)5614.
- [323] K. Matyjaszewski and J. Xia, *Chem. Rev.* 101(2001)2921.
- [324] K. Matyjaszewski, *Chem. Eur. J.* 5(1999)3095.
- [325] V. Coessens, T. Pintauer and K. Matyjaszewski, *Prog. Polym. Sci.* 26(2001)337.
- [326] M. Kato, M. Kamigaito, M. Sawamoto and T. Higashimura, *Macromolecules* 28(1995)1721.
- [327] J.S. Wang and K. Matyjaszewski, *Macromolecules* 28(1995)7901.
- [328] K. Matyjaszewski, T.E. Patten and J. Xia, *J. Am. Chem. Soc.* 119(1997)674.

- [329] K.L. Beers, S.G. Gaynor, K. Matyjaszewski, S.S. Sheiko and M. Moeller, *Macromolecules* 31(1998)9413.
- [330] H.G. Boerner, D. Duran, K. Matyjaszewski, M. Da Silva, S.S. Sheiko, *Macromolecules* 35(2002)3387.
- [331] D. Neugebauer, Y. Zhang, T. Pakula and K. Matyjaszewski, *Polymer* 44(2003)6863.
- [332] S. Qin, K. Matyjaszewski, H. Xu and S.S. Sheiko, *Macromolecules* 36(2003)605.
- [333] K. Yamada, M. Miyazaki, K. Ohno, T. Fukuda and M. Minoda, *Macromolecules* 32(1999)290.
- [334] S.G. Roos, A.H. Mueller and K. Matyjaszewski, *Macromolecules* 32(1999)8331.
- [335] H. Shinoda and K. Matyjaszewski, *Macromol. Rapid Commun.* 22(2001)1176.
- [336] H. Shinoda, K. Matyjaszewski, L. Okrasa, M. Mierzwa and T. Pakula, *Macromolecules* 36(2003)4772.
- [337] H. Shinoda and K. Matyjaszewski, *Macromolecules* 34(2001)6243.
- [338] S.C. Hong and S. Jia, *J. Polym. Sci. Part A: Polym. Chem.* 40(2002)2736.
- [339] K. Matyjaszewski, K.L. Beers, A. Kern and S.G. Gaynor, *J. Polym. Sci. Part A: Polym. Chem.* 36(1998) 823.
- [340] J. Pyun and K. Matyjaszewski, *Chem. Mater.* 13(2001)3436.
- [341] K. Matyjaszewski, P.J. Miller, N. Shukla, B. Immaraporn, A. Gelman, B.B. Luokala, T.M. Siclovan, G. Kickelbick, T. Vallant, H. Hoffmann and T. Pakula, *Macromolecules* 32(1999)8716.
- [342] J. Pyun, J. Xia and K. Matyjaszewski, *ACS Symp. Ser.* 838(2003)273.
- [343] M. Ejaz, S. Yamamoto, Y. Tsujii and T. Fukuda, *Macromolecules* 35(2002) 1416.
- [344] J. Pyun, K. Matyjaszewski, T. Kowalewski, D. Savin, G. Patterson, G. Kickelbick and N. Huesing, *J. Am. Chem. Soc.* 123(2001)9445.
- [345] J. Pyun, S. Jia, T. Kowalewski, G.D. Patterson and K. Matyjaszewski, *Macromolecules* 36(2003)5094.
- [346] D.A. Savin, J. Pyun, G.D. Patterson, T. Kowalewski and K. Matyjaszewski, *J. Polym. Sci. Part B: Polym. Phys.* 40(2002)2667.
- [347] T. Kowalewski, R.D. McCullough and K. Matyjaszewski, *Eur. Phys. J. E: Soft Matter* 10(2003)5.
- [348] A. Carlmark and E. Malmstroem, *J. Am. Chem. Soc.* 124(2002)900.

- [349] M. Ejaz, Y. Tsujii and T. Fukuda, *Polymer* 142(2001) 6811.
- [350] T. Peng and Y.L. Cheng, *Polymer* 42(2001)2091.
- [351] I.E. Uflyand, I.A. Ilchenko, V.N. Sheinker and V.S. Savostyanov, *Polymer* 17(1992)289.
- [352] A. Bhattacharya, A. Das and A. De, *Ind. J. Chem. Tech.* 5(1998)135.
- [353] J. Chen, H. Iwata, Y. Maekawa, M. Yoshida and N. Tsubokawa, *Radiat. Phys. Chem.* 67(2003)397.
- [354] P. Marmey, M.C. Porte and C. Baquey, *Nucl. Instrum. Methods B* 208(2003)42.
- [355] T. Yamaki, M. Asano, Y. Maekawa, Y. Morita, T. Suwa, J. Chen, N. Tsubokawa, K. Kobayashi, H. Kubota and M. Yoshida, *Radiat. Phys. Chem.* 67(2003)403.
- [356] I. Kaur, R. Barsola, A. Gupta and B.N. Misra, *J. Appl. Polym. Sci.* 54 (1994).
- [357] I. Kaur, B.N. Misra, M.S. Chauhan and S. Chauhan, *J. Appl. Polym. Sci.* 59(1996)389.
- [358] S. Basu, A. Bhattacharya, P.C. Mondal and S.N. Bhattacharyya, *J. Polym. Sci. Polym. Chem.* 32(1994) 2251.
- [359] S. Aich, A. Bhattacharya and S. Basu, *Radiat. Phys. Chem.* 50(1997)347.
- [360] S. Aich, T. Sengupta, A. Bhattacharya and S. Basu, *J. Polym. Sci. Polym. Chem.* 37(1999)3910.
- [361] S.N. Bhattacharyya, D. Maldas and V.K. Pandey, *J. Polym. Sci. A24* (1986)2507.
- [362] A. Kitamura, S. Hamamoto, A. Taniike, Y. Ohtani, N. Kubota and Y. Furuyama, *Radiat. Phys. Chem.* 69(2004)9171.
- [363] R. Mazzei, D. Tadey, E. Smolko and C. Rocco, *Nucl. Instrum. Methods B* 208(2003)411.
- [364] I.R. Bellobono, S. Calgari, M.C. Leonari, E. Selli and E.D. Paglia, *Die Angewandte Makromolekulare Chemie* 100(1981)135.
- [365] H. Kubota, I.G. Suka, S. Kuroda and T. Kondo, *Eur. Polym. J.* 37(2001)1367.
- [366] A. Wenzel, H. Yamgishita, D. Kitamoto, A. Endo, K. Haraya, T. Nakane, N. Hanai, H. Matsuda, H. Kamuswetz and D. Paul, *J. Membr. Sci.* 179 (2000)69.
- [367] T. Yamaguchi, S. Yamahara, S. Nakao and S. Kimura, *J. Membr. Sci.* 95(1994)39.
- [368] T. Chen, G. Kumar, M.T. Harries, P.J. Smith and G.F. Payne, *Biotechnol. Bioeng.* 70(2000)564.

- [369] S. Cosnier, D. Fologen, S. Szunerits and R.S. Marks, *Electrochem. Commun.* 2(2000)827.
- [370] A. K. Noor, S. L. Venneri, D. B. Paul and M. A. Hopkins, *Computers & Structures*, 74(2000) 507.
- [371] J. A. Balta, F. Bosia, V. Michaud, G. Dunkel, J. Botsis and J. A. Månson, activation and control, *Smart Materials & Structures*, 14(2005) 457.
- [372] C. Fischer, S. A. Braun, P. E. Bourban, V. Michaud, C. J. G. Plummer and J. A. E. Månson, *Smart Materials & Structures*, 15(2006)1467.
- [373] L. M. Mathieu, T. L. Mueller, P. E. Bourban, D. P. Pioletti, R. Muller and J. A. E. Månson, *Biomaterials*, 27(2006) 905.
- [374] J. Verrey, M. D. Wakeman, V. Michaud and J. A. E. Månson, 37(2006)9.
- [375] N. Bernet, V. Michaud, P. E. Bourban and J. A. E. Månson, *J. Composite Mater.*, 33(1999)751.
- [376] P. E. Bourban, N. Bernet, J. E. Zanetto and J. A. E. Månson, *Composites Part a-Appl. Sci. & Manufacturing*, 32(2001)1045.
- [377] J. Karger-Kocsis, *Polypropylene structure, blends and composites*, Chapman & Hall, London etc., (1995)
- [378] X. Wang, W. M. Hou, J. J. Zhou, L. Li, Y. Li and C. M. Chan, *Coll.& Polym. Sci.*, 285(2007)449.
- [379] K. Mezghani and P. J. Phillips, *Polymer*, 38(1997)5725.
- [380] J. Karger-Kocsis, *Polypropylene an a-z reference*, Kluwer Academic Publ., Dordrecht etc.(1999)
- [381] J. Jancar, *Advances in Polymer Science*, 1999; 139
- [382] J. R. Fried, *Polym. Sci. & technol.* Prentice Hall, Englewood Cliffs, NJ, (1995)
- [382] C. H. Hong, Y. B. Lee, J. W. Bae, J. Y. Jho, B. U. Nam and T. W. Hwang, *J. Appl. Polym. Sci.*, 98(2005)427.
- [384] S. M. Zebarjad, M. Tahani and S. A. Sajjadi, *J. Materi. Proc. Technol.* 155(2004)1459.
- [385] Q. Yuan and R. D. K. Misra, *Polymer*, 47(2006) 4421.
- [386] A. V. Shenoy, *Rheology of filled polymer systems*, Kluwer Academic Publishers, Dordrecht, (1999)
- [387] R. N. Rethon, *Mineral fillers in thermoplastics: filler manufacture and characterization*, *Advances in Polymer Science*, 1999; 139

- [388] P. M. McGenity, J. J. Hooper, C. D. Paynter, A. M. Riley, C. Nutbeem, N. J. Elton and J. M. Adams, *Polymer*, 33(1992)5215.
- [389] W. C. J. Zuiderduin, C. Westzaan, J. Huetink and R. J. Gaymans, *Polymer*, 44(2003)261.
- [390] Z. Demjen, B. Pukanszky and J. Nagy, *Composites Part A, App. Sci. & Manufacturing*, 29(1998)323.
- [391] L. Jilken, G. Malhammar and R. Selden, *Polym. Test.* 10(1991)329.
- [392] P. F. Bright, R. J. Crowson and M. J. Folkes, *J. Mater. Sci.* 13(1978)2497.
- [393] M. Drubetski, A. Siegmann and M. Narkis, *J. Mater. Sci.* 42(2007)1.
- [394] J. Gassan and A. K. Bledzki, *Composites Part A, App. Sci. & Manufacturing*, 28(1997)1001.
- [395] A. Ziabicki, *Fundamentals of fibre formation the science of fibre spinning and drawing*, Wiley, London a.o., (1976)
- [396] B. V. Gupta and K. V. Kothari, *Manufactured fibre technology*, Chapman & Hall, London, (1997)
- [397] Y. Ide and J. L. White, *Journal of Non-Newtonian Fluid Mechanics*, 2(1977)281.
- [398] F. Fourné, *Synthetic Fibers. Machines and Equipment, Manufacture, Properties*, Hanser Publishers, Munich, (1998)
- [399] X. Qian, M. Liao and W. Zhang, *Polym. Int.* 56(2007)399.
- [400] J.H. Shim, E.S. Kim, J.H. Joo and J.S. Yoon, *Appl. Polym. Sci.* 102(2006)4983.
- [401] A. Akelah, A. Rehab, T. Agag and M. Betiha, *J.Appl.Polym.Sci.*103 (2007)3739.
- [402] M. Heper, L. Türker, N.S. Kincal, *J. Colloid. & Interface Sci.*306 (2007)11.
- [403] P.H. Blanchard and E.Q. Geiger, *Sugar Technol.Rev.*11 (1984)1.
- [404] S.C. Tjong, *Mater. Sci. & Eng.* 53(2006)73.
- [405] M.K. Zahran, *J.Polym.Res.*,13(2006)65.
- [406] A. Hebeish, A.H. Zahran, A.M. Rabie and A.M. El-Naggar, *Die Angewandte Makromolekulare Chemie* 134(1975)37.
- [407] L.Razafimahefa, S.Chlebicki, I.Vroman and E. Devaux, *Society of Dyers and Colourists, Color. Technol.* 124(2008)86.
- [408] M. Pulat, E. Memis, M. Gümüsderelioglu, *J. Biomater. Appl.*17 (2003)237.
- [409] A.I. Vogel, *Elementary Practical Organic Chemistry Part 3: Quantitative Organic Analysis*, 2nd ed.; Longman: London, (1975)652.
- [410] ASTM D2240-05. *Annu. Book, ASTM Stand.* 1976.
- [411] C. Peter, W. Zhen and P. Thomas, *Appl. Clay Sci.* 15(1999)11.

- [412] S. Sinan, M. Mine, N. Nihan and N. Turgut, *Polym. Int.* 55(2006)216.
- [413] M. Alexander and P. Dubois, *Mater. Sci. Eng.* 28(2000)1.
- [414] C. Zilg, R. Thomson, R. Mulhaupt and J. Finter, *J. Adv. Mater.* 11(1999)49.
- [415] D. Yui, H. Y. Chang, S. Kuo, J. Huang and F. Chang, *J. Polym. Sci. Polym. Phys.* 45(2007)1781.
- [416] A. Petrella, M. Tamborra, M. Curri, L.P. Cosma, M. Striccoli, P.D. Cozzoli and A. Agostiano, *J. Phys. Chem.* 109(2005)1554.
- [417] T. Xin, Z. Haicha, T. Tao, F. Zhiliu and H. Baotong, *J. Polym. Sci. Polym. Chem.* 40(2002)1706.
- [418] A. Okoda, M. Kawasumi, A. Usuki, Y. Kojima, T. Kurauchi and O. Kamigaito, *Mater. Res. Soc. Prog.* 171(1990),45.
- [419] M. Miroslava, O. Maria, P. Petra, P. Andras, P. Bela and P. Jürgen, *Polym. Adv. Technol.* 17(2006)715.
- [420] H. Lu, Y. Hu, L. yang, Z. Wang, Z. Chen and W. Fan, *J. Mater. Sci.* 40(2005)43.
- [421] D.Garcia-Lopez, O.Picazo, J.C.Merino and J.M.Pastor, *European Polym.J.* 39:945(2003).
- [422] M.Abolfazl, B.Joao, P.Souares and Leonard C.Simon, *Macromol.Symp.* 243:277(2006).
- [423] W.Kaminsky, A.Funk and K.Wiemann, *Macromol.Symp.* 236:1(2006).
- [424] W.B.Xu, H.B.Zhai, H.Y.Guo, Z.F.Zhou, N.Whitely and W.P.Pan, *J. Thermal Analysis and Calorimetry*, 78:101(2004).
- [425] M.L.Lopez-Quintanilla, S.Sanchez-Valdes, L.F.Ramos de Valle and F.J.Medellin, *J.Appl.Polym.Sci.* 100:4748(2006).
- [426] E.Moore, *Polypropylene Handbook*; Hanser: Munich, 1996.
- [427] E.Manias, A.Touny, L.Wu, K.Strawhecker, B.Lu and T.C.Chung, *Chem.Mater.* 13(2001)3516.
- [428] M.Kawasumi, N.Kato, M.Usuki and A.Okada, *Macromol.* 30:6333(1997).
- [429] P. Ding and B. Qu, *J. Colloid & Interface Sci.* 8(2005)291.
- [430] Z. Matusinovic, M. Rogosic and J. Sipusic, *Polym. Degrad. & Stab.* 95 (2009)94.
- [431] Z.A. Kusmono, I. Mohd, W.S. Chow, T. Takeichi and R. Rochmadi, *Composites: Part A* 39(2008)1802.
- [432] E.J.Blanchard, E.F.Graves, *J.Text.Res.* 72(2002)39.
- [433] F. Effenberger, M. Schweizer and W.S.Mohamed, *J. Appl. Polym.Sci.* 113 (2009)492.

- [434] M.Pulat and C.Isakoca, J.Appl.Sci. 100(2006)2343.
- [435] N.Abidi and E.Hequet, J.Appl.Polym. 93(2004)145.
- [436] B.Abd El-Hady and M.N: Ibrahim, J.Appl.Polym.Sci. 93(2004)271.
- [437] G.S.Chauhan, L.Guleria and H.Lai, Polym.Compos. 11(2003)19.
- [438] V.Cornelia, C.Marinescu, R.Vornico and G.Staikos, J.Polym.Sci. 87(2003)1383.
- [439] M.W.Sabaa and S.M.Mokhtar, Polym.Test, 21(2002)337.
- [440] A.H.Zahran, A.M.Dessouki and M.Abozeid, Radiat.Phys.Chem. 29(1987)105.
- [441] R. Samu, A. Moulee and V.G. Kumar, J. Colloid.Interface Sci. 220(1990)220.
- [442] E. Elalfy, S.H. Samaha and F.M. Tera, Presented at the International Symposium on Fiber Science and Technology, Yokohama, Japan, Oct 1994.
- [443] S.R. Karmaker, Colourage Annu 1991.
- [444] S.Zhang and A.R. Horrocks. Prog. Polym. Sci. 28(2003)1517.
- [445] A.R. Horrocks, B.K. Kandola, G. Smart , S. Zhang and T.R. Hull, J. Appl. Polym. Sci. 106(2007)1707.
- [446] S. Bourbigot, J.W. Gilman and C.A. Wilkie ,Polym. Deg. Stab. 84(2004)483.
- [447] F. Gong, M. Feng, C. Zhao, S. Zhang and M. Yang, Polym. Deg. Stab. 84(2004) 289.
- [448] M.Heper, L.Türker, N.S.Kincal, J.Colloid&Interface Sci. 11(2007)306.
- [449] G.Smart, B.K.Kandola, A.R.Horrocks, S.Nazare and D.Marney, Polym. Adv.Technol.19 (2008)658.
- [450] A. Würz, Melliand Textilber., 36 (1955) 466.
- [451] C. L. Bird and W. S. Boston, Theory of Coloration of Textiles (Bradford: SDC, 1975).
- [452] Q. Fan, Y. Yang, S. C. Ugbolue and A. R. Wilson, National Textile Center, C01-D20 Annual Report-2001. (Available at:<http://www.ntcresearch.org/pdf-rpts/AnRp01/C01-D20-A1.pdf>) (Accessed 25 February 2008).
- [453]. Q Fan, S C Ugbolue, A R Wilson and Y S Dar, AATCC Rev. 3 (2003)25.
- [454] Y. Yang, S. Han, Q. Fan and S. Ugbolue, Text. Res. J., 75(2005)622.

CURRICULUM VITAE

Wael Sabry Mohamed



PERSONAL DATA

Born : Cairo, Egypt, 10th. August 1976

Nationality : Egyptian.

E-mail : wael.sabry@ipoc.uni-stuttgart.de

wsabry1976@yahoo.com

EDUCATIONAL BACKGROUND

Helwan University, Department of Chemistry, Faculty of Science, Egypt

M.Sc. in Organic Chemistry, August 2002.

M.Sc. Thesis examined "*Grafting Emulsion Polymerization of some vinyl monomers onto leather by using chemical and Gamma ray initiation systems*".

Helwan University, Department of Chemistry, Faculty of Science, Egypt

Pre-M.Sc. courses in Organic Chemistry, October 1999.

Helwan University, Department of Chemistry, Faculty of Science, Egypt.

B. Sc. in Chemistry May 1998.

General Estimation of "**Very good**".

PROFESSIONAL EXPERIENCE

- Jan. 2007-Sep.2009* Doctoral studies in chemistry
Institute for Polymer Chemistry
Stuttgart University
with Prof. Dr. Dr. h.c.F. Effenberger
- May. 2004-Dec.2006* **National Research Centre (NRC),**
Polymer Chemistry Department, Cairo, Egypt.
Assistant Lecturer
- Aug. 2002-May2004* **National Centre of Radiation Research And
Technology (NCRRT).**
Polymer Chemistry Department,
Nasr City, Cairo, Egypt .
Research Assistant
- Oct. 1998-Aug.2002* **Faculty of Science-Helwan University**
Chemistry Department, Helwan, Cairo, Egypt.
Research Assistant

PUBLICATIONS

- 1- Modification of Natural Leather by Grafting Emulsion Copolymerization Technique.
A.S.Badran, H.E.Nasr, N.R.El-Halawany and W.S.Mohamed
Polymer-Plastic Technology and Engineering. Vol.46, P.79 (2007)
- 2- Grafting Emulsion Polymerization of Glycidyl Methacrylate onto Leather by Chemical Initiation System.
K.A.Shaffei, A.B.Moustafa and W.S.Mohamed
Journal of Applied Polymer Science. Vol.109, P.3923 (2008)
- 3- Synthesis and Characterization of Some Polyacrylate / Montmorillonite Nanocomposites by In Situ Emulsion Polymerization using Redox Initiation System.
F.Effenberger, M.Schweizer and W.S.Mohamed
Journal of Applied Polymer Science. Vol.112, P.1572 (2009)
- 4- Elucidation of the Nanoparticle Effect on the Grafting of Vinyl Monomers onto Cotton Fabric.
F.Effenberger, M.Schweizer and W.S.Mohamed
Journal of Applied Polymer Science. Vol.113, P.492 (2009)

5- Novel Applications of Montmorillonite Nanoparticles and Solution Preparation of Polyolefin / Montmorillonite Nanocomposites

F.Effenberger, M.Schweizer and W.S.Mohamed

Polymer-Plastic Technology and Engineering. (In Press)

6- Effect of Montmorillonite Clay Nanoparticles on the Properties of Polypropylene Fibres

F.Effenberger, M.Schweizer and W.S.Mohamed

Polymer-Plastic Technology and Engineering. (In Press)